



Norwegian University of  
Science and Technology

# Wet Gas Compressor Transient Operation

**Ingeborg Mæland Dolve**

Master of Science in Mechanical Engineering

Submission date: June 2018

Supervisor: Lars Eirik Bakken, EPT

Co-supervisor: Martin Bakken, EPT

Tor Bjørge, EPT

Norwegian University of Science and Technology  
Department of Energy and Process Engineering



EPT-M-2018-23

**MASTER THESIS**

for

Student Ingeborg Dolve

Spring 2018

Wet Gas Compressor Transient Operation

*Transiente driftsforhold for våtgasskompressor***Background and objective**

Natural gas is one key to reduce emission and optimize efficiency. Increased production of gas demands new field development based on sub-sea production. Several wet gas compressors have been installed subsea at Gullfaks and Åsgard and novel experience from first operating phases is achieved.

Operation of subsea wet gas compressor systems represents challenges related to transient response at different inlet conditions. Of specific interest is to document compressors and throttle valves transient response to variations in gas mass fraction. Advanced techniques for transient analyses (e.g. HYSYS Dynamics) and comparison between different cases are prioritised. If required, test data should preferably be based on the existing NTNU wet gas compressor test rig.

**The following tasks are to be considered:**

1. Literature review to document compressor and throttle valve performance behaviour at different gas mass fraction (GMF).
2. Perform sensitivity analyses and document wet gas compressor transient response to variation in gas mass fraction.
3. Based on literature and lab tests, implement dry and wet valve characteristics in HYSYS Dynamics. Analyse and document different valve characteristics impact on the system response.

-- ” --

Within 14 days of receiving the written text on the master thesis, the candidate shall submit a research plan for his project to the department.

When the thesis is evaluated, emphasis is put on processing of the results, and that they are presented in tabular and/or graphic form in a clear manner, and that they are analyzed carefully.

The thesis should be formulated as a research report with summary both in English and Norwegian, conclusion, literature references, table of contents etc. During the preparation of the text, the candidate should make an effort to produce a well-structured and easily readable report. In order to ease the evaluation of the thesis, it is important that the cross-references are correct. In the making of the report, strong emphasis should be placed on both a thorough discussion of the results and an orderly presentation.

The candidate is requested to initiate and keep close contact with his/her academic supervisor(s) throughout the working period. The candidate must follow the rules and regulations of NTNU as well as passive directions given by the Department of Energy and Process Engineering.

Risk assessment of the candidate's work shall be carried out according to the department's procedures. The risk assessment must be documented and included as part of the final report. Events related to the candidate's work adversely affecting the health, safety or security, must be documented and included as part of the final report. If the documentation on risk assessment represents a large number of pages, the full version is to be submitted electronically to the supervisor and an excerpt is included in the report.

Pursuant to "Regulations concerning the supplementary provisions to the technology study program/Master of Science" at NTNU §20, the Department reserves the permission to utilize all the results and data for teaching and research purposes as well as in future publications.

The final report is to be submitted digitally in DAIM. An executive summary of the thesis including title, student's name, supervisor's name, year, department name, and NTNU's logo and name, shall be submitted to the department as a separate pdf file. Based on an agreement with the supervisor, the final report and other material and documents may be given to the supervisor in digital format.

- Work to be done in lab (Water power lab, Fluids engineering lab, Thermal engineering lab)
- Field work

Department of Energy and Process Engineering, 15. January 2018



---

L E Bakken  
Academic Supervisor

Research Advisor:  
T. Bjørge  
M. Bakken

## Preface

This report is the final result of my master thesis: *Wet gas compressor transient operation*. The work presented was performed during the spring of 2018 as the final part of my Master of Science program at the Norwegian University of Science and Technology.

I would like to thank my supervisor, professor Lars E. Bakken, for excellent guidance this semester and for always being available for questions. A special thanks to Erik Langørgen and my co-supervisor Martin Bakken for their valuable advice and help in the compressor lab. I also wish to thank my family for supporting and encouraging me throughout my studies.

Ingeborg Mæland Dolve

A handwritten signature in black ink, reading "Ingeborg Dolve". The signature is written in a cursive style with a dotted line underneath the name.

Juni 2018, Trondheim



# Abstract

Over the past years, the oil and gas industry has directed its attention towards subsea wet gas compression. Previous research has demonstrated that the operation of subsea wet gas compressors represents challenges related to transient response at various inlet conditions. Experimental work has been conducted to study the effects of wet gas on compressor aerodynamic and mechanical performance, which has presented many challenges in quantifying the effect of liquid presence on the compressor performance.

To date, the wet gas research has focused on the compressor and little attention has been given to the control valves surrounding the compressor. Control valves are an important part of the compression process, increasing the operational range and making the operation more flexible. Consequently, it is important to consider the effects of wet gas on the control valves. This thesis evaluates the performance of a centrifugal compressor and its discharge control valve at both wet and dry condition. The main objective of this thesis is to document the control valve performance at different gas mass fractions. Previous research on the wet gas compressor is presented, but the experimental campaign focuses on investigating valve wet gas performance.

No standard performance analysis for wet gas throttling through control valves exists. Thus, various methods are used in the industry. The valve performance calculation procedure used in this thesis is the Addition method. An experimental campaign was conducted in the NTNU wet gas compression test facility. Two different experimental set-ups were used to document the control valve performance. Water was injected either upstream or downstream of the compressor. The volume flow through the system was varied by altering the control valve opening. The gas mass fraction was varied from 1 to 0.8. Dry gas experiments were conducted to compare data from the valve manufacturer and the wet gas tests.

The results demonstrated that liquid properties influenced the control valve and compressor performance. A reduced volume flow and an increased pressure differential were observed for each valve opening when liquid was introduced. This indicated an increased throttling effect due to liquid blockage. The valve flow coefficient was reduced and a shift towards a linear valve characteristic was observed when the gas mass fraction was reduced. Additionally, a shift in operational point and system resistance curve was observed when liquid was introduced. The results in this thesis confirm the need for improved understanding of wet gas control valve throttling.





## Sammendrag

Olje- og gassindustrien har de siste årene rettet sin oppmerksomhet mot undervannsprosessering, spesielt gasskompresjon. Utviklingen av undervannskompressorer krever økt kunnskap om kompressorytelse og om hvordan endringer i driftsforhold påvirker kompressoren. Både teoretisk og eksperimentelt arbeid har blitt utført for å studere virkningen av våtgass på kompressorens aerodynamiske og mekaniske ytelse. Forskningen har fremhevet mange utfordringer knyttet til å kvantifisere effekten av våtgass på kompressorens ytelse.

Per dags dato har våtgassforskningen i hovedsak fokusert på kompressoren. Lite oppmerksomhet har blitt gitt til ventilene som omgir kompressoren. Ventiler er en viktig del av kompresjonsprosessen ettersom de utvider driftsområdet og gjør operasjonen mer fleksibel. Det er derfor viktig å vurdere effekten av våtgass på ventilen. Denne oppgaven evaluerer ytelsen til en sentrifugalkompressor og dens utløpsventil i både våt og tørr tilstand. Hovedformålet med denne oppgaven er å dokumentere ventilens ytelse og oppførsel ved ulike gassmassefraksjoner. Tidligere forskning på våtgass kompressoren presenteres, men de eksperimentelle forsøkene fokuserer på å undersøke ventilens ytelse.

I dag eksisterer ingen standard metode for å analysere våtgassventilytelse. Følgelig brukes ulike metoder i industrien. I denne oppgaven ble Addisjonsmetoden brukt for å beregne ventilytelsen. Eksperimentelle forsøk ble utført i våtgasskompresjonslaboratoriet ved NTNU. To forskjellige eksperimentelle oppsett ble brukt til å dokumentere våt ventilytelse. Vann ble injisert enten oppstrøms eller nedstrøms for kompressoren. Volumstrømmen gjennom systemet ble variert ved å kontrollere åpningen til utløpsventilen. Gassmassefraksjonen ble variert fra 1 til 0.8. Det ble også utført et tørrgasseksperiment for å sammenligne data fra ventilprodusenten og våtgassforsøkene.

Resultatene viste at introduksjonen av væske påvirket både ventilens og kompressorens ytelse. En redusert volumstrøm og en økt trykkdifferanse ble observert ettersom gassmassefraksjonen ble redusert. Dette indikerte en økt strupingseffekt på grunn av væskeblokkering. Ventilstrømningskoeffisienten ble redusert, og en forskyvning mot en lineær ventilkarakteristikk ble observert når gassmassefraksjonen ble redusert. I tillegg forflyttet kompressorens driftspunkt og systemmotstandskurven seg, når væske ble introdusert. Resultatene i denne oppgaven bekrefter behovet for en bedre forståelse av våtgass struping gjennom ventiler.



# Nomenclature

## Symbols

C	Orifice coefficient of discharge	-
$C_v$	Valve flow coefficient in US units	gpm
D	Internal diameter of piping	mm
$d_o$	Orifice diameter	mm
F	Pressure recovery	bar
f	Compressor path correction factor	-
$F_\gamma$	Specific heat ratio factor	-
$F_d$	Valve style modifier	-
$F_l$	Liquid pressure recovery factor	-
$F_p$	Piping geometry factor	-
H	Head	kJ
h	Entalphy	kJ
$K_v$	Valve flow coefficient in SI-units	$m^3/h$
L	Pipe length	mm
m	Mass	kg
MW	Molar mass	kg/kmol
N	Compressor speed	rpm
n	Polytropic exponent	-
P	Power	W
p	Pressure	bar
$P_R$	Valve pressure drop ratio	-
Q	Volume flow	$m^3/s$
R	Specific gas constant	J/kg K

$R_o$	Universal gas constant	J/K mol
$s$	Entropy	J/K kg
SG	Specific gravity	-
T	Temperature	K
V	Volume	$m^3$
$v$	Specific volume	$m^3/kg$
$v$	Velocity	m/s
X	Schultz' compressibility function	-
$x$	Pressure ratio differential	-
$x_T$	Pressure differential ratio factor at choked condition	-
Y	Expansion factor	-
Y	Schultz' compressibility function	-
Z	Compressibility factor	-
$\alpha$	Gas volume fraction	-
$\beta$	Beta ratio	-
$\beta$	Gas mass fraction	-
$\Delta$	Differential	-
$\dot{m}$	Mass flow rate	kg/s
$\epsilon$	Orifice expansibility factor	-
$\eta$	Efficiency	-
$\gamma$	Specific heat ratio	-
$\kappa$	Isentropic exponent	-
$\rho$	Density	$kg/m^3$
<b>Subscripts</b>		
1	Inlet	-

2	Outlet	-
c	Compressor	-
g	Gas	-
l	Liquid	-
L1	Upstream valve	-
L2	Downstream valve	-
m	Mechanical	-
max	Maximum	-
o	Orifice	-
p	Polytropic	-
ref	Reference	-
rel	Relative	-
s	Isentropic	-
T	Temperature	-
tot	Total	-
v	Valve	-
v	Volume	-
vc	Vena contracta	-

### Abbreviations

DN	Diameter nominal	mm
DPT	Differential pressure transmitter	-
EOS	Equation of state	-
FT	Flow transmitter	-
FTC	Flow to close	-
FTO	Flow to open	-
GMF	Gas mass fraction	-

GVF	Gas volume fraction	-
HEM	Homogeneous equilibrium model	-
HNE	Homogeneous non-equilibrium	-
HNE-DS	Homogeneous non-equilibrium-Diener/Schmidt	-
HT	Humidity transmitter	-
HYSYS	Process simulation software	-
IEC	International electrotechnical commission	-
IGV	Inlet guide vane	-
ISO	International Organization for Standardization	-
NPS	Nominal pipe size	inch
NTNU	Norwegian University of Science and Technology	-
PT	Pressure transmitter	-
ST	Speed transmitter	-
TM	Torque transmitter	-
TT	Temperature transmitter	-

# Contents

<b>Preface</b>	<b>i</b>
<b>Abstract</b>	<b>iii</b>
<b>Sammendrag</b>	<b>v</b>
<b>Nomenclature</b>	<b>vii</b>
<b>Table of Contents</b>	<b>xiii</b>
<b>List of Figures</b>	<b>xvii</b>
<b>List of Tables</b>	<b>xix</b>
<b>1 Introduction</b>	<b>1</b>
1.1 Background . . . . .	1
1.2 Thesis Statement . . . . .	2
1.3 Limitations of Scope . . . . .	2
1.4 Structure of Thesis . . . . .	3
<b>2 Compressor Fundamentals: From Dry to Wet Condition</b>	<b>5</b>
2.1 Compressibility . . . . .	5
2.2 Centrifugal Compression: An Overview . . . . .	5
2.2.1 Instabilities . . . . .	7
2.3 Dry Gas Performance . . . . .	8
2.3.1 Characteristics . . . . .	9
2.4 Wet Gas Performance . . . . .	10
2.4.1 Wet Gas Effects . . . . .	11
2.4.2 Wet Gas Performance Models . . . . .	14
2.5 Summary . . . . .	15
<b>3 Valve Fundamentals</b>	<b>17</b>
3.1 Control Valves: An Overview . . . . .	17
3.2 Flow Through Control Valves . . . . .	19
3.3 Valve Characteristics . . . . .	21
3.4 Flashing and Cavitation . . . . .	23
3.5 Single-Phase Valve Performance Prediction Models . . . . .	24
3.5.1 Incompressible Fluids . . . . .	25
3.5.2 Compressible Fluids . . . . .	25
3.6 Multi-Phase Valve Performance Prediction Models . . . . .	27
3.6.1 Homogeneous Equilibrium Models . . . . .	27

3.6.2	Homogeneous Non-Equilibrium Models . . . . .	28
3.6.3	Conclusion . . . . .	29
3.7	Summary . . . . .	30
<b>4</b>	<b>Compressors and System Resistance</b>	<b>31</b>
4.1	System Resistance Curve . . . . .	31
4.2	Compressor Discharge Throttling . . . . .	31
4.3	Summary . . . . .	34
<b>5</b>	<b>NTNU Wet Gas Compression Lab</b>	<b>35</b>
5.1	General Explanation of the Lab . . . . .	35
5.2	Sensors and Instrumentation . . . . .	37
5.3	Equipment Specifications . . . . .	37
5.3.1	Compressor . . . . .	37
5.3.2	Discharge Valve . . . . .	38
5.3.3	Flow Measurement Device and Calculations . . . . .	42
5.4	Summary . . . . .	45
<b>6</b>	<b>Experimental Campaign</b>	<b>47</b>
6.1	Experimental Set-Ups . . . . .	47
6.2	Purpose of Test . . . . .	49
6.3	Test Matrix . . . . .	49
6.4	Test Procedure . . . . .	50
6.5	Results and Discussion . . . . .	50
6.5.1	Dry Gas Tests . . . . .	51
6.5.2	Wet Gas Tests . . . . .	52
6.5.3	Operational Point and System Resistance Curve . . . . .	57
6.6	Summary and Conclusion . . . . .	60
<b>7</b>	<b>HYSYS Dynamics</b>	<b>63</b>
7.1	General . . . . .	63
7.2	Valve Characteristics and Operation . . . . .	64
7.3	Centrifugal Compressor Characteristic and Operation . . . . .	66
7.4	Summary . . . . .	67
<b>8</b>	<b>Conclusion</b>	<b>69</b>
<b>9</b>	<b>Further Work</b>	<b>71</b>
	<b>References</b>	<b>73</b>
	<b>Appendix A: Research Plan</b>	<b>I</b>



Appendix B: Research Log	II
Appendix C: Risk Assessment	III
Appendix D: The Schultz Polytropic Analysis of Centrifugal Compressors	X
Appendix E: Affinity Laws	XII
Appendix F: Inherent NPS 8 V150 Fisher Valve Characteristics	XIII
Appendix G: Lab Results	XIX
Appendix H: Calculated Performance Parameters	XXVIII



## List of Figures

1	Cross section of the centrifugal compressor at the NTNU wet gas compression lab (Ferrara, 2016). . . . .	6
2	Theoretical characteristic of a centrifugal compressor (Saravanamuttoo, 2009, p 181). . . . .	7
3	Centrifugal compressor characteristic (Saravanamuttoo, 2009, p 184). . . . .	9
4	Annular flow. . . . .	11
5	Compressor temperature ratio for various GMFs at 9000 rpm (Bakken, 2017b). . . . .	13
6	Compressor pressure ratio for various GMFs at 9000 rpm (Bakken, 2017b). . . . .	13
7	Compressor polytropic head for various GMFs at 9000 rpm (Bakken, 2017b). . . . .	14
8	Compressor polytropic efficiency for various GMFs at 9000 rpm (Bakken, 2017b). . . . .	14
9	Various control valves (Borden and Friedmann, 1998, p 38). . . . .	18
10	Simple illustration of (a) linear globe valve and (b) rotary ball valve. . . . .	18
11	General sketch of flow through a control valve. . . . .	19
12	Typical expansion line for a single-stage valve. The recovery from the vena contracta is shown as wavy because it is not well defined. (Borden and Friedmann, 1998, p 7) . . . . .	20
13	Inherent control valve characteristics. . . . .	21
14	How the equal percentage characteristic changes from inherent to installed condition for various valve pressure drop ratios. . . . .	22
15	Cavitation. . . . .	23
16	Flashing. . . . .	24
17	System resistance curve. . . . .	31
18	Simple illustration of discharge throttling. . . . .	32
19	How change in discharge valve opening affects the compressor performance at constant compressor speed. . . . .	33
20	Simple illustration of NTNU wet gas compressor test facility. . . . .	36
21	Compressor discharge valve at the NTNU wet gas compression test rig. . . . .	39
22	$C_v$ 1820 V150 NPS 8 Fisher inherent valve characteristic for single-phase water and air. . . . .	40
23	Different valve orientations. . . . .	40
24	Accumulation of water in front of valve at the NTNU wet gas compression lab. . . . .	41
25	Appropriate pressure tap locations (IEC, 2015). . . . .	42

26	Simple illustration of an orifice plate. . . . .	43
27	Illustration of the inlet section at the NTNU wet gas compression lab. . . . .	44
28	Experimental set-up 1: Water injection upstream of compressor. . . . .	48
29	Experimental set-up 2: Water injection downstream of compressor. . . . .	48
30	Comparison of dry gas flow coefficients ( $C_v$ ) for various valve openings at installed and inherent condition. . . . .	51
31	Comparison of dry gas relative flow coefficients ( $C_v$ ) for various valve openings at installed and inherent condition. . . . .	52
32	Valve inlet temperature curves for various GMFs in relation to volume flow (9000 rpm). . . . .	53
33	Total valve inlet density curves for various GMFs in relation to volume flow (9000 rpm). . . . .	53
34	Valve inlet volume flow curves for various GMFs in relation to valve opening (9000 rpm). . . . .	54
35	Valve differential pressure curves for various GMFs in relation to valve opening (9000 rpm). . . . .	55
36	Valve differential pressure curves for various GMFs in relation to volume flow (9000 rpm). . . . .	55
37	Flow coefficient curves for various GMFs (9000 rpm). . . . .	56
38	Relative flow coefficient curves for various GMFs (9000 rpm). . . . .	57
39	Compressor discharge pressure curves for various GMFs in relation to volume flow (9000 rpm). . . . .	58
40	How the compressor operational point is affected by wet gas at low volume flows (valve opening 40 %, 9000 rpm). . . . .	59
41	How the compressor operational point is affected by wet gas at high volume flows (valve opening 90 %, 9000 rpm). . . . .	59
42	Example of how the system resistance curve and operational point may change from wet to dry condition. . . . .	66
43	Valve inlet pressure curves for various GMFs in relation to volume flow (9000 rpm). . . . .	XXIII
44	Valve inlet pressure curves for various GMFs in relation to valve opening (9000 rpm). . . . .	XXIII
45	Total valve inlet density curves for various GMFs in relation to valve opening (9000 rpm). . . . .	XXIV
46	Valve inlet temperature curves for various GMFs in relation to valve opening (9000 rpm). . . . .	XXIV
47	Valve pressure ratio ( $P_2/P_1$ ) curves for various GMFs in relation to volume flow (9000 rpm). . . . .	XXV

48	Valve pressure ratio ( $P_2/P_1$ ) curves for various GMFs in relation to valve opening (9000 rpm). . . . .	XXV
49	Valve pressure ratio ( $P_1/P_2$ ) curves for various GMFs in relation to volume flow (9000 rpm). . . . .	XXVI
50	Valve pressure ratio ( $P_1/P_2$ ) curves for various GMFs in relation to valve opening (9000 rpm). . . . .	XXVI
51	Compressor discharge pressure curves for various GMFs in relation to valve opening (9000 rpm). . . . .	XXVII



# List of Tables

1	How valve opening affects valve performance parameters. . .	30
2	Effects of dry gas discharge throttling at constant compressor speed (Dolve, 2017). . . . .	34
3	NTNU compressor rig configurations. . . . .	38
4	NTNU discharge valve rig details. . . . .	38
5	Test matrix. . . . .	49
6	Research log. . . . .	II
7	NPS 8 V150 Fisher valve characteristics $C_v$ 1750 (Fisher Controls, 2018). . . . .	XVIII
8	NPS 8 V150 Fisher valve characteristics $C_v$ 1820 (Fisher Controls, 2018). . . . .	XVIII
9	Explanation of lab parameters used in Table 10-12. . . . .	XIX
10	Dry gas test results (9000 rpm). . . . .	XX
11	Set-up 1 wet gas test results (9000 rpm). . . . .	XXI
12	Set-up 2 wet gas test results (9000 rpm). . . . .	XXII
13	Explanation to the parameters used in Table 14-16. . . . .	XXVIII
14	Dry gas calculated performance parameters, based on Table 10. . . . .	XXIX
15	Set-up 1 wet gas calculated performance parameters, based on Table 11. . . . .	XXX
16	Set-up 2 wet gas calculated performance parameters, based on Table 12. . . . .	XXXI





# 1 Introduction

In this section, the background and the objective of this thesis are introduced. Limitations of the scope and the thesis' structure are displayed.

## 1.1 Background

It is an increasing focus on energy efficiency and environmental emission today. To reduce operational cost, meet environmental restrictions and optimise the production capacity, new and improved technology is continuously implemented in various processes and industries. The oil and gas industry is no exception.

Over the past years, the oil and gas industry has directed its attention towards subsea processing and gas compression in particular. The subsea gas compression will make it possible to develop fields in deep waters and harsh environments, where development would have been impossible before. Today many of the major oil and gas fields on the Norwegian continental shelf are entering the last phases of their lifetime. Many of these fields are heavily pressure depleted and thereby limited when it comes to production rates and lifting capacity. Consequently, the subsea compressors are installed to lift out more gas and condensate from the reservoirs and increase the fields' lifetime. A major advantage of subsea compression is that the efficiency and production rates increase the closer the compression process is to the wellhead. Equinor is one of the main driving forces for subsea processing. Several compressors have been installed subsea at Gullfaks and Åsgard, and novel experience from first operating phases have been achieved. Various technologies exist for subsea compression. Åsgard is a dry gas compression system which means that liquids are separated from the gas before compression. Gullfaks, on the other hand, is a subsea wet gas compression facility which does not depend on separation of liquid before compression. (Equinor, 2018)

In recent years, researchers have focused on investigating the wet gas performance of the main subsea compression component: namely the compressor. Experimental work has been conducted to study the effects of wet gas on compressor aerodynamic and mechanical performance, which has presented many challenges in quantifying the effect of liquid presence on the compressor performance (Musgrove et al., 2014b). However, a compressor never operates alone but is integrated into a bigger process scheme. Consequently, the compressor performance is affected by the surrounding equipment and vice versa. Valves are examples of such equipment that are close coupled to

the compressor. Control valves are an important part of the compression process, increasing the operational range and making the operation more flexible. The correlations between pressure drop and volume flow through the valves will affect the performance of the compressor. A process is only as strong as its weakest link, consequently it is of great interest making sure that the control valves are not detrimental to process optimisation.

Control valves are an increasingly vital component of modern manufacturing all around the world. They are frequently used in the oil and gas industry to control fluid mixtures that comprise both single-phase and two-phase flow. Despite this, control valves are usually oversized and the control range of these valves often does not fit the control requirements (Diener and Schmidt, 2005). A valve must be of sufficient size to pass the required flow by the process under all contingencies. However, an oversized control valve is a detriment to process optimisation (Fisher Controls, 2017). Properly sized control valves have the potential to increase efficiency, safety, profitability, and ecology in the various processes (Fisher Controls, 2017). There is a significant knowledge gap in making conclusions about the operation of valves with liquid and gas (Musgrove et al., 2014a). No standards of multi-phase flow through valves currently exist. To make accurate models and simulations of the complete compression system, investigations on this topic are needed. Consequently, it is of specific interest to investigate the behaviour of the control valves when exposed to wet gas.

## **1.2 Thesis Statement**

The main objective of this thesis is to document a control valve's transient response to variations in gas mass fraction (GMF). This thesis focuses on documenting variations in control valve performance parameters when the GMF is varied. An experimental campaign is conducted investigating wet and dry gas characteristics of a V-ball rotary valve placed downstream of a centrifugal compressor. Additionally, a discussion concerning valve and compressor characteristics in HYSYS Dynamics is conducted.

## **1.3 Limitations of Scope**

In consultation with the supervisor, it was decided to focus mainly on control valve performance. The reason for this was that much of the previous research had focused on the wet gas compressor. Wet gas control valve performance on the other hand, was a poorly investigated field of research. Fundamental theory and previous research on compressor performance for both dry and wet conditions are presented, but the experimental campaign

focused on the control valve.

Additionally, it was decided together with the supervisor to not focus on HYSYS Dynamics simulations. This was because the latest version of the HYSYS model of the NTNU test facility was developed in a pilot version of HYSYS not available for the author of this thesis.

## **1.4 Structure of Thesis**

This thesis is constructed as a scientific report, with fundamental theory, literature review and discussion followed by an experimental campaign, results and a final conclusion. The main content of each section is listed below:

Section 1: The background and the objective of the master thesis are introduced. Limitations of the scope and the thesis' structure are displayed.

Section 2: Fundamental theory of centrifugal compression is presented. Emphasis is put on explaining how the compressor performance changes from dry to wet condition.

Section 3: The fundamental theory of control valves is presented. Various performance calculation procedures are discussed.

Section 4: An explanation of the system resistance curve and how it affects the compressor operating point is given.

Section 5: An overview of the NTNU compressor lab and its key features are displayed.

Section 6: The experimental campaign with results and discussion is displayed.

Section 7: A discussion on how to implement wet and dry valve characteristics in HYSYS Dynamics is conducted.

Section 8: Final conclusion.

Section 9: Ideas for further work in relation to this thesis are presented.



## 2 Compressor Fundamentals: From Dry to Wet Condition

In this section the fundamental theory of centrifugal compression is presented. Emphasis is put on explaining how the compressor performance changes from dry to wet condition. Focus is not put on the basic thermodynamic theory and dry gas performance models, because these were focused on in the author's project thesis (Dolve, 2017). However, the concept of compressibility is included because it is vital when calculating gas properties in the NTNU lab and in the procedure described in Appendix D.

### 2.1 Compressibility

Compressibility is used to indicate the relative volume change of a fluid as a response to changes in pressure. For ideal gases the ideal gas law applies, as presented in Equation (1). An equation of state (EOS) is a thermodynamic equation which describes the state of a fluid under different physical conditions. The ideal gas law is such an equation and gives the relation between pressure ( $p$ ), volume ( $V$ ) and temperature ( $T$ ) for a specific amount of gas ( $m$ ). There are several EOSs that all fit different purposes and situations.

$$pV = mRT \quad (1)$$

For real gases, the ideal gas law falls short. To quantify the real gases deviation from the ideal, it is necessary to study the compressibility factor ( $Z$ ).

$$Z = \frac{pvMW}{R_oT} \quad (2)$$

The compressibility factor can be found using a generalised compressibility map or by using an EOS. Generalised maps should only be used for estimation purposes. For real gas performance calculations, a proper EOS should be selected and used. In Equation (2),  $R_o$  is the universal gas constant and  $MW$  is the molar weight of the gas. The molar weight can be found by summation of the molar weight of each component multiplied by the mole fraction. (Bakken, 2017a)

### 2.2 Centrifugal Compression: An Overview

The main task of a centrifugal compressor is to increase the pressure of a fluid. This is done by first accelerating the flow, and then transforming kinetic energy to potential energy.

The centrifugal compressor consists essentially of a stationary casing containing an impeller, a diffuser and a volute. The impeller is the rotating part, where the fluid is drawn in at high speed. The fluid trapped between the impeller blades is forced to move around with the blades due to centrifugal forces. This results in a pressure increase from eye to tip in the impeller. The diffuser transforms the kinetic energy at the impeller outlet into static pressure. The diffuser can be either vaneless or vaned. (Saravanan, 2009) Generally, the diffuser is followed by a volute. The volute is a spiral-shaped channel of increasing cross-sectional area, whose goal is to deliver the discharge flow from the diffuser to the downstream piping system (Ferrara, 2016). Figure 1 illustrates a centrifugal compressor with its main parts.

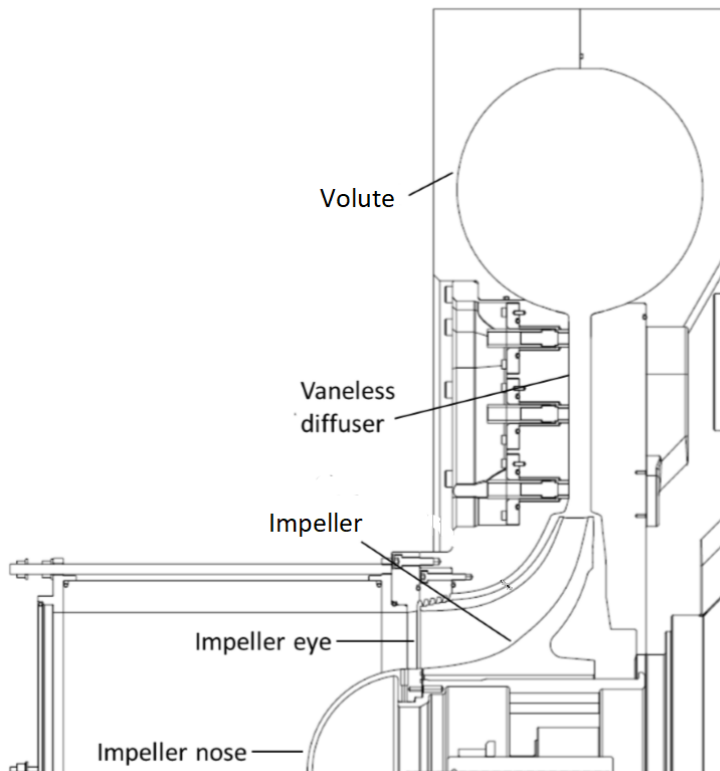


Figure 1: Cross section of the centrifugal compressor at the NTNU wet gas compression lab (Ferrara, 2016).

### 2.2.1 Instabilities

Figure 2 illustrates how the pressure ratio will *theoretically* vary with mass flow for a given compressor speed. Other similar curves for other compressor speeds could have been plotted, but for simplicity, only one curve is included in Figure 2. When there is no mass flow through the compressor the pressure ratio will be at some value A. When the mass flow increases the pressure ratio will increase and reach its maximum in point B, where the efficiency approaches its maximum. If the mass flow is further increased the efficiency and the pressure ratio will begin to decrease. (Saravanamuttoo, 2009)

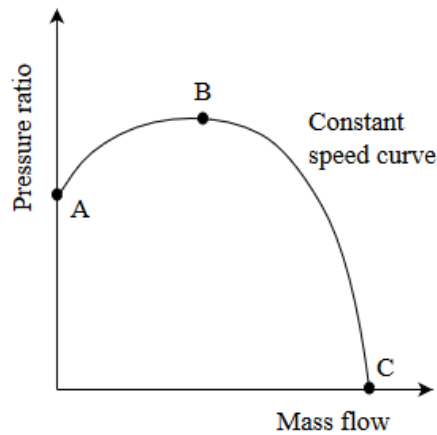


Figure 2: Theoretical characteristic of a centrifugal compressor (Saravanamuttoo, 2009, p 181).

The effective operating range of a centrifugal compressor is limited by phenomena such as surge, stall and choke (Saravanamuttoo, 2009). Surge is defined as pulsations in flow and pressure. This phenomenon can be described using Figure 2.

Suppose that the compressor is operating at some point between A and B in Figure 2. Because the slope is positive a reduction in mass flow will be followed by a decrease in discharge pressure. The pressure ratio will decrease, and the compressor loses its ability to produce the pressure existing in the discharge pipe. The pressure in the discharge pipe will be higher than the pressure of the compressor and the fluid will reverse its direction towards the resulting pressure gradient. Reversal flow will occur in this situation. The compressor discharge pressure drops and is re-established in high frequency cycles resulting in unsteady operation. On the contrary, suppose that the compressor is operating at some point between B and C

where the slope is negative. In this case, a reduction in mass flow will be accompanied with an increase in pressure ratio. In this case there will be no reversal flow because the pressure of the compressor is higher than the pressure of the discharge pipe, hence stable operation is maintained. The surging can vary in intensity, but intense surging can cause complete destruction of compressor parts in seconds and should therefore be avoided. (Hundseid and Bakken, 2006a; Saravanamuttoo, 2009)

Stall is another source of instability and poor performance. Stall may contribute to surge but can also exist during stable operation. Rotating stall may lead to vibrations resulting in fatigue failures in downstream equipment. Stall occurs when the fluid is separated from the walls in the channels between diffuser vanes and impeller blades. This separation is usually caused by non-uniformity in the channel geometry or in the flow. The separation in one channel may lead to changes in angle of incidence in other channels. Stall can propagate from channel to channel, *stalling* the flow. (Saravanamuttoo, 2009)

A third phenomenon that limits the operating range is called *choke*. Choke occurs somewhere between operating point B and C in Figure 2 at the point where no further increase in mass flow can be obtained. (Saravanamuttoo, 2009)

### 2.3 Dry Gas Performance

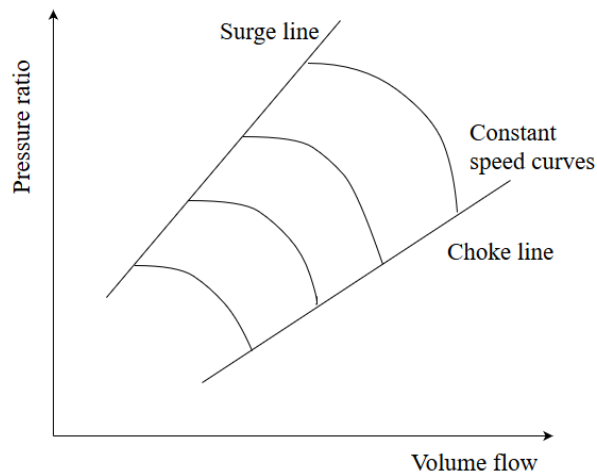
An accurate compression calculation is essential for estimating the real gas performance parameters (Bakken, 2017a). Essentially, there are two ways to model a compression process: the isentropic and the polytropic approach. For details about these two models see Dolve (2017) or Bakken (2017a). However, other modified approaches based on the two mentioned methods exist. The Schultz approach is an example of a modified polytropic analysis. Schultz' procedure accounts for the variations in the polytropic volume exponent. In the isentropic and polytropic procedure this exponent is assumed to be constant along the compression path. Schultz showed that it would be more convenient to include two compressibility functions in the polytropic analysis (Schultz, 1962). A major advantage of these compressibility functions is that the head and efficiency are determined explicit from the performance equations (Bakken, 2017a). This corrected method ensures more accurate results for real gas compression (Schultz, 1962). Both Bakken (2017a) and Hundseid et al. (2008) accentuates the superiority of Schultz' method compared to the isentropic and the polytropic approach. Additionally, both the ASME and ISO Standard for power testing of dry



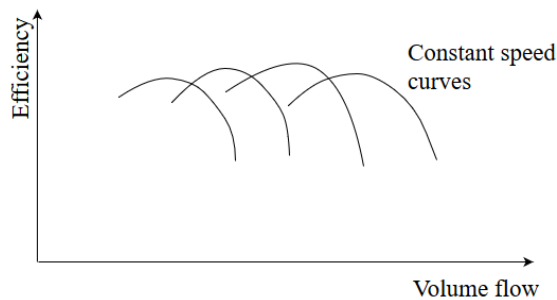
gas performance in centrifugal compressors are based on Schultz approach (Hundseid et al., 2008). As a result, the preferred method for dry gas performance calculations is the Schultz polytropic analysis. Consequently, Schultz' method is the approach used for performance calculations in this report. The Schultz procedure can be found in Appendix D.

### 2.3.1 Characteristics

Once the geometry of the compressor has been fixed at design point, then the *compressor characteristic* or *compressor map* can be generated. The purpose of generating the characteristic is to determine the performance of the compressor at off-design conditions. A typical centrifugal compressor characteristic is shown in Figure 3.



(a)



(b)

Figure 3: Centrifugal compressor characteristic (Saravanamuttoo, 2009, p 184).

Figure 3(a) illustrates the actual variation in pressure over the entire range of volume flow and compressor speed. These curves are equal to the one presented in Figure 2, only here curves for various speeds are included. Additionally, the surge line and the choke line have been included. These lines set the limits for stable operation. Figure 3(b) shows how the efficiency varies over the entire range of volume flow and compressor speed.

Together these figures represent the characteristic of a given compressor. The characteristic is dependent on physical properties of the working fluid, such as the compressor inlet pressure, temperature and composition. Altering the inlet conditions will change the characteristic and generate new pressure curves in Figure 3(a). The correlations in Figure 3(a) and 3(b) can be retrieved using suitable performance calculation methods such as discussed in Section 2.3. Even though it is dangerous to operate the compressor close to the surge line, it is also highly desirable because of the high efficiency in this area. As the figure above displays, only a limited number of characteristic curves can be included in a compressor map. Consequently, if an operating point lies outside or between these curves, the affinity laws are used for calculating the head, efficiency and volume flow (Dahlhaug, 2017). These laws are presented in further detail in Appendix E.

## 2.4 Wet Gas Performance

This far in the thesis, only dry gas performance has been discussed. In this subsection wet gas performance is introduced. Research shows that the presence of liquid affects the performance of the compressor to a high degree and that the models for dry gas performance are no longer valid (Hundseid et al., 2008). A wet gas compression process follows a compression path given by the efficiency in the same way as for dry gas. Wet gas is defined as a gas containing up to 5 % of liquid on a volume basis (Hundseid et al., 2008). The gas volume fraction (GVF) is defined according to Equation (3), while the gas mass fraction (GMF) is defined by Equation (4) (Bakken, 2017a).

$$\alpha = \frac{Q_g}{Q_g + Q_l} = \frac{\beta \rho_l}{\beta \rho_l + (1 - \beta) \rho_g} \quad (3)$$

$$\beta = \frac{\dot{m}_g}{\dot{m}_g + \dot{m}_l} = \frac{\alpha \rho_g}{\alpha \rho_g + (1 - \alpha) \rho_l} \quad (4)$$

The total wet gas density is calculated as a weighted average of the single-phase fluids as demonstrated in Equation (5).

$$\rho_{tot} = \alpha \rho_g + (1 - \alpha) \rho_l \quad (5)$$

Wet gas flow is usually described as annular flow due to the high velocities and relative low liquid content (Hundseid et al., 2008). The liquid transports as a thin film on the pipe wall while the gas flows in the centre of the pipe. The liquid may also be transported as dense droplets in the core of the gas phase as illustrated in Figure 4.

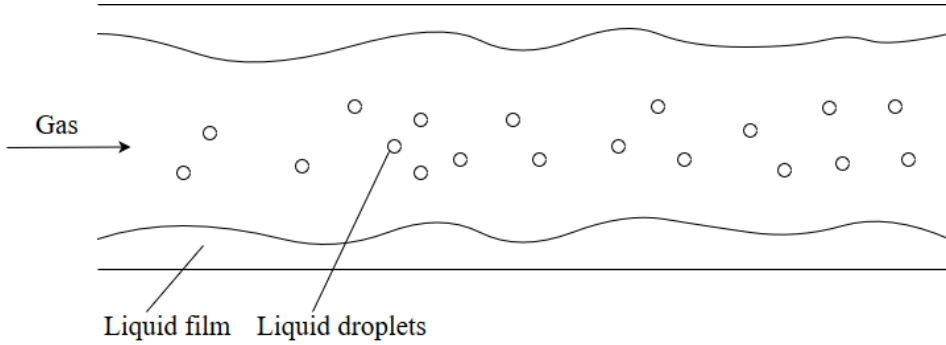


Figure 4: Annular flow.

#### 2.4.1 Wet Gas Effects

This subsection describes the main effects of introducing two-phase flow in the compressor. The general trends observed in wet gas compression research are documented. Attention is paid to the phenomena that occur and how they affect the performance of the compressor.

The interactions between the phases contribute to multi-phase effects not present in single-phase flow. The dynamics of multi-phase flow involve heat, mass and momentum transfer (Hundseid et al., 2008). Hundseid et al. (2008) demonstrated several effects of wet gas that influences the thermodynamics of the compressed fluid and the aerodynamics of the compressor. For starters, compression of wet gas may result in an evaporative cooling of the compressed fluid. This is a phenomenon where the liquid phase evaporates into gas phase. Because the gas phase has a lower heat capacity than the liquid phase there will be a difference in compressor discharge temperature. The liquid phase is more resistant towards temperature change and will have a lower discharge temperature compared to the gas. The temperature difference causes heat and mass transfer between the phases resulting in an increase in entropy of the compressed fluid.

Under wet conditions there is also a possibility of liquid entrainment and deposition. Liquid atomisation and droplet deposition are associated with losses. When the entrained liquid is accelerated, kinetic energy from the

high-velocity gas is reduced. Additionally, the total kinetic energy is reduced when droplets deposit on the liquid film. The velocity difference between the phases is often called slip. Hundseid et al. (2008) also pinpointed the effect of liquid film formation on the impeller surface. The film increases the surface roughness and results in increased blockage. The physical blockage reduces the flow area and is also associated with increased frictional losses. This results in less volume flow through the compressor.

Musgrove et al. (2014b) documented the general trends in wet gas compression. The study showed that the compressor temperature ratio decreases when liquid is introduced due to evaporative cooling. Additionally, the pressure ratio normally increases due to the increased density and molecular weight. Musgrove et al. (2014b) also pinpointed that the volume flow through the compressor decreases when liquid is introduced. Both Musgrove et al. (2014b) and Hundseid and Bakken (2015) stated that liquid droplet size is not an important parameter in wet gas compression if the liquid injection occurs far enough upstream the compressor.

Brenne et al. (2005) and Hundseid et al. (2008) demonstrated a significant reduction in specific polytropic head with increasing liquid content, because the mass fraction of liquid is increased due to larger internal losses in the compressor. The increasing density difference leads to a considerable increase in the mass fraction entering the compressor. In wet condition, a reduction in suction pressure reduces the specific polytropic head even further. An increase in total polytropic head is also observed due to the change in pressure ratio (Hundseid et al., 2008). Brenne et al. (2005) showed that the efficiency drops when the amount of liquid is increased due to increased power consumption. The effect is more pronounced at lower pressures due to the increasing density difference between the phases when the suction pressure is reduced while holding the GMF constant.

Ferrara and Bakken (2015) investigated the wet gas flow behaviour at the impeller eye during surge. Their experiments revealed a liquid “doughnut” formation upstream the inlet area. This phenomenon transpires because the main flow fails to transport the high-density particles into the impeller due to the increased fluid density. Consequently, wet gas conditions increase the risk of liquid accumulation and blockage in front of the impeller eye.

The figures below display the same observations as discussed above. Figures 5-8 are experimental results obtained at the NTNU wet gas test facility (Bakken, 2017b). See Section 5 for details about the test facility. Figure 5 demonstrates that the temperature ratio decreases when the GMF is re-

duced. Figure 6 shows that the pressure ratio increases when the GMF is reduced. The figure also demonstrates that the increase is more pronounced at low volume flows. Figure 7 shows that the polytropic head decreases when the GMF is reduced. Figure 8 shows that the polytropic efficiency also decreases as the GMF is reduced.

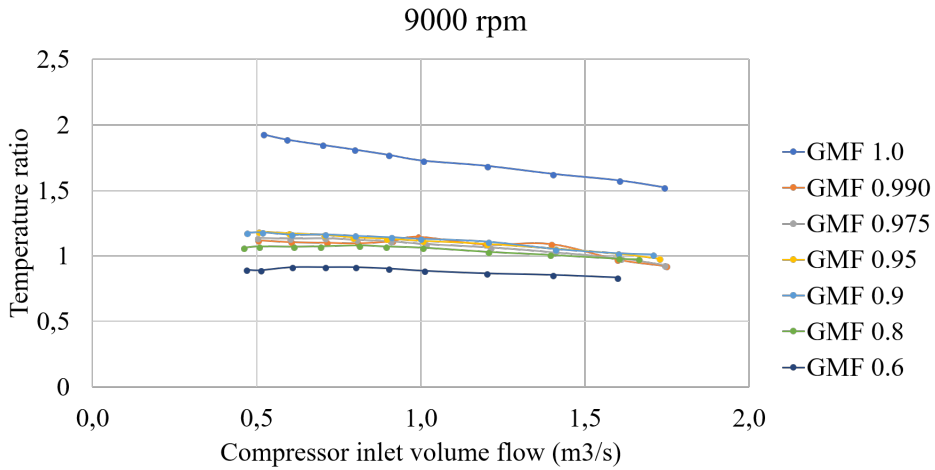


Figure 5: Compressor temperature ratio for various GMFs at 9000 rpm (Bakken, 2017b).

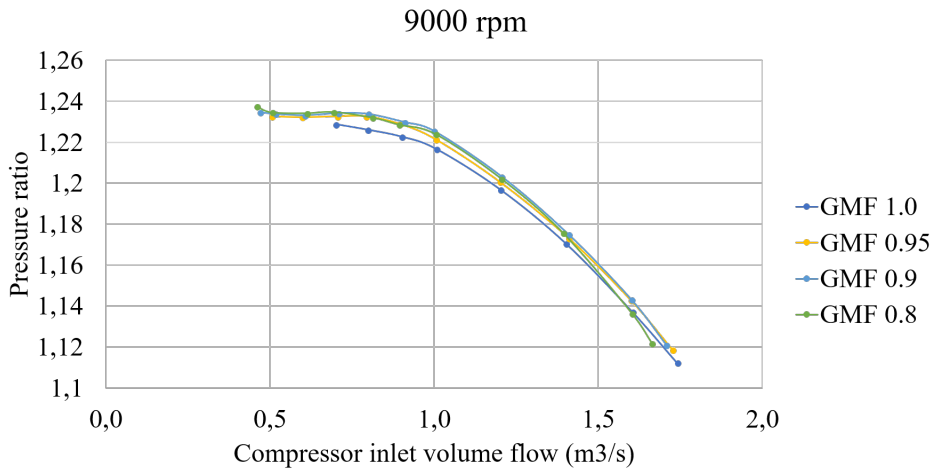


Figure 6: Compressor pressure ratio for various GMFs at 9000 rpm (Bakken, 2017b).

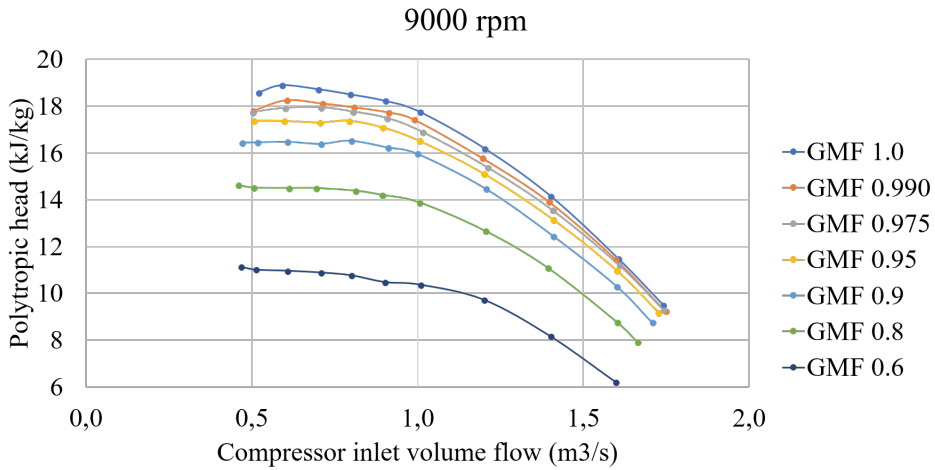


Figure 7: Compressor polytropic head for various GMFs at 9000 rpm (Bakken, 2017b).

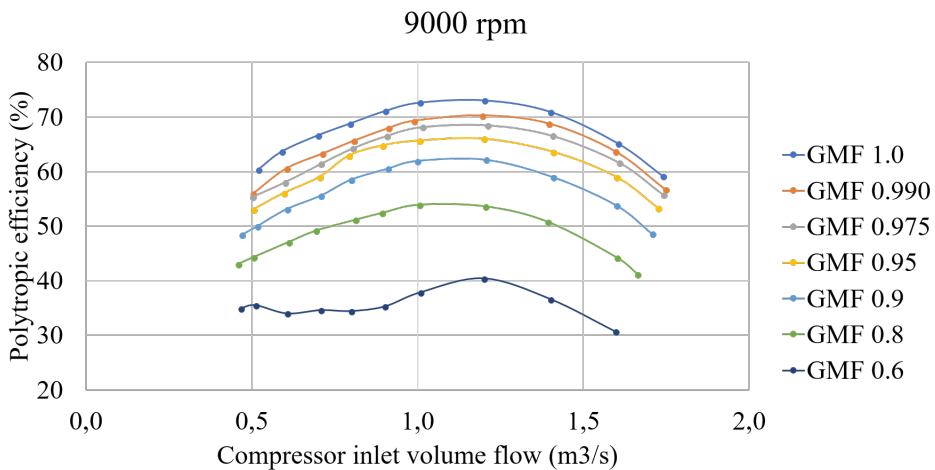


Figure 8: Compressor polytropic efficiency for various GMFs at 9000 rpm (Bakken, 2017b).

#### 2.4.2 Wet Gas Performance Models

Hundseid et al. (2008) clarified that the standard parameters based on dry gas theory are not applicable for estimating wet performance, especially because of sensitivity to temperature variation. The effects due to density changes, phase interactions and compressibility variations make the standard calculations inadequate, so new methods to estimate performance are

fundamental (Ferrara, 2016). Various wet gas performance models exist. Bakken (2017a) mentioned the two-fluid model and the total fluid model. The two-phase model approach assumes that the fluid phases do not interact with each other. The total head is the sum of the gas and liquid head, adjusted according to the GVF like a weighted average. This approach is mainly used for multi-phase pumps at low GVFs. On the other hand, the total fluid model includes fluid and thermodynamic properties of all components. Also, Hundseid et al. (2008) proposed a corrected formula to calculate the polytropic head and efficiency, using Wood’s model that allows for a direct comparison of dry and wet gas performance.

Hundseid and Bakken (2006b) and Bakken (2017a) suggested a direct integration method that utilises the real gas properties along the polytropic compression path. This method divides the compression process into many sub-compressions and considers any phase change through the compression. Hundseid and Bakken (2006b) pin-pointed the importance of estimating the volume flow along the compressor path. However, this polytropic direct integration procedure is currently based on phase and thermal equilibrium. Wet gas tests have revealed non-equilibrium conditions (Bakken, 2017a). Thus, Bakken (2017a) accentuated the need for precise performance models that include non-thermal and non-equilibrium behaviour through the compressor.

## 2.5 Summary

In this section, an introduction of centrifugal compression is given. Compressor wet gas performance was presented and the effects of introducing liquid were discussed. Previous research showed how the pressure ratio increased and the temperature ratio decreased along the entire curve when the GMF was reduced. Additionally, the polytropic head and efficiency decreased along the entire curve when the GMF was reduced. Some of the most important discoveries from this section are listed below.

Multi-phase phenomena include:

- Evaporative cooling.
- Liquid entrainment and deposition.
- Heat and mass transfer between phases.
- Liquid film formation.
- Liquid “doughnut” formation during surge.

- Velocity variations between phases.

Multi-phase effects on compressor performance parameters include:

- Decreased temperature ratio.
- Increased pressure ratio, especially at low flows.
- Increased fluid density.
- Decreased specific polytropic head.
- Increased power consumption.
- Decreased efficiency.



## 3 Valve Fundamentals

In this section, the fundamental theory of control valves is introduced. Emphasis is put on explaining the valve characteristic and various performance calculation procedures.

### 3.1 Control Valves: An Overview

Valves are mechanical devices commonly used in pipelines and pipe networks for industrial applications, including the oil and gas industry. A valve can control the flow rate, pressure and temperature of a fluid. Borden and Friedmann (1998) defines a control valve in the following way:

*A control valve is a power operated device which modifies the fluid flow rate on a process control system. It consists of a valve connected to an actuator mechanism that is capable of changing the position of a flow controlling element in the valve in response to a signal from the controlling system.* (Borden and Friedmann, 1998, p. 1)

A control valve essentially consists of a body, closure member, flow control orifice and stem. The body is the part of the valve that provides the fluid flow passage and connects the valve to the surrounding piping. The closure member is the movable part of the valve which is placed in the flow path to modify the flow rate through the valve. The flow control orifice is the part of the flow passageway that works together with the closure member to modify the flow rate through the valve. The stem is the shaft that connects the actuator to the closure member. These parts can be designed differently and some control valve types are listed in Figure 9.

Usually, control valves are classified based on what motion moves the closure member. This motion can either be linear or rotary. The flow area in a linear valve is dictated by the position of the closure member relative to its flow control orifice, while the flow area in a rotary valve depends on the angular position of a disc (Thomas, 1999). Figure 10(a) illustrates a linear control valve, while Figure 10(b) shows a rotary control valve.

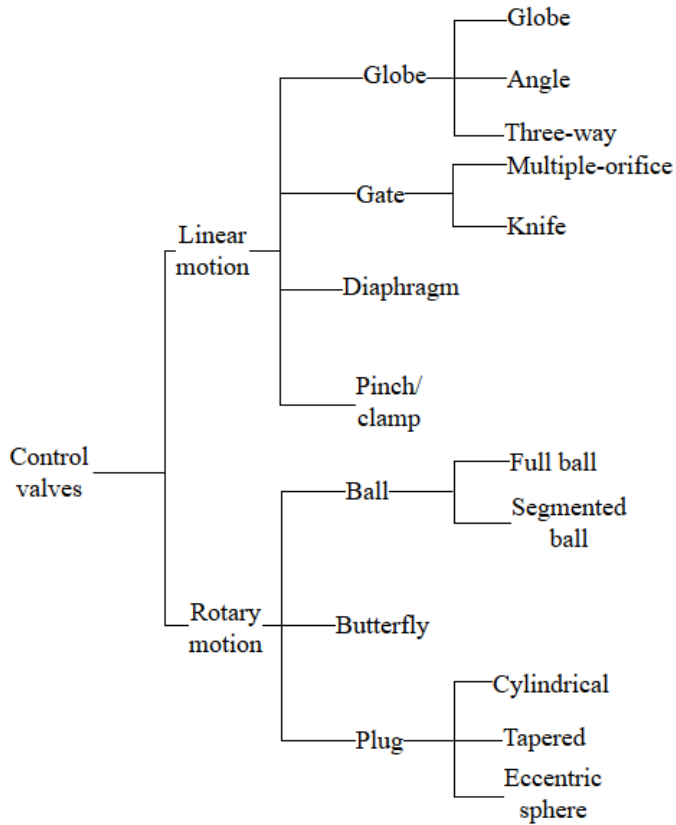


Figure 9: Various control valves (Borden and Friedmann, 1998, p 38).

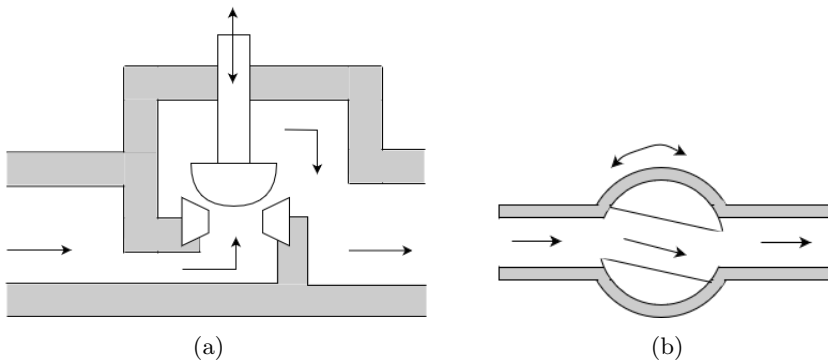


Figure 10: Simple illustration of (a) linear globe valve and (b) rotary ball valve.

Valves are also classified by which direction the flow travels: Flow to open (FTO) or flow to close (FTC). Figure 10(a) illustrates a classic FTO valve.

The fluid pushes on the closure member trying to open it, like the water in a garden hose. Imagine that the flow direction in Figure 10(a) is reversed. Then the fluid would push on the closure member trying to close it, like the water on a bathtub plug. In this scenario, the valve would be a FTC valve. Sometimes FTO is called forward flow and FTC is called reversed flow. (Lipták, 1995)

The mechanism for opening and closing a valve is called an actuator. Manually operated valves require someone in attendance to adjust them using a direct or geared mechanism attached to the valve stem. Power-operated actuators allow the valve to be operated remotely. These actuators use gas pressure, hydraulic pressure or electricity to supply force and motion to the closure member. (Borden and Friedmann, 1998, p 37)

### 3.2 Flow Through Control Valves

Fluid flowing through a valve obeys the basic laws of conservation of energy and mass. Figure 11 is a simple illustration of the pressure and velocity profile through a valve.

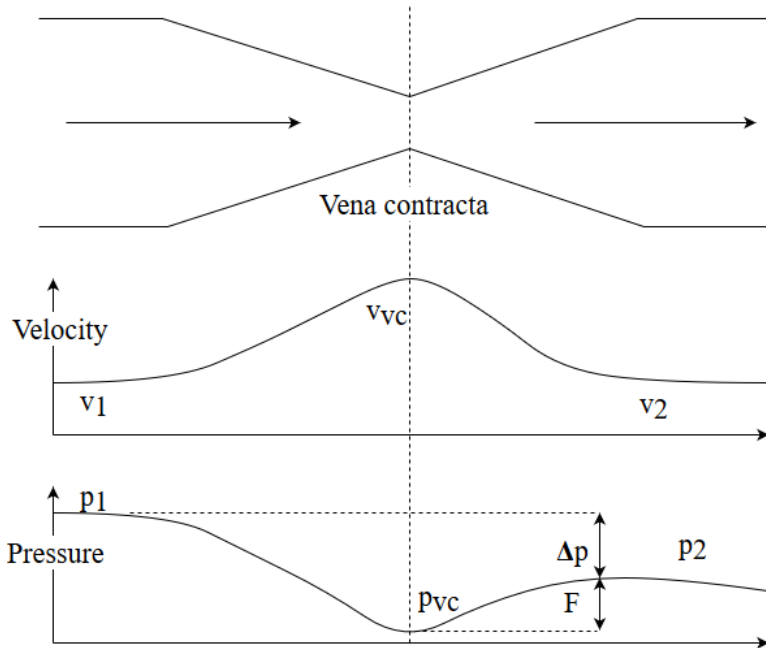


Figure 11: General sketch of flow through a control valve.

The valve is illustrated as a simple convergent-divergent section. In reality, the flow path will be much more complex and vary according to valve

type and design. The relationship between pressure and velocity can be obtained by Bernoulli's equation. The valve acts as a restriction in the flow stream, limiting the flow area. As the fluid approaches the valve, its velocity increases for the full flow to pass through the restriction. Energy for this increase in velocity comes from a corresponding decrease in pressure. (Bahadori, 2014)

The enthalpy of the fluid does not change through the valve, but the process is irreversible with an accompanying increase in entropy, indicating that the energy has become less useful (Borden and Friedmann, 1998, p 7). Some of the kinetic energy of the fluid is converted to heat and lost as the fluid travels through the valve. Exactly what portion of the kinetic energy that is lost, largely depends on the valve type and construction. The throttling process of a control valve is illustrated in an enthalpy-entropy diagram in Figure 12.

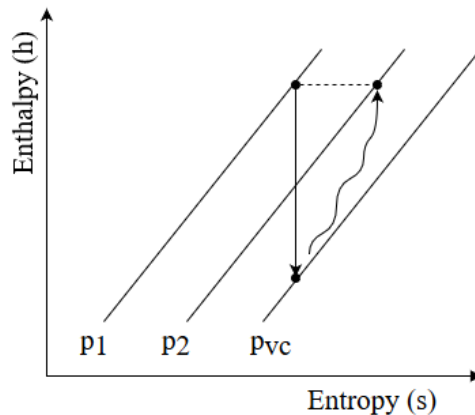


Figure 12: Typical expansion line for a single-stage valve. The recovery from the vena contracta is shown as wavy because it is not well defined. (Borden and Friedmann, 1998, p 7)

The vena contracta is the location where the cross-sectional area of the flow is at a minimum. Consequently, it is also the location where the fluid velocity is at a maximum and the pressure is at a minimum. The vena contracta normally occurs just downstream of the actual physical restriction in a control valve. (Borden and Friedmann, 1998, p 219)

Pressure recovery is the increase in pressure that occurs when the fluid moves from the vena contracta to the valve's outlet and downstream piping (Borden and Friedmann, 1998, p 165). Exactly how large the pressure re-

covery is, depends on valve type. The pressure recovery is illustrated by F in Figure 11.

As mentioned, the valve opening and thus the valve performance parameters can be controlled by varying the position of the closure member. When the valve opening is reduced, the flow area is reduced resulting in increased velocity at the vena contracta. The increase in velocity is followed by a similar decrease in pressure. Thus, the valve differential pressure will increase across the valve and the valve inlet pressure increases. On the contrary, if the valve opening is increased the valve will experience the opposite effects.

### 3.3 Valve Characteristics

The valve characteristic is defined as the relationship between the valve opening position and the flow through the valve. It is common to distinguish between *inherent* and *installed* characteristic. Inherent flow characteristic is defined as the relationship between valve opening position and the relative flow through the valve at constant pressure differential. These characteristics are normally supplied by the valve manufacturer and the most common are sketched in Figure 13.

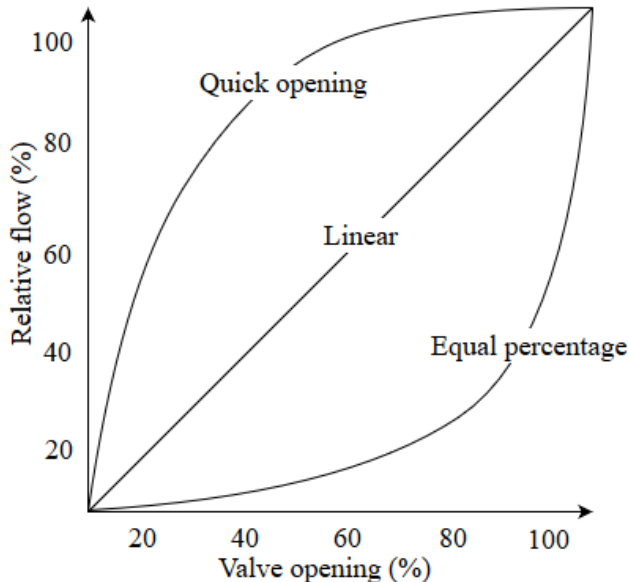


Figure 13: Inherent control valve characteristics.

In the linear case in Figure 13, the flow is directly proportional to the valve opening position. For the quick opening characteristic, the high flows are

achieved for low valve openings and as the valve opens further the flow increases at a slower rate. Contrary, the equal percentage characteristic initially obtains very low flows at low valve openings, but the flow will increase more rapidly as the valve opens to its full position. (Borden and Friedmann, 1998, p 4)

When a valve is installed with other process equipment, such as compressors or pumps, the pressure drop across the valve will vary depending on the complete process scheme and changes in the system. Consequently, the inherent characteristic does not reflect the actual performance of the valve. The installed characteristic is defined as the relationship between the relative flow and valve opening under the system's actual operating conditions. In this case, the pressure difference is not constant and the characteristic will be unique for each specific installed system or process. Kinetic pressure drop in the piping and equipment in series with the valve make the installed characteristic decidedly different from the inherent characteristics. (Borden and Friedmann, 1998, p 4)

Figure 14 illustrates the change in an equal percentage characteristic as it moves from inherent condition to installed condition.

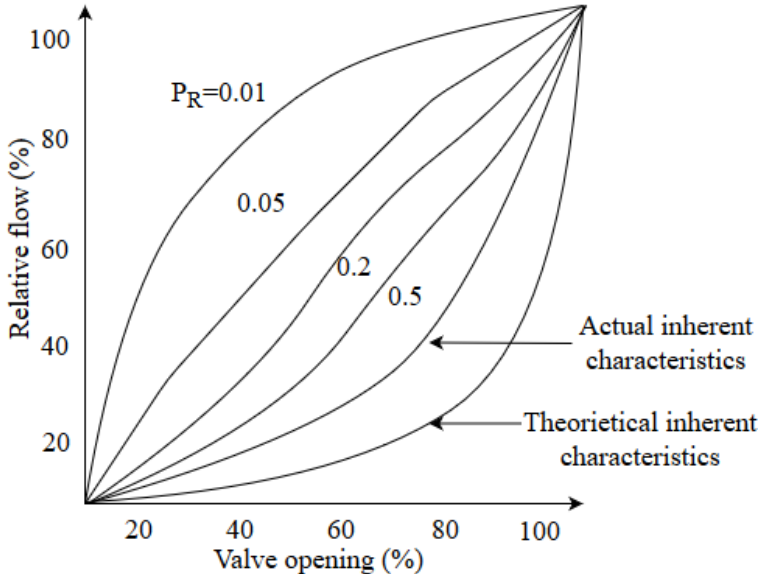


Figure 14: How the equal percentage characteristic changes from inherent to installed condition for various valve pressure drop ratios.

The equal percentage inherent valve characteristic moves towards an linear installed characteristic as the valve pressure drop ratio decreases (Borden and Friedmann, 1998, p 5). The valve pressure drop ratio is found by Equation (6). The denominator is the sum of the differential pressure upstream, downstream and across the valve.

$$P_R = \frac{\Delta p_v}{\Delta p_v + \Delta p_{L1} + \Delta p_{L2}} \quad (6)$$

### 3.4 Flashing and Cavitation

*Cavitation* occurs in liquid systems when local pressure fluctuations near the liquid's vapour pressure result in the sudden growth and collapse of vapour bubbles (cavities) within the liquid. The vena contracta area is vulnerable to this phenomenon because cavitation occurs in regions with low pressures. As illustrated in Figure 15, cavities start to form when the static pressure is at or below the fluid's vapour pressure. The vapour pressure of a fluid is the pressure where both liquid and gas phase exists in equilibrium. After the vena contracta the static pressure rises above the vapour pressure and the cavities collapse. The cavity collapse produces localised shock waves and liquid microjets. If the collapse occurs close to a solid surface it may cause significant damage to the body of the valve. (Borden and Friedmann, 1998, p 164-167)

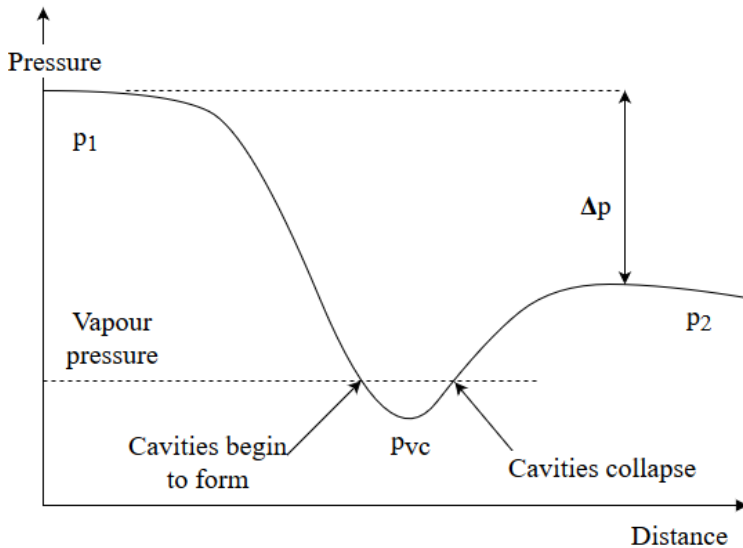


Figure 15: Cavitation.

*Flashing* is a vaporising process similar to cavitation. However, flashing differs from cavitation in that the vapour phase persists and continues downstream of the valve. For this to happen, the static pressure after the pressure recovery region must be at or below the vapour pressure as illustrated in Figure 16. (Borden and Friedmann, 1998, p 211-212).

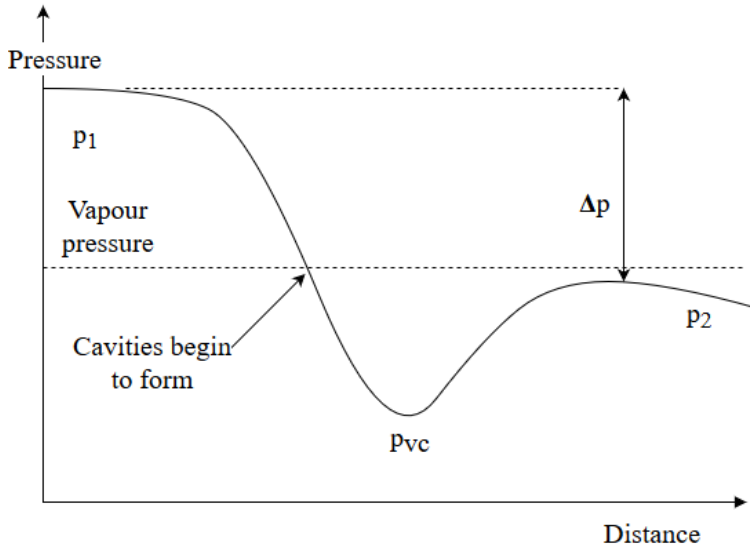


Figure 16: Flashing.

### 3.5 Single-Phase Valve Performance Prediction Models

The concept of  $C_v$  was developed years ago by valve manufacturers.  $C_v$  is a flow coefficient which relates to the geometry of a given valve for a given valve opening position.  $C_v$  is numerically equal to the number of U.S. gallons of water at 60°F that will flow through the valve in one minute when the pressure differential across the valve is one pound per square inch (Fisher Controls, 2017, p 16). This is not a normal situation in practice, but it provides a systematic way of comparing one valve characteristic to another. The size of a control valve is dependent on the maximum flow through the valve (Diener and Schmidt, 2005). Consequently, the flow coefficient plays an important role when selecting and purchasing valves.

The flow coefficient varies with both size and style of the valve but provides an index for comparing capacities of different valves under a standard set of conditions. The general flow coefficient equation is given by Equation (7). However, the equation needs modifications depending on the fluid and flow properties. It should be noted that the equations in this subsection are



only valid for single-phase flow.

$$Q = C_v \sqrt{\frac{\Delta p}{SG}} \quad (7)$$

The specific gravity (SG) is the ratio of density between a substance and a reference substance and is defined by Equation (8). For liquids, the reference is almost always water at its densest (4°C). For gases, the reference substance is almost always air at room temperature (25°C).

$$SG = \frac{\rho}{\rho_{ref}} \quad (8)$$

$K_v$  is an alternative SI system flow coefficient. The relationship between these two coefficients are shown in Equation (9).

$$K_v = 0.865C_v \quad (9)$$

The numerical constants in the equations below allow the input parameters to be specified in SI units ( $m^3/h$ , bar, K, kg), but still the equations yield the flow coefficient in the unit which it is defined .

### 3.5.1 Incompressible Fluids

The IEC 60534-2-1 Standard (IEC, 2011) presents flow capacity equations for incompressible fluids, such as liquids. When a fluid is incompressible the density is assumed constant. Equation (10) determines the flow rate of a liquid through a valve under turbulent, non-vaporising flow conditions. The equation assumes no cavitation or flashing through the valve. The IEC standard also specifies that the equations for incompressible flow are not to be applied for non-Newtonian fluids, fluid mixtures, multi-phase mixtures, slurries or for liquid-solid systems.

$$C_v = \frac{Q}{0.865F_p} \sqrt{\frac{SG_l}{p_1 - p_2}} \quad (10)$$

The piping geometry factor ( $F_p$ ) is equal to 1 when the valve size and the adjoining pipe sizes are identical.  $SG_l$  represents the specific gravity of the liquid.

### 3.5.2 Compressible Fluids

The IEC standard (IEC, 2011) also presents sizing equations for compressible fluids in the turbulent flow regime. Equation (11) establishes the relationship between the flow rate, flow coefficient, fluid properties, installed

factors and conditions for control valves handling a gas or vapour. Equation (11) is derived using the gas law (Equation (2)) and the fundamental model for compressible fluids in the turbulent flow regime (IEC, 2011).

$$C_v = \frac{Q}{417F_p p_1 Y} \sqrt{\frac{SG_g T_1 Z}{x}} \quad (11)$$

$SG_g$  is the specific gravity of the gas. The parameter  $F_p$  represents the piping geometry factor as explained in Section 3.5.1. The ratio of pressure differential to inlet pressure is defined by Equation (12).

$$x = \frac{p_1 - p_2}{p_1} \quad (12)$$

The expansion factor ( $Y$ ) accounts for the change in density of the fluid as it transports from the valve inlet to the vena contracta. It also accounts for the change in area of the vena contracta as the pressure drop is varied. The expansion factor is defined in Equation (13).

$$Y = 1 - \frac{x}{3F_\gamma x_T} \quad (13)$$

In theory the expansion factor is affected by the following parameters:

1. Ratio of the flow control orifice area to body inlet area.
2. Internal geometry of the valve.
3. Pressure drop ratio ( $x$ ).
4. Reynolds number.
5. Ratio of specific heats ( $\gamma$ ).

The factor  $F_\gamma$  accounts for the effect of the ratio of specific heats for compressible fluids.  $F_\gamma$  has the value of 1 for air at moderate temperatures and pressures.

$$F_\gamma = \frac{\gamma}{1.4} \quad (14)$$

The pressure differential ratio factor ( $x_T$ ) accounts for parameters 1-3 and can be found by Equation (15). All parameters in Equation (15) are at choked condition. (IEC, 2015)

$$x_T = \left[ \frac{Q_{max}}{0.667C_v 2250p_1} \right]^2 \left[ \frac{MWT_1 Z}{F_\gamma} \right] \quad (15)$$

### 3.6 Multi-Phase Valve Performance Prediction Models

The IEC 60534-2-1 Standard is primarily applied to calculate the performance of single-phase flow in the form of liquid or gas as described in Section 3.5.1 and 3.5.2. Any limitations in mass flow capacity attributed to cavitation and flashing of liquid are considered by empirically developed correction factors. If two-phase mixtures are to be considered at the inlet of the valve these standards are no longer applicable (Diener and Schmidt, 2005; Diener et al., 2005; Darby et al., 2001). In these cases, plant operators and manufacturers use various methods for predicting the flow through the valve according to own experience. Consequently, this leads to different, incomparable results depending on fluid properties and operating conditions. (Diener et al., 2005).

The most common valve prediction model for two-phase flow in the industry is the Addition model. It is a simple model that deals with each phase separately using the equations in the IEC 60534-2-1 Standard. The flow coefficient for single-phase gas and single-phase liquid are added as a weighted average leaving an overall flow coefficient (Diener and Schmidt, 2005). No heat, momentum or mass transfer is considered in this model. Therefore, this method may lead to highly over- or underestimations (Diener and Schmidt, 2005). The Addition method is presented in Equation (16).

$$C_v = \alpha \frac{Q}{417F_p p_1 Y} \sqrt{\frac{SG_g T_1 Z}{x}} + (1 - \alpha) \frac{Q}{0.865F_p} \sqrt{\frac{SG_l}{p_1 - p_2}} \quad (16)$$

Sheldon and Schuder (1965) proposed a correction factor to correct for the over- or underestimations. The factor was based on the volume fraction of the phases at the valve inlet. Nevertheless, the model still gives inaccurate results for boiling liquids and mixtures of flashing liquids and vapours.

Two main types of prediction models exist: The Homogeneous Equilibrium Model (HEM) and the Homogeneous Non-Equilibrium model (HNE). Both models assume that the two-phase flow is homogeneously mixed and that the fluid can be described as a "pseudo-single phase" fluid obeying the laws of single-phase flow with properties that are weighted averages of each phase (Darby et al., 2001).

#### 3.6.1 Homogeneous Equilibrium Models

The homogeneous equilibrium model is the simplest method for analysing two-phase flow. This model assumes that the phases are in both thermody-

namic and mechanical equilibrium, i.e. they have equal pressures, temperatures and velocities. Any phase change occurs under equilibrium conditions at saturation pressure and the phases are assumed uniformly distributed over the flow cross-section. These conditions are only true for spray or wet vapour having only small droplets of liquid in the vapour (Diener and Schmidt, 2005). The advantage of the HEM is that the compressibility coefficient is only dependent on inlet property data which is generally available in the industry (Schmidt and Egan, 2009). Various models are based on the HEM, amongst them is the most common “omega-model” developed by Leung (1986). In the omega-model, the density is represented as a linear function of the pressure and the thermal/physical properties of the fluid at stagnation state (Darby et al., 2001). The model is primarily used for mixtures with low gas fractions. However, Diener and Schmidt (2005) argued that the model provides acceptable results for higher fractions because acceleration in the valve mixes the phases thoroughly and the flow can be seen on as largely homogeneously distributed. Diener and Schmidt (2005) accentuated the uncertainties of the omega-model when mixtures of steam and boiling water are passed through control valves. However, Darby et al. (2001) argued that the HEM is adequate in most cases for two-phase flow through long nozzles and pipes, for both non-flashing and flashing flow.

### 3.6.2 Homogeneous Non-Equilibrium Models

In contrast, the homogeneous non-equilibrium models consider both thermodynamic and mechanical non-equilibrium of the flow. Mechanical non-equilibrium or *slip* occurs as a result of an expansion of gas. It is a phenomenon where the gas accelerates relative to the liquid, resulting in a velocity difference and a corresponding drag force between the phases. Slip is expected to be most pronounced when the pressure gradient is large, such as in the entrance section of a nozzle or valve. (Darby et al., 2001)

Diener et al. (2005) developed a model that considers these non-equilibrium effects of the flow. The Homogeneous Non-Equilibrium-Diener/Schmidt (HNE-DS) model considers how the mixture density flowing through the valve affects the flow capacity. The model is an extension of the HNE model including a boiling delay coefficient to account for the delayed boiling of the liquid in the valve (Diener and Schmidt, 2005). The most difficult physical situation to account for in the models is when the fluid entering the valve is either saturated liquid, liquid just above the saturation pressure or a two-phase saturated mixture with low gas content (Darby et al., 2001). In these cases, extensive flashing is likely to occur. The formation of cavities is usually a fast process, but the high velocity experienced in the valve may

result in significant fluid travel before the flashing is complete. This scenario is called delayed boiling. Diener and Schmidt (2005) pin-pointed that the HNE-DS method can be applied equally to various throttling devices including orifices, control valves and safety relief valves. Diener et al. (2005) showed that for mixtures of steam and boiling water the HNE-DS method is more accurate than the previous mentioned methods.

Other more complex models based on more accurate physical assumptions exist. These depend on extended property data including densities, enthalpies and entropies which are rarely available in the industry. Additionally, iterative solutions of the mathematical equations are necessary. (Diener et al., 2005) Consequently, such models are not discussed in this thesis.

### **3.6.3 Conclusion**

To sum up, various models for predicting the flow through valves exist. To limit the scope, only a selection is presented in this subsection. Each model has a set of assumptions making the model valid for certain specific conditions and less accurate for other conditions. Consequently, there is no "best" method, each case must be evaluated individually to choose the right method. If there are reasons to suspect flashing or boiling liquid through the valve, models such as the HNE-DS or omega-model should be used. In the NTNU test facility the pressure differentials are low and the working fluid is a mixture of air and water at high gas fractions. For these reasons, the risk of cavitation and flashing is considered minimal. Additionally, there is not much probability of boiling. Consequently, the valve performance calculation procedure used in this thesis is the Addition model.

### 3.7 Summary

In this section the fundamental theory of control valves was introduced. Various methods for calculating valve performance was discussed. It was concluded to use the Addition method for valve performance calculations in this thesis. Table 1 summarises how valve opening affects valve performance.

Table 1: How valve opening affects valve performance parameters.

Cause	Effect on valve
Decreased valve opening	Increased velocity at vena contracta Decreased pressure at vena contracta Increased inlet pressure Increased pressure differential
Increased valve opening	Decreased velocity at vena contracta Increased pressure at vena contracta Decreased inlet pressure Decreased pressure differential

## 4 Compressors and System Resistance

A compressor or valve seldom operate alone but are integrated into a bigger system or process. Consequently, it is important to have knowledge of how the various components affect each other. This section explains what a system resistance curve is and how it affects the compressor operating point with emphasis on compressor discharge throttling. This section only includes dry gas effects.

### 4.1 System Resistance Curve

The system resistance curve is based on losses in the system the compressor is a part of (Forsthoffer, 2006). These losses are associated with pressure drop due to friction, bends and large piping lengths in e.g. piping, valves or other equipment surrounding the compressor (Forsthoffer, 2006). Figure 17 illustrates a compressor map with an additional system resistance curve. The compressor operating point is determined by the intersection between the compressor characteristic curve and the system resistance curve. This is because the compressor and the system resistance interact to drive the flow to a point of equilibrium (Forsthoffer, 2006).

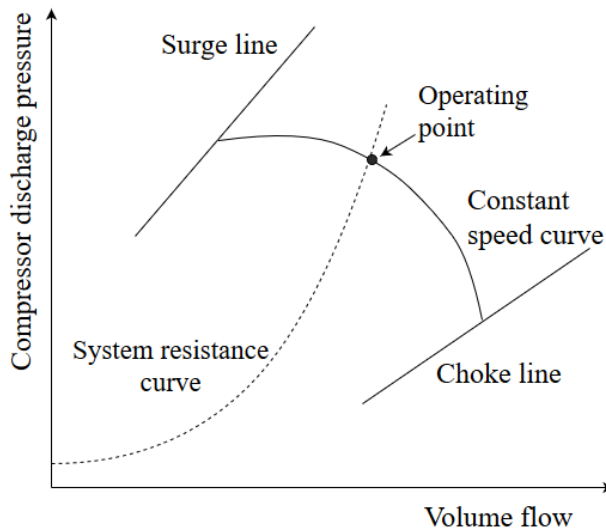


Figure 17: System resistance curve.

### 4.2 Compressor Discharge Throttling

There are various methods for controlling the compressor's operational point. Several of these methods were discussed in the author's project thesis (Dolve,

2017). In this thesis, only one of them will be discussed in detail, namely; discharge throttling.

Compressor discharge throttling is a control method where a valve is placed downstream the compressor as illustrated in Figure 18. To explain the concept of discharge throttling and to disclose how the discharge valve can affect the compressor performance, one must combine the theory of compressors (Section 2) and control valves (Section 3).

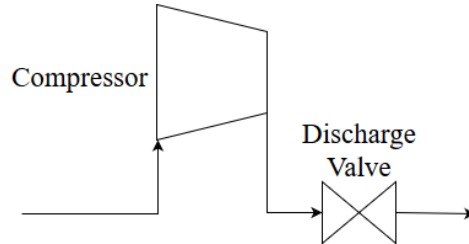


Figure 18: Simple illustration of discharge throttling.

Suppose that the compressor operates at point A in Figure 19. At this point the valve has a given opening. When the compressor operates at a constant speed, the operational point must follow the constant speed curve. If the valve opening is reduced the valve inlet pressure will increase and thus the compressor discharge pressure will increase. The volume flow through both the compressor and the valve will decrease. Consequently, the operating point will move to the left towards e.g. point C and a new system resistance curve is generated. A new curve is generated because the change in valve opening alters the pressure drop in the system. If the compressor inlet pressure is kept relatively constant the decreased valve opening will result in an increased compressor polytropic head. This can be seen using Equation (30) from Appendix D.

Likewise, if the valve opening is increased the operating point will move to the right towards e.g. point B and a different system curve is generated. This is the result of a decrease in valve inlet pressure and thus a decrease in compressor discharge pressure. Subsequently, the compressor polytropic head will decrease. HYSYS simulations from the author's project thesis also confirm these effects of varying the valve opening (Dolve, 2017).



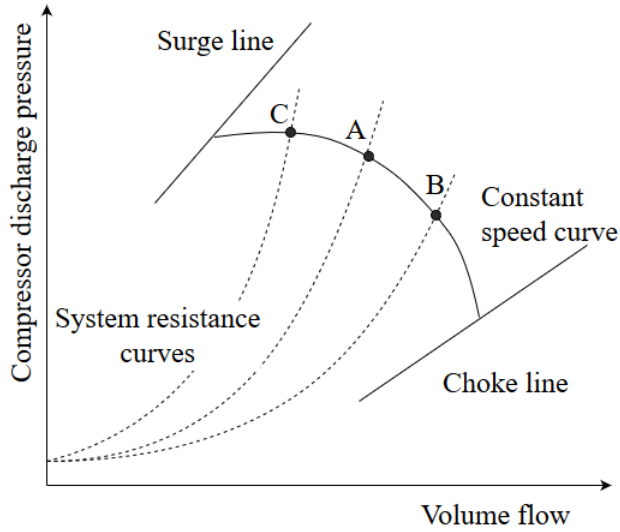


Figure 19: How change in discharge valve opening affects the compressor performance at constant compressor speed.

Other factors may also affect and alter the system resistance curve and consequently the compressor's operational point. Slight changes in inlet parameters contribute to changes in density which alter the friction drop in the surrounding equipment (Forsthoffer, 2006). A given system resistance curve will change when composition, pressure, temperature and/or velocity change (Forsthoffer, 2006). Changes in inlet conditions will also alter the discharge pressure along the entire curve. Together with supervisor it was decided to not discuss this further as discharge throttling is the focus of this thesis. However, the impact of wet gas on discharge throttling will be discussed later in the thesis.

### 4.3 Summary

This section explained how the discharge valve can be used to alter the compressor's operational point for dry gas. The effects of discharge throttling are summarised in Table 2.

Table 2: Effects of dry gas discharge throttling at constant compressor speed (Dolve, 2017).

Cause	Effect
Reduced valve opening	Decreased volume flow Increased valve inlet pressure Increased valve differential pressure Increased compressor differential pressure Increased compressor discharge pressure Increased compressor polytropic head
Increased valve opening	Increased volume flow Decreased valve inlet pressure Decreased valve differential pressure Decreased compressor differential pressure Decreased compressor discharge pressure Decreased compressor polytropic head

## 5 NTNU Wet Gas Compression Lab

In this section, a presentation of the NTNU compressor test facility is given. All experiments done in relation to this thesis were conducted in this facility. First, a general explanation of the facility is given. Then, the instrumentation and equipment considered most essential for this thesis are presented in detail.

### 5.1 General Explanation of the Lab

The lab was developed to identify the fundamental mechanisms related to wet gas compression and was installed in 2006 at NTNU (Hundseid and Bakken, 2015). Since then, modifications have been made, resulting in a module-based lab with the possibility of testing various designs for the various components. The facility is used both for academic purposes and industry related research. Figure 20 is a simplified overview of the open-loop installation.

The working mediums are water and air and the suction condition is atmospheric. Water and air can either be mixed upstream the compressor through the injection module or downstream the compressor through the pulse valve. The water injection module consists of 16 nozzles distributed around the pipe wall. The nozzle size can be varied to give different droplet sizes. (Hundseid and Bakken, 2015)

The lab is equipped with both a suction and a discharge valve. The valves are coupled to a hydraulic actuator system making it possible for the valves to respond fast and with high accuracy. Observation slots have been installed at the impeller and diffuser section. These slots can give valuable insight into the fundamentals of wet gas compression. The slots are illustrated with the "plexiglas" module in Figure 20. Downstream of the discharge valve, water and air are separated. (Hundseid and Bakken, 2015)

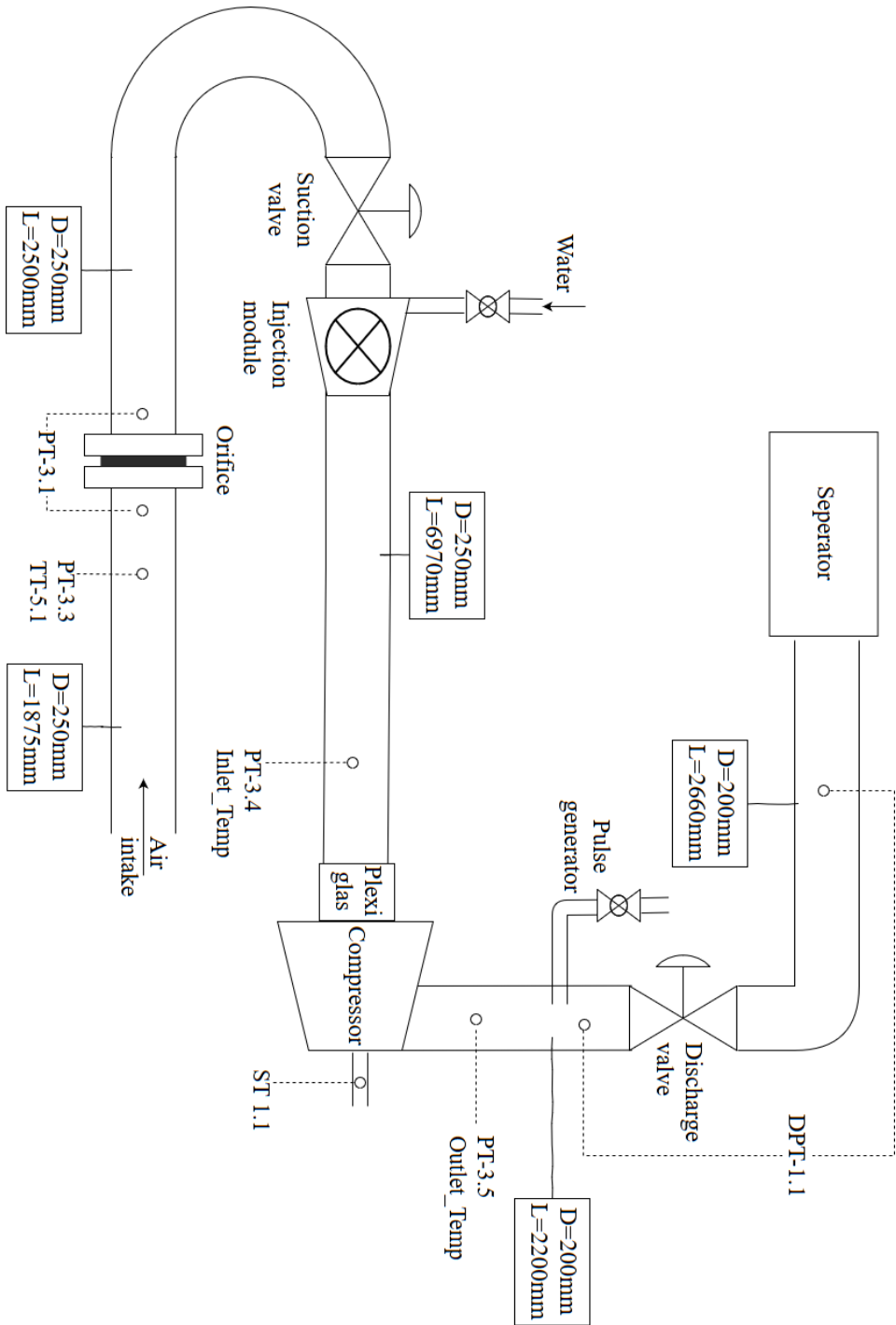


Figure 20: Simple illustration of NTNU wet gas compressor test facility.

## 5.2 Sensors and Instrumentation

The lab is instrumented with various transmitters as shown in Figure 20. There are seven different transmitters:

- Differential pressure transmitter (DPT)
- Flow transmitter (FT)
- Humidity transmitter (HT)
- Pressure transmitter (PT)
- Speed transmitter (ST)
- Torque transmitter (TM)
- Temperature transmitter (TT)

These transmitters allow for pressure, temperature and flow to be measured several places in the system. Likewise, the torque and speed are measured at the compressor shaft. The measured parameters are all sampled by the control system, facilitating accurate measurements of performance parameters. The acquisition system for the lab is the National Instruments PXI solution, which permits synchronous sampling up to 20kHz (Hundseid and Bakken, 2015). Figure 20 only displays the most essential transmitters used for this thesis' performance calculations. Overall piping lengths and diameters are included, but exact sensor locations are displayed later in the thesis in appropriate sections. See Appendix G Table 9 for explanation of the various sensors' names.

## 5.3 Equipment Specifications

The instrumentation is in accordance with ASME PTC-10 Standard for compressors and exhausters. (Hundseid and Bakken, 2015)

### 5.3.1 Compressor

The lab is equipped with a full-scale low-pressure ratio single-stage centrifugal compressor including a vaneless diffuser and a symmetric circular volute that delivers the flow to the discharge pipe. The compressor section is module-based, which allows for testing of different impeller and diffuser designs. The compressor is driven by a high-speed electrical motor with a maximum speed of 11000 rpm. The motor is connected to an advanced controlling system which makes it possible to monitor the performance of

the compressor. The variable speed drive is delivered by ABB. The compressor inlet and outlet pipe diameter is respectively 250 mm and 200 mm. (Hundseid and Bakken, 2015) The experiments conducted in relation to this thesis used the compressor rig configurations described in Table 3.

Table 3: NTNU compressor rig configurations.

Component	Specification
Impeller	NWI
Diffuser	-3
Inducer	Long

### 5.3.2 Discharge Valve

The compressor discharge valve is a Fisher V-ball V150 valve, which is a type of rotary valve where the closure member is a segment of a sphere. The segment is V-shaped and has a travel course of 90 degrees. All details of the discharge valve are given in Table 4. The valve and the actuator are displayed in Figure 21.

Table 4: NTNU discharge valve rig details.

Manufacturer	Emerson
Valve size NPS	8 inches
Valve size DN	200 mm
Characteristic	Equal percentage
Cv	1820
Type	Fisher V150
Travel Course	90 degrees
Flow	Forward (FTO)



Figure 21: Compressor discharge valve at the NTNU wet gas compression test rig.

### Valve Characteristics

As seen from Table 4 the valve is classified with an equal percentage characteristic and a maximum flow coefficient of 1820. It was desirable to have the entire inherent valve characteristic as a baseline to compare with results from the test campaign. Consequently, contact was made with the valve manufacturer: Emerson. Emerson provided the characteristics for V150 Fisher valve for two flow coefficients: 1820 and 1750. The data received from Emerson can be found in Appendix F. Emerson contributed with a detailed valve sizing calculation for single-phase water and air for the flow coefficient 1750. These calculations revealed that single-phase air and water have the same characteristic. However, the valve in the lab has a flow coefficient of 1820 and the correct inherent characteristic is given in Table 8 in Appendix F. These are the parameters used further in this thesis. Figure 22 demonstrates the inherent flow coefficient characteristic of the valve in the lab.

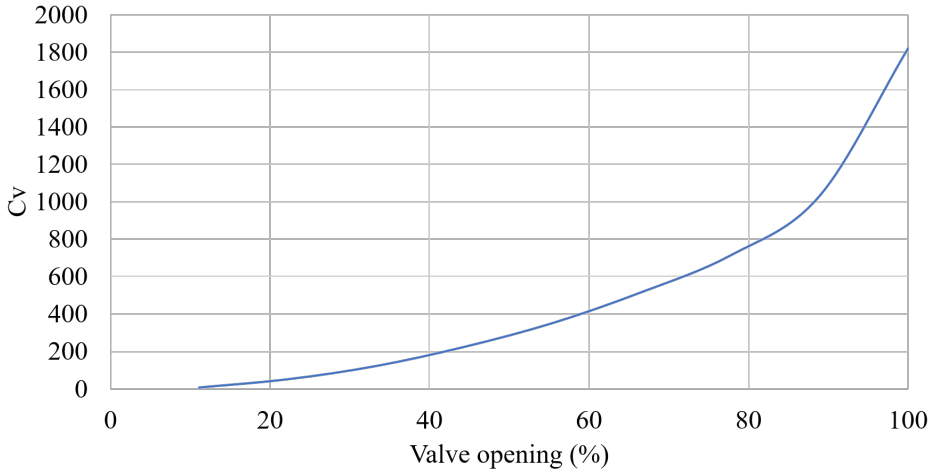


Figure 22:  $C_v$  1820 V150 NPS 8 Fisher inherent valve characteristic for single-phase water and air.

### Valve Orientation

It is possible to change the orientation of the valves in the lab. The original orientation of the discharge valve is shown in Figure 23(a). Due to water accumulation in front of the discharge valve it was proposed to rotate the valve 90 degrees, as shown in Figure 23(b). The segmented part of the valve was facing downwards inhibiting water accumulation. This orientation was used in all the experiments conducted in relation to this thesis. Figure 24 shows how the water accumulated in front of the valve before the rotation.

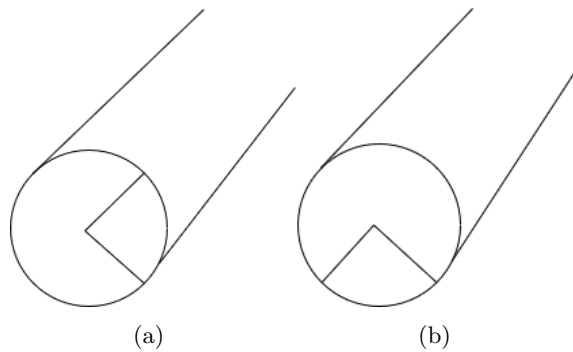


Figure 23: Different valve orientations.



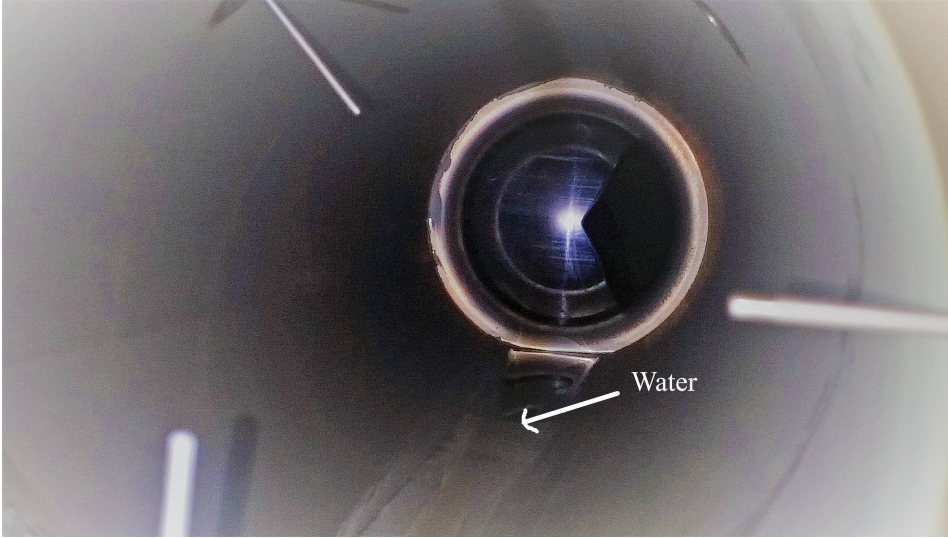


Figure 24: Accumulation of water in front of valve at the NTNU wet gas compression lab.

### **Differential Pressure Measurement**

Both dry and wet gas tests were performed already in February 2018 as seen from the research log in Appendix B. However, the measured pressure differentials across the discharge valve were highly fluctuating. The in-percentage pressure deviations were high, especially for high valve openings where the deviations in some cases came above 100 %. Due to the unstable test results, an investigation of appropriate pressure tap locations for the differential pressure measurement device was conducted. The investigation revealed that the pressure taps were not in accordance with the IEC 60534-2-3 Standard for test procedures for industrial process control valves (IEC, 2015). The original pressure taps were located too close to the valve inlet and outlet, leaving the taps vulnerable to turbulent flow. As explained in Section 3.2 increased velocity is followed by reduced pressure. Hence, the location of the pressure taps should be a specific number of straight pipe diameters upstream and downstream of the valve (IEC, 2015). This is to assure a stable flow through the taps reducing the risk of large pressure fluctuations.

The IEC 60534-2-3 Standard proposed that the upstream pressure tap should be located 2 pipe diameters upstream of the valve inlet and that the downstream pressure tap should be located 6 pipe diameters downstream of the valve outlet. The standard also pin-pointed the importance of *straight* pipe diameters. Bends may also contribute to turbulence, consequently the

downstream pressure tap should be located 6 pipe diameters downstream of the bend. Figure 25 illustrates the appropriate pressure tap locations according to the IEC 60534-2-3 Standard.

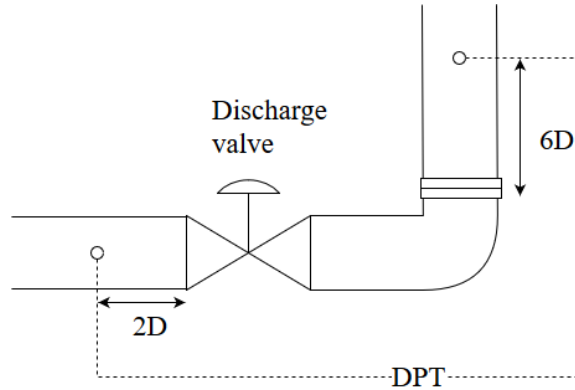


Figure 25: Appropriate pressure tap locations (IEC, 2015).

As a part of this thesis, modifications were done to approach the set-up in Figure 25. Together with supervisor it was decided that the upstream pressure tap should be kept. This was because there was already a pressure sensor installed further upstream the valve (See Figure 20) that could be used as a substitute. The downstream pressure tap was moved 1320 mm downstream of the bend. The new pressure tap location was not exactly in accordance with the IEC 60534-2-3 Standard, but together with the supervisor the location was assumed to be good enough for more stable results. Comparison of tests conducted before and after the modification confirmed this assumption.

### 5.3.3 Flow Measurement Device and Calculations

The air inlet flow was measured with an orifice plate 1875 mm downstream the air intake. The orifice is a circular metal plate having a pointed hole at the centre, such that the sharp edge of the hole faces upstream. A simple illustration of an orifice is given in Figure 26.

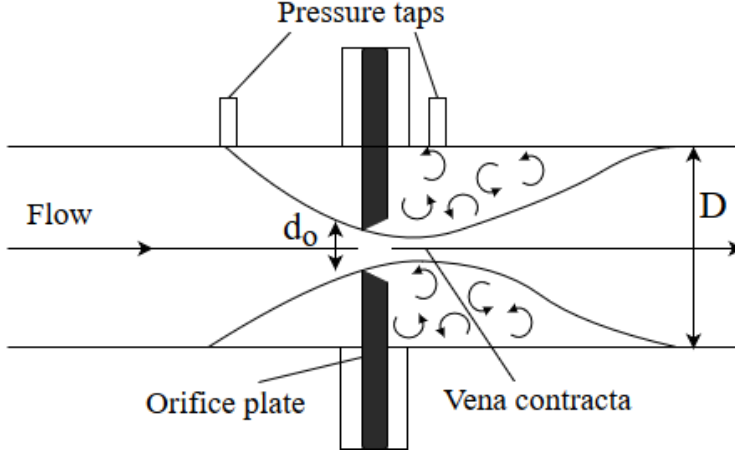


Figure 26: Simple illustration of an orifice plate.

The change in cross section is abrupt and consequently the pressure drops suddenly. The orifice acts similar to a valve and so the pressure-velocity relationship is the same as discussed in Section 3.2. The vena contracta is formed a little distance away from the orifice. Two pressure taps are installed to measure the differential pressure across the valve. Orifices are classified by the *beta ratio*. The value is defined as the diameter of the orifice hole divided by the pipe's internal diameter. (Kaleem, 2015)

$$\beta = \frac{d_o}{D} \quad (17)$$

A large beta ratio represents an orifice with a large hole, and consequently a smaller pressure drop. Likewise, a small beta ratio means a larger pressure drop. The beta ratio of the plate in the lab is 0.64.

Figure 27 is a simple illustration of the air inlet section of the NTNU compression lab. Based on the orifice differential pressure (PT-3.1), inlet temperature (TT-5.1) and inlet pressure (PT-3.3) the flow can be calculated. The orifice inlet density is also calculated based on the same parameters using Equation (2). The air mass flow rate is determined using Equation (18) which is in accordance with the ISO 5167-2 Standard for fluid flow measurements through orifice plates (ISO, 2003).

$$\dot{m} = \frac{C}{\sqrt{1 - \beta^4}} \epsilon \frac{\pi}{4} d_o^2 \sqrt{2 \Delta p_o \rho_{1,o}} \quad (18)$$

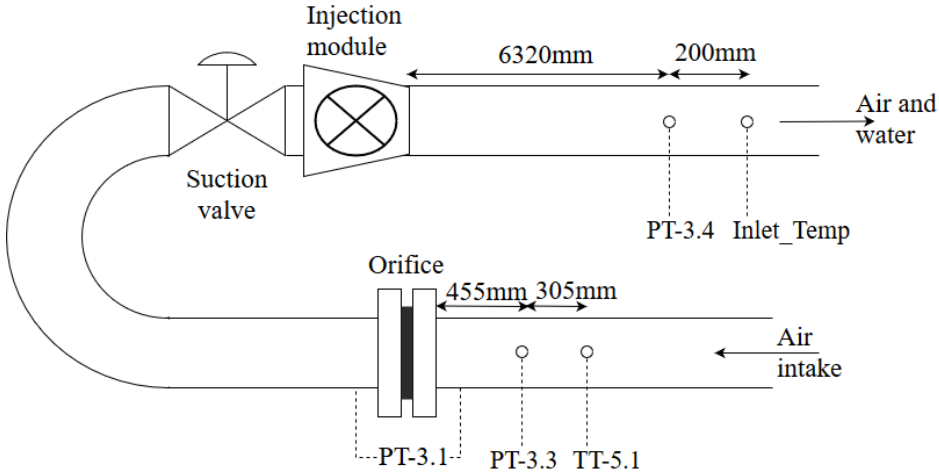


Figure 27: Illustration of the inlet section at the NTNU wet gas compression lab.

$C$  is the coefficient of discharge which is dependent of the Reynolds number and the mass flow itself. Consequently, the discharge coefficient should, according to the ISO Standard, be determined by iteration to get the most accurate results. (ISO, 2003) However, such iterations are time demanding and the results without such iterations are considered accurate enough. As a result, the lab engineers have implemented a simplified calculation procedure in the NTNU lab's virtual workbench (LabVIEW). The method used for calculating the coefficient of discharge is given by Equation (19).

$$C = 0.5959 + 0.0312\beta^{2.1} - 0.184\beta^8 \quad (19)$$

The expansibility or expansion factor is an adjustment factor that considers the compressibility of the fluid. Equation (20) is used in the NTNU lab.

$$\epsilon = 1 - (0.351 + 0.256\beta^4) \frac{\Delta p_o}{\kappa p_{1,o}} \quad (20)$$

Baker (2016) pin-pointed new discoveries that showed errors in Equation (19) and (20). Additionally, the ISO 5167-2 Standard recommends a different calculation procedure for calculating the coefficient of discharge and the expansibility factor. Thus, there may be some inaccuracy in the calculations of the air inlet mass flow. The author suggests an upgrade of the orifice calculation procedure at the NTNU lab in accordance with the ISO Standard. However, no further investigation or modifications were done, as this is beyond the scope of this thesis.

When the mass flow and the density at the orifice are calculated, the volume flow can be determined using the relationship in Equation (21).

$$Q = \frac{\dot{m}}{\rho} \quad (21)$$

Volume flow varies with pressure, temperature and compressibility (Forsthofer, 2006, p. 104). Equation (21) was used to calculate the volume flow through the lab. The mass flow through the test facility was assumed constant. The density was recalculated for the various pressures and temperatures at desired locations in the lab.

## 5.4 Summary

In this section, an overview of the NTNU test facility was given. Details about the compressor, discharge valve and flow measurement device were discussed. The inherent characteristic of the discharge valve received from the valve manufacturer was presented. Additionally, a new differential pressure measurement device was installed across the discharge valve as a part of this thesis.



## 6 Experimental Campaign

This section reports the results obtained from an experimental test campaign conducted in the NTNU wet gas compression lab. A description of the test procedure and results are presented. The objective of this section is divided into 3 parts:

1. Comparison of dry gas valve performance data collected in the NTNU lab with data from the valve manufacturer.
2. Investigation of the difference between injecting water upstream and downstream of the compressor.
3. Comparison of valve performance parameters for dry and wet condition.

### 6.1 Experimental Set-Ups

Two experimental set-ups were used in the test campaign. Figure 28 illustrates the experimental set-up for injecting water *upstream* of the compressor. This set-up will be called set-up 1 through the thesis. Water and air were mixed in the injection module before entering the compressor. The injection module was placed 6970 mm upstream of the compressor. Figure 29 illustrates the experimental set-up for injecting water *downstream* of the compressor. This set-up will be called set-up 2 through the thesis. In set-up 2, water and compressed air were mixed in the pipe downstream of the compressor. Only air travelled through the compressor. The water was injected through a valve already installed in the lab, with the original purpose of generating pulses. The water injection occurred 660 mm upstream of the discharge valve.

The main difference between the two set-ups was obviously the placement of the water injection device. Additionally, the injection methods were different. In set-up 1 the injection module consisted of a set of nozzles that allowed for uniformly spraying of liquid droplets in the same direction as the airflow. However, Section 2.4.1 explained that the injection method does not affect the compressor performance and consequently not the valve inlet conditions. In set-up 2 water was injected as a single spray through the pulse valve. Because of the placement of the pulse valve the water was sprayed in the opposite direction of the air flow. This may have led to a blockage of liquid affecting the flow through the valve. No further investigation of the flow regime was done in relation to this thesis. However, if further work is to be conducted, an investigation of the flow behaviour downstream the

compressor is suggested. A proposal is to install observation slots and explore how various water injection methods and flow regimes affect the valve performance.

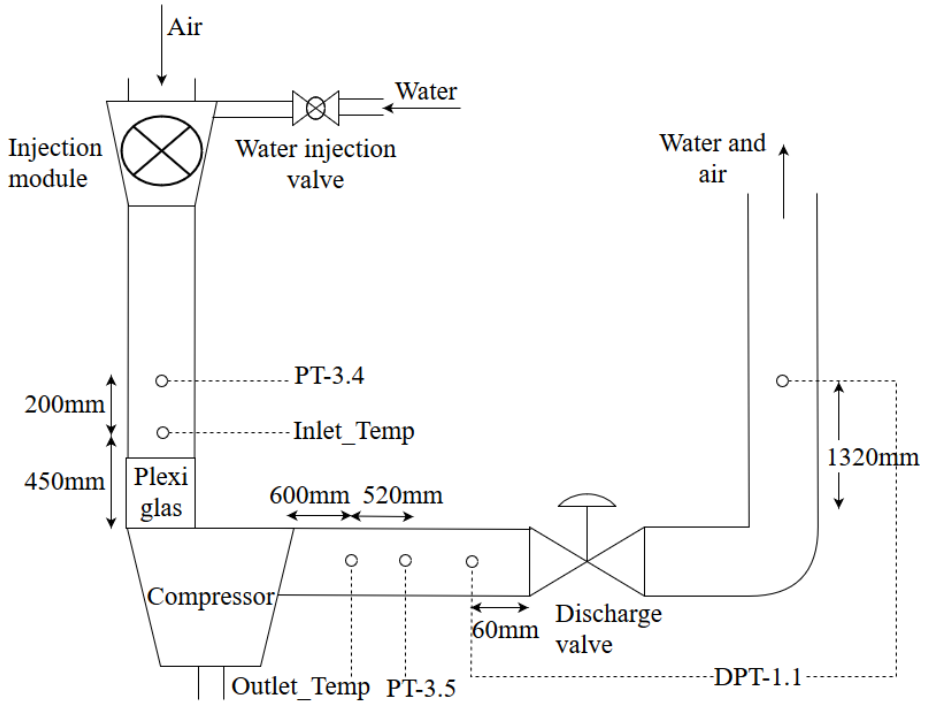


Figure 28: Experimental set-up 1: Water injection upstream of compressor.

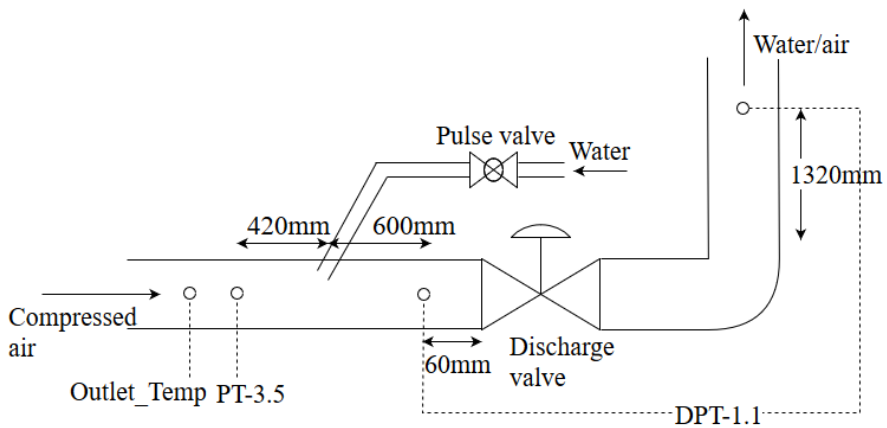


Figure 29: Experimental set-up 2: Water injection downstream of compressor.



The reason for testing two experimental set-ups was to document how sensitive the valve performance parameters, especially the flow coefficient, were to changes in inlet conditions. A comparison of the results from the two set-ups may provide valuable insight into how the upstream compression affects the valve performance. Additionally, in real process systems, various pipelines containing various fluids often unite at some point in the process. The fluids intertwining can be at different temperatures and pressures, similarly as the fluids in set-up 2. Consequently, set-up 2 is a realistic scenario because a process valve is at risk of facing various fluids with various inlet conditions.

## 6.2 Purpose of Test

There were 4 main purposes of conducting the experimental campaign:

1. Establish dry gas baseline curves and compare them with data from valve manufacturer to document the transition from inherent to installed condition.
2. Compare dry gas baseline performance curves with wet gas curves.
3. Investigate the effect of injecting water upstream and downstream of the compressor on valve performance parameters.
4. Document potential changes in system resistance curve and compressor operational point when liquid is introduced.

## 6.3 Test Matrix

The test matrix for the experiments is shown in Table 5. The compressor speed was kept constant in all the tests. A speed of 9000 rpm was chosen because this is the compressor's design speed. The GMF was varied from 1 to 0.8 in order to see potential trends when decreasing the GMF. For each GMF, the valve opening was varied from 100 % to 30 %. To avoid entering the surge region, it was decided that 30 % was the minimum valve opening.

Table 5: Test matrix.

Speed	GMF	Valve opening	Set-up
9000 rpm	1	100%-30%	1
9000 rpm	0.95	100%-30%	1,2
9000 rpm	0.8	100%-30%	1,2

## 6.4 Test Procedure

1. Change to experimental set-up 1.
2. Follow the start-up procedure.
3. Accelerate to 9000 rpm.
4. At GMF 1, incrementally decrease the valve opening from 100 % to 30 %. (8 increments)
5. At GMF 0.95, incrementally decrease the valve opening from 100 % to 30 %. (8 increments)
6. At GMF 0.8, incrementally decrease the valve opening from 100 % to 30 %. (8 increments)
7. Change to experimental set-up 2.
8. Follow the start-up procedure.
9. Accelerate to 9000 rpm.
10. At GMF 0.95, incrementally decrease the valve opening from 100 % to 30 %. (8 increments)
11. At GMF 0.8, incrementally decrease the valve opening from 100 % to 30 %. (8 increments)

## 6.5 Results and Discussion

The test results from the lab experiments are presented tabulated in Appendix G. Calculated parameters based on the experiments are presented tabulated in Appendix H. The calculation procedure for the flow through the orifice was as discussed in Section 5.3.3. The Addition method was used to calculate the flow coefficient as discussed in Section 3.6. Due to limitations in the lab, the compressor was not able to deliver enough flow to measure the choked flow through the discharge valve. Consequently, the pressure differential ratio factor ( $x_T$ ) was assumed to be equal to the inherent data from Emerson in Table 8 in Appendix F. A complete research log is presented in Appendix B. A risk assessment in relation to the experiments was also conducted and is displayed in Appendix C. The modified pressure differential measurement set-up (See Section 5.3.2), gave more stable results with a maximum in-percentage deviation of 20 % for both dry and wet condition. The volume flow used in the figures below is the total volume flow.

### 6.5.1 Dry Gas Tests

A dry gas baseline flow coefficient performance curve was established to compare with the inherent characteristic from Emerson. Figure 30 displays the flow coefficients obtained from the experiment at the NTNU lab and the inherent coefficients collected from Emerson. A considerable increase in flow coefficients were observed when going from inherent to installed condition. The exception was at 100 % valve opening where the installed flow coefficient was lower than the inherent. Generally, the installed curve shifted upwards in relation to the inherent curve. For instance, at a valve opening of 70 % the coefficient increased with 21 % when going from inherent to installed condition. The most significant deviations were observed between the valve openings 80 % to 90 %. The results were consistent with the theory from Section 3.3 stating that the installed and inherent characteristics will deviate.

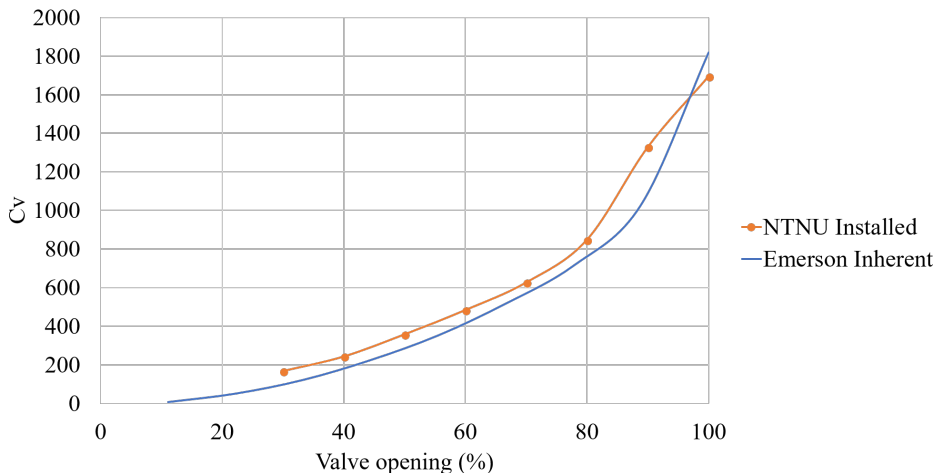


Figure 30: Comparison of dry gas flow coefficients ( $C_v$ ) for various valve openings at installed and inherent condition.

Figure 31 shows the characteristics of the relative flow coefficient for both installed and inherent condition. The installed curve had a valve pressure drop ratio ( $P_R$ ) of 0.5. Section 3.3 explained how the installed curve shifts towards a linear characteristic when the pressure drop ratio is reduced. The test results were in compliance with this theory as Figure 31 demonstrates. The installed characteristic lay above the inherent curve. The results clearly confirmed a shift towards a linear valve characteristic when comparing installed and inherent characteristics.

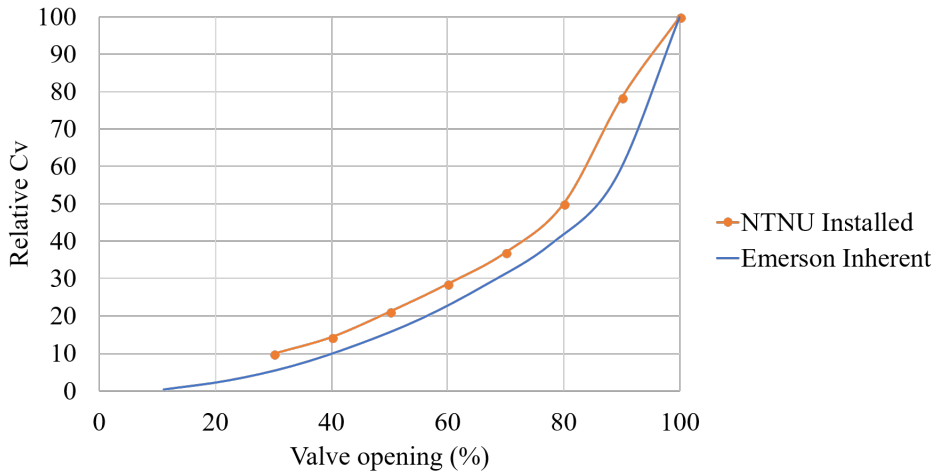


Figure 31: Comparison of dry gas relative flow coefficients ( $C_v$ ) for various valve openings at installed and inherent condition.

### 6.5.2 Wet Gas Tests

Curves marked with (1) represent results from set-up 1 and curves marked with (2) represents results from set-up 2. The dry gas baseline curves are included in the figures for comparison.

Figure 32 displays the temperature of the flow entering the discharge valve for various GMFs. A decrease in temperature was observed when liquid was introduced for both set-ups. The figure also demonstrates that the temperature was considerably lower for set-up 1 compared with set-up 2. This observation can be explained by a certain degree of liquid evaporation as the liquid passed through the compressor in set-up 1. A certain cooling effect was observed for set-up 2 as well because the hot compressed air was mixed with colder water. It should be mentioned that the temperature sensor was installed 1600 mm upstream of the pulse valve, as seen in Figure 29. Thus, the temperature may not be completely representative of the actual valve inlet temperature in set-up 2. It is possible that the valve inlet temperature was lower due to water cooling further downstream of the temperature sensor. Temperature changes could have an extended effect on other performance parameters. Thus, this should be investigated further for future work.

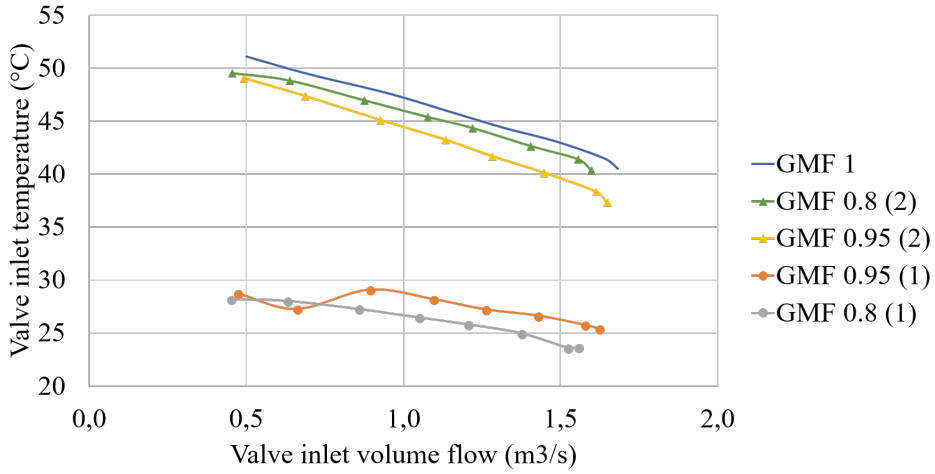


Figure 32: Valve inlet temperature curves for various GMFs in relation to volume flow (9000 rpm).

Figure 33 demonstrates how the total valve inlet density ( $\rho_{tot}$ ) varied with volume flow for various GMFs. The figure shows that the density increased when liquid was introduced. This was a result of decreased valve inlet temperature and increased molecular weight caused by the liquid presence. The densities from set-up 1 were clearly higher compared to set-up 2. This can be explained by the higher valve inlet temperature for set-up 2 resulting in a lower density.

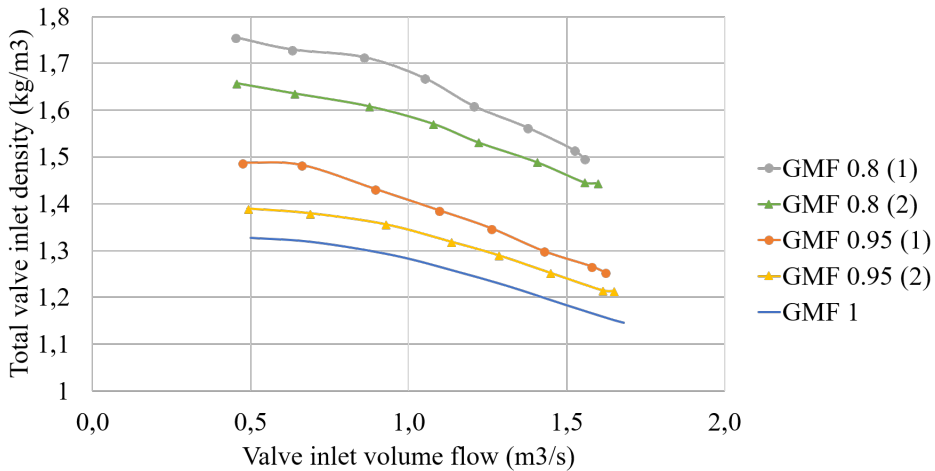


Figure 33: Total valve inlet density curves for various GMFs in relation to volume flow (9000 rpm).

A reduction in volume flow was observed when liquid was introduced. Figure 34 displays how the volume flow varied for the various GMFs. Section 2.4.1 explained how the presence of liquid could lead to increased blockage and consequently decreased volume flow through the compressor. The same principle can be used to explain the reduced flow through the valve. The volume flow for set-up 2 was lower compared to set-up 1. This applied to both GMF 0.95 and GMF 0.8. This can be explained by leakage or liquid evaporation through the compressor, resulting in less liquid blockage through the valve for set-up 1.

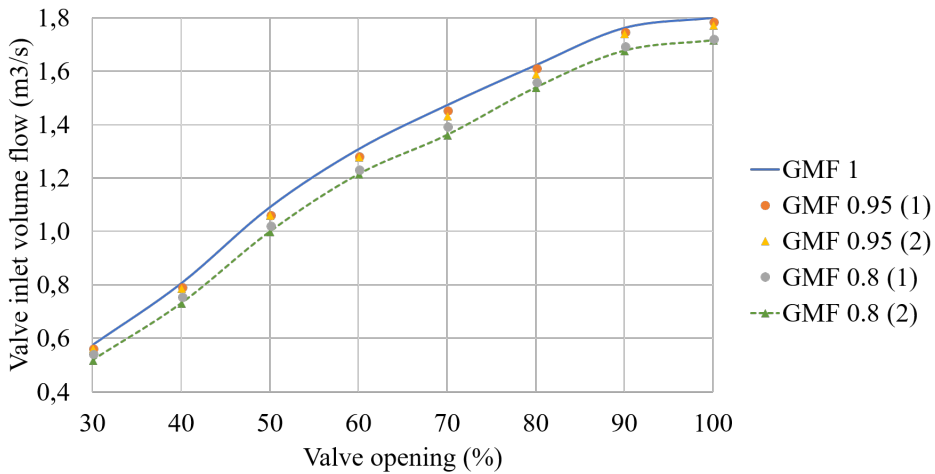


Figure 34: Valve inlet volume flow curves for various GMFs in relation to valve opening (9000 rpm).

Figure 35 demonstrates how the valve differential pressure changed in relation to valve opening for various GMFs. An increase in differential pressure was observed for each valve opening when liquid was introduced. For example, at a valve opening of 70 % the pressure differential increased with 14.2 % for set-up 2 when going from GMF 1 to 0.8. As mentioned, the introduction of liquid decreased the flow area through the valve due to liquid blockage. This will increase the throttling effect at each valve opening, resulting in an increased valve pressure differential. The increase in differential pressure was more pronounced at high valve openings.

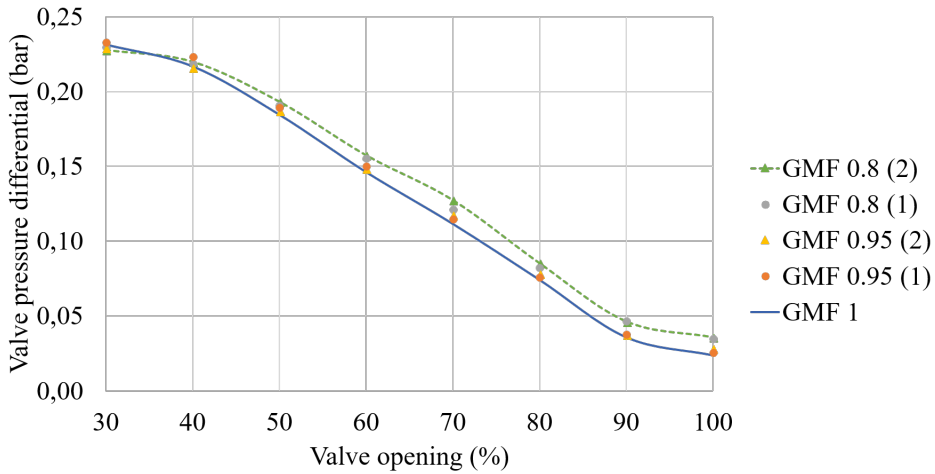


Figure 35: Valve differential pressure curves for various GMFs in relation to valve opening (9000 rpm).

Figure 36 shows how the valve differential pressure varied with volume flow for various GMFs. The figure displays that the differential pressure curve shifted to the left when the GMF was reduced. This can be explained by the reduction in volume flow discussed above. Figure 36 demonstrates that the shift was more pronounced at high volume flows.

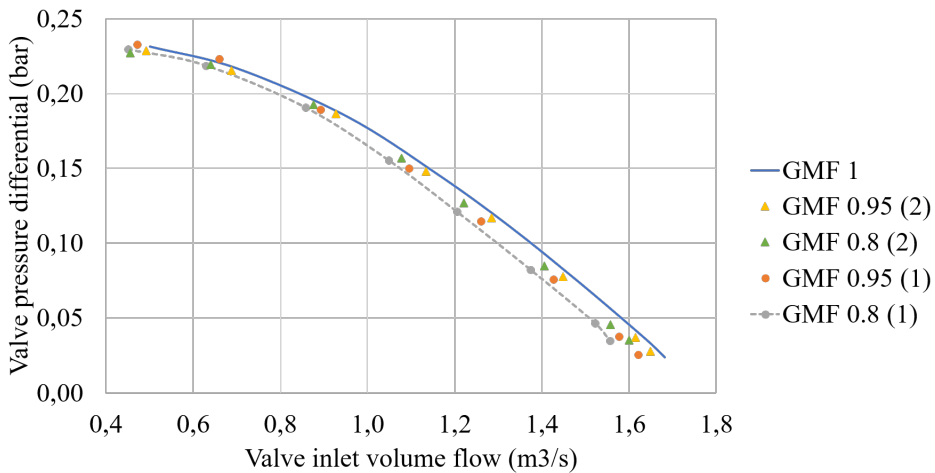


Figure 36: Valve differential pressure curves for various GMFs in relation to volume flow (9000 rpm).

Figure 37 demonstrates how the flow coefficient varied with valve opening

for various GMFs. The figure clearly shows a decrease in flow coefficient as the GMF was decreased. The wet gas curves for set-up 1 and set-up 2 were approximately identical, especially at low valve openings. Based on Figure 37, there is a reason to believe that the choice of set-up had an insignificant effect on the flow coefficient when using the Addition method. This was observed despite the temperature difference between set-up 1 and 2, which indicates that the temperature had a minor impact on the flow coefficient. Equation (16) shows that the changes in density and temperature equalises each other. Thus, it was likely the reduction in volume flow and the increase in pressure differential that resulted in the reduced flow coefficient. For instance, with set-up 1 and at the valve opening 70 %, the in-percentage deviation of the flow coefficient was 29.4 % when going from GMF 1 to GMF 0.8. By comparison, at the same conditions the volume flow was reduced with 9 % and the differential pressure increased with 8.7 %.

Additionally, the deviations from the dry gas baseline were significantly higher at high valve openings. This can be explained by the more pronounced increase in differential pressure for high valve openings. It should be mentioned that due to the low water content on a volume basis, the single-phase water flow coefficient generally contributed to approximately 1 % of the total flow coefficient.

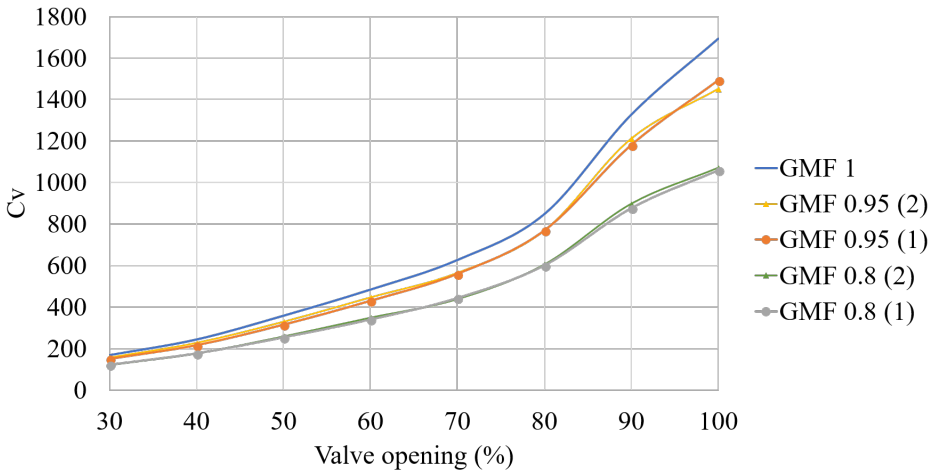


Figure 37: Flow coefficient curves for various GMFs (9000 rpm).

Figure 38 displays the variation in the relative flow coefficient for various GMFs. An increased relative flow coefficient was observed as the GMF was reduced. The figure shows that the characteristic shifted towards a linear characteristic when liquid was introduced. The valve pressure drop



ratio did not change when going from dry to wet condition for low valve openings. However, for high valve openings it varied between 0.42 to 0.5 in wet condition, as seen in Appendix H.

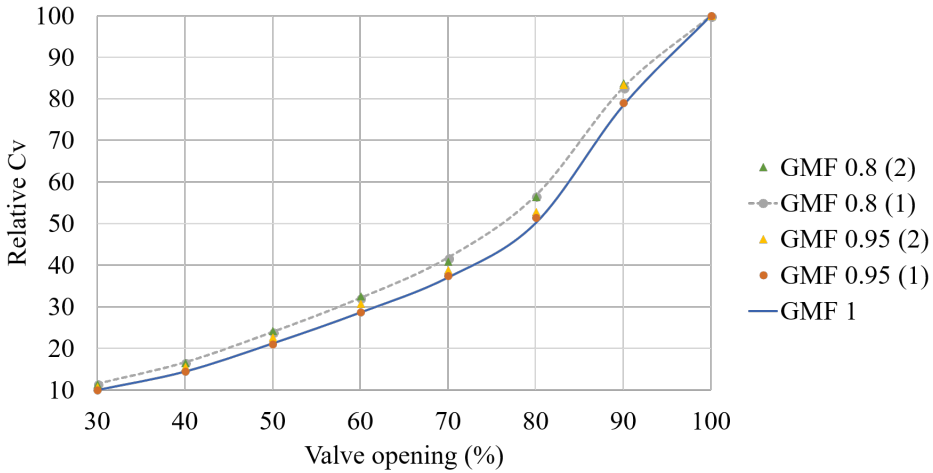


Figure 38: Relative flow coefficient curves for various GMFs (9000 rpm).

As mentioned in Section 3.5 and 3.6, various valve performance calculation procedures exist. Consequently, the author suggests comparing and exploring various valve performance calculation methods to see potential variations in flow coefficient and to evaluate the sensitivity of choice of calculation procedure. It is also possible to explore new correction procedures to account for wet gas effects. However, the accuracy of the addition method will not be discussed further in this thesis but should be considered if further work is to be conducted.

### 6.5.3 Operational Point and System Resistance Curve

As explained in Section 4 the system resistance curve change when the process conditions change. Section 4 did not discuss how the system resistance curve and operational point reacts to variations in GMF. Consequently, the results from the experimental campaign will be used to explain this.

Figure 39 displays the compressor discharge pressure curves for various GMFs. The dots represent the operational points at constant valve openings. The figure shows that the operational point shifts differently for high and low volume flows. Consequently, it was decided to “zoom-in” on the operational points at 40 % and 90 % valve opening to disclose any differences. For simplicity, the compressor discharge pressure curve from set-up

2 with GMF 0.8 is used to explain how the operational point shifts.

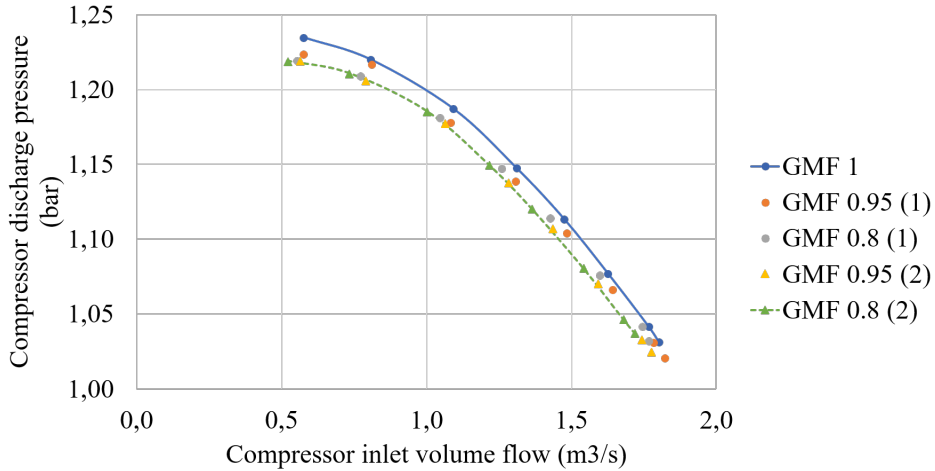


Figure 39: Compressor discharge pressure curves for various GMFs in relation to volume flow (9000 rpm).

Figure 40 demonstrates how the operational point shifted from dry to wet condition at low volume flows. The operational point shifted from point A (dry) to point B (wet). The valve opening was kept constant at 40 %. When moving from point A to B the compressor discharge pressure was reduced with 0.009 bar which was a 0.75 % deviation from dry condition. The volume flow was reduced with 9.4 % compared to dry condition.

Figure 41 demonstrates how the operational point shifted from dry to wet condition at high volume flows. The operational point shifted from point A (dry) to point B (wet). The valve opening was kept constant at 90 %. When moving from point A to B the compressor discharge pressure was increased with 0.005 bar which was a 0.5 % deviation from dry condition. The volume flow was reduced with 5 % compared to dry condition.

The reduction in volume flow and compressor discharge pressure were generally more significant for low volume flows. When the volume flow increased the difference in compressor discharge pressure became less. For the intermediate valve opening of 60 % the discharge pressure was constant when going from dry to wet condition. For the highest valve openings, the compressor discharge pressure was increased when going from dry to wet condition. Consequently, the results show that the introduction of liquid does change the compressor operational point.

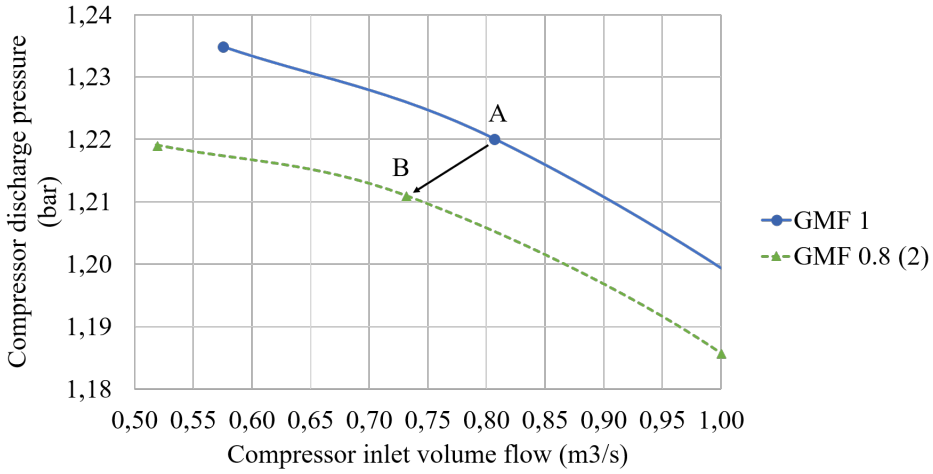


Figure 40: How the compressor operational point is affected by wet gas at low volume flows (valve opening 40 %, 9000 rpm).

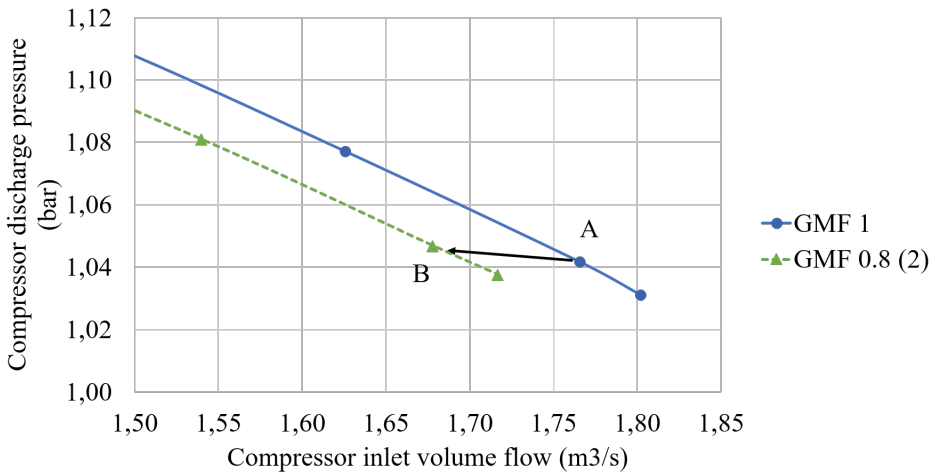


Figure 41: How the compressor operational point is affected by wet gas at high volume flows (valve opening 90 %, 9000 rpm).

The system resistance curves are not plotted in the figures in this subsection. To plot the system resistance curves several new experimental tests would have to be carried out. The compressor speed would have to be varied from minimum speed to maximum speed while keeping the GMF and the valve opening constant. This would have to be done for each GMF and all the valve openings. Together with supervisor it was decided to not focus on this. However, the results in this section demonstrate that the pressure in

the equipment and piping changes for the various GMF. Thus, the system resistance curve will change when liquid is present. Additionally, Figure 39 demonstrates that the operational point shifts, making it impossible for the operational point to follow the dry gas system resistance curve. This is especially clear for the intermediate flows when the wet operational point is aligned with the dry operational point. Thus, there is reason to believe that the system resistance curve will shift to the left when going from dry to wet condition.

## 6.6 Summary and Conclusion

In this section, the results from dry and wet gas experiments were presented and discussed. A comparison of the installed dry gas valve characteristics and inherent characteristics from the valve manufacturer was made. The installed characteristics shifted towards a linear characteristic which follows fundamental valve theory. The dry gas flow coefficients obtained in the lab was somewhat higher compared to the manufacturer's coefficients.

Two different experimental set-ups were tested. The deviations from the dry gas baselines were generally more pronounced for set-up 1, but the same trends were observed for both set-ups. Reduction in volume flow and increased differential pressure indicated a more pronounced throttling effect when liquid was introduced. The results from both set-ups showed that the introduction of liquid reduced the flow coefficient along the entire curve. The results indicated that the flow coefficient was independent of whether experimental set-up 1 or 2 were used. When analysing the relative flow coefficient, a shift towards a linear characteristic was observed as the GMF was reduced.

A shift in compressor operational point and system resistance curve was also observed when going from dry to wet condition. Based on the results from this section one can conclude that the presence of liquid does affect the valve performance and characteristic.

A list of general trends observed from the experimental campaign is given below. When the GMF was decreased the following was observed:

- Valve inlet temperature decreased.
- Valve pressure differential increased.
- Valve inlet volume flow decreased.
- Valve inlet density increased.

- Flow coefficient decreased.
- Relative flow coefficient increased.
- Compressor operational point changed.



## 7 HYSYS Dynamics

The objective of this section is to explain how to implement wet and dry valve characteristics in HYSYS Dynamics. Also, emphasis is put on the compressor operation and how wet gas possibly affects the HYSYS Dynamics simulations. The information in this section is mainly retrieved from Aspen Technology (2016).

### 7.1 General

Aspen HYSYS Dynamics, delivered by Aspentech, is a dynamic process simulation software that has been integrated into Aspen HYSYS. The software makes it possible to convert steady-state process models into dynamic process simulation models to study time-dependent oil and gas processes.

An HYSYS model of the NTNU wet gas facility, introduced in Section 5, has been developed. The model has progressed over a course of years by master students, PhD candidates and employees at the Department of Energy and Process Engineering. The latest version of the model is developed in a pilot version of HYSYS not available for the author of this thesis. Consequently, it was decided together with supervisor to not conduct any simulations in HYSYS Dynamics. However, a brief explanation of today's procedure for implementing valve and compressor characteristics in HYSYS is given. Additionally, a discussion regarding the implementation of wet gas characteristics is conducted.

Physical operations in HYSYS are governed by thermodynamics and mass and energy balances together with operation specific relations. An operation can e.g. be a compressor, valve, pipe or other equipment. The dynamic models simulate the thermal, equilibrium and reactive behaviour of a chemical system in a similar manner as the steady-state models. However, the dynamic model uses a different set of conservation equations which account for changes occurring over time. The equations for material, energy, and composition balances include an additional accumulation term which is differentiated with respect to time. Numerical integration is used to determine the process behaviour at distinct time steps.

Additionally, HYSYS Dynamics uses lumped models for all of the operations. In reality, most chemical engineering systems have thermal or component concentration gradients in three dimensions as well as in time. A lumped model considers all physical properties to be equal in space. Only the time gradients are considered in such analysis'. Besides, HYSYS uses

a "Degrees of Freedom" approach when modelling the various operations. For most operations, the user must provide specific information to begin a simulation. Based on the implemented parameters, HYSYS calculates any unknowns.

## 7.2 Valve Characteristics and Operation

To date, HYSYS allows the user to specify details primarily relating to the inherent valve parameters. The default sizing method is the ANSI/ISA S75.01 Standard which is equivalent to the IEC 60534-2 Standard described in Section 3.5. For two-phase flow, HYSYS practices the addition model described in Section 3.6. However, this does not happen automatically. The user must choose the "handle multi-phase flows rigorously"-option. HYSYS calculates the valve pressure drop as a function of valve opening and the valve characteristic implemented by the user. The user must specify the variables:  $C_v$ ,  $F_l$ ,  $F_p$  and  $x_T$  for the maximum inherent flow coefficient. For the discharge valve in the NTNU lab, these values would be the ones specified in Table 8 for the maximum valve opening. Additionally, it is essential that the user selects the valve operating characteristics most appropriate. The options are the following:

1. Linear

$$\%C_v = \%ValveOpening \quad (22)$$

2. Quick opening

$$\frac{\%C_v}{100} = \sqrt{\frac{\%ValveOpening}{100}} \quad (23)$$

3. Equal percentage

$$\frac{\%C_v}{100} = \left( \frac{\%ValveOpening}{100} \right)^3 \quad (24)$$

4. User table

These characteristics are explained in detail in Section 3.3. If any of options 1-3 are chosen, the theoretical characteristic is used as shown in the associating equations. The option "User Table" allows the user to implement a distinct and customised characteristic. Two columns must be specified: the valve opening (%) and the corresponding relative flow coefficient. These two columns are plotted against each other, creating the distinctive valve characteristic curve. The author suggests choosing "User Table" because it



allows for the installed characteristics to be implemented creating a more accurate simulation of the valve performance. Based on the theory and experimental results in this thesis, the installed and theoretical characteristic will deviate and thus option 4 is likely to be the better choice.

The user can manually change the characteristic curve to document the system's steady-state response to variations in the GMF and hence characteristic. This can be done by altering the "User Table" for the various characteristics. In practice, this would e.g. mean implementing the various curves in Figure 38 depending on the GMF chosen for the simulation. It should be noted that this can be somewhat time demanding and cumbersome. On contrary, analysing transient responses to variations in valve characteristics is not possible in today's HYSYS. To the author's knowledge, there is no way to vary the characteristic during a dynamic simulation. In dynamic mode, the user can analyse the valve opening's impact on the system response with a constant valve characteristic. Additionally, it is possible to use a HYSYS spreadsheet to set a correlation between GMF and maximum flow coefficient. If such a spreadsheet is made, valve performance will change when the maximum flow coefficient is decreased or increased. This makes it possible to analyse the maximum flow coefficient's impact on the system response in dynamic mode. But, the characteristic will still be the same, unable to correct for wet gas effects.

The experimental results in Section 6.5 clearly show that the valve characteristic is affected by liquid introduction. The characteristic establishes the relationship between pressure, flow and valve opening. Alterations in the characteristic would affect not only the valve discharge parameters, but possibly the entire system's response. Consequently, the ability to implement both dry and wet characteristic in HYSYS is much needed. Such an implementation would open for the possibility of dynamically analysing different valve characteristics and GMFs impact on the system's response.

The author suggests adding a feature that allows for the implementation of plural characteristic curves for various GMFs. When the GMF is altered, this feature will automatically change to the corresponding valve characteristic. Such a feature would simplify the steady-state simulations and make wet gas dynamic valve simulations possible. However, such a feature would require a standard procedure for calculating the wet gas valve characteristics. Otherwise, there is a risk of incomparable and inconclusive simulation results.

### 7.3 Centrifugal Compressor Characteristic and Operation

In HYSYS the operating mode of the compressor and the calculation procedure are specified by the user. In relation to this thesis, the proper choice would be respectively centrifugal compression and Schultz polytropic procedure. Also, the user must specify the distinctive characteristic curves of the desired compressor. This involves implementing a set of polytropic head and efficiency curves into the model. The specified curves allow for accurate simulations and recreations of in-field compressors. In contrast to the valve, the compressor has a feature that permits the implementation of various compressor curves in HYSYS. The "Multiple IGV Curve" selections allows for insertion of compressor curves for various GMFs. This feature allows for dynamic simulations of the system's response to variations in GMF. To simulate the compressor at the NTNU lab, the curves in Figure 7 and 8 would be implemented. Based on the inlet flow rate, inlet pressure, compressor speed and characteristic HYSYS calculates the compressor discharge parameters. The affinity laws are used if the operational point lies outside the implemented set of curves.

Figure 42 is an example of how the system resistance curve and compressor operational point may change from dry to wet condition based on the results from Section 6.5.3.

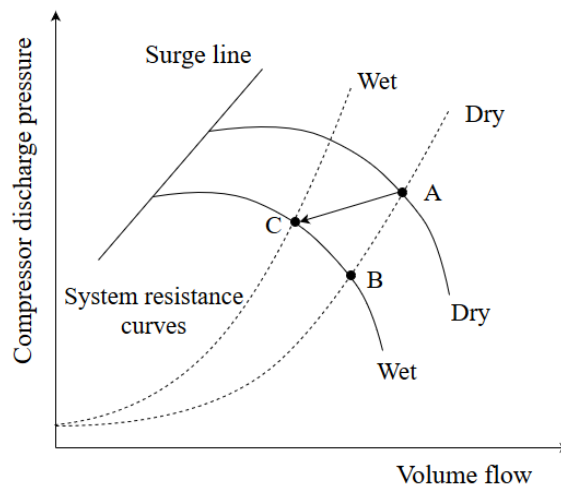


Figure 42: Example of how the system resistance curve and operational point may change from wet to dry condition.

The experiments showed that the compressor's operational point will shift. However, any changes in wet gas effects are not taken into consideration

when using the affinity laws in HYSYS. Additionally, the valve characteristic will not change when going from dry to wet condition in HYSYS Dynamics. Consequently, the operating point will shift from point A to B in HYSYS, following the dry gas system resistance curve. But in reality, the operational point actually shifts from point A to C. Thus, there will be some inaccuracy in the wet gas compressor simulations that potentially could affect the entire process' response. Hence, there is a need for comparing the experimental results from this thesis with simulations in HYSYS to validate this hypothesis.

## 7.4 Summary

This section explains how to implement valve and compressor characteristics in HYSYS. The results from this thesis can be directly implemented in HYSYS Dynamics. Based on the experimental results, this section concludes that there is a need for a feature that allows for the implementation of plural valve characteristic curves in HYSYS Dynamics to document the process's response to variations in GMF. This would require a standard wet gas valve performance calculation procedure. Comparison of the experimental results from this thesis and simulations in HYSYS Dynamics is necessary to validate potential deviations.



## 8 Conclusion

The work presented in this thesis has focused on an experimental test campaign with a centrifugal compressor and a rotary V-ball discharge valve. The goal of the thesis was to document compressor and control valve wet gas performance. Because previous wet gas research has focused on the compressor, it was decided to mainly focus on the wet gas valve behaviour in the experimental campaign. However, previous research in wet gas compression was documented.

A dry gas baseline characteristic was experimentally obtained to compare with wet gas results and the inherent characteristic from the valve manufacturer. The dry gas flow coefficients obtained in the lab was somewhat higher compared to the manufacturer's coefficients. The installed dry gas valve characteristic shifted towards a linear characteristic compared to the inherent. This is in compliance with fundamental valve theory.

Based on the results of the experimental campaign it can be concluded that the presence of liquid does affect the valve performance and characteristic. The presence of liquid increased the throttling effect through the valve. A decrease in volume flow was observed along with an increase in valve differential pressure. Additionally, the valve inlet temperature decreased and the valve inlet density increased when liquid was introduced.

Two experimental set-ups were tested. In both set-ups, the flow coefficient was reduced when the GMF was reduced. The results also indicated that the flow coefficient was independent of which set-up was used. When the GMF decreased the installed characteristic shifted towards a linear characteristic. A shift in compressor operational point and system resistance curve was also observed when going from dry to wet condition.

Additionally, this thesis emphasises the need for a standardised wet gas control valve performance calculation procedure. Especially if dynamic simulations on wet gas valve performance are to be conducted. This thesis confirms the need for further investigation of wet gas control valve performance.



## 9 Further Work

Throughout the work of this thesis, several interesting areas for further examination have emerged. Among them is further investigation of the flow regime downstream of the compressor, at the discharge valve inlet. A study of how the wet gas valve performance is affected by the flow regime can give valuable insight. A suggestion is to install visualisation slots downstream of the compressor. The author also proposes to investigate the placement of the valve inlet temperature sensor.

Additionally, wet gas valve simulations should be made using the HYSYS model of the NTNU test facility. After implementing the valve characteristics from this thesis, simulations should be made to analyse and document different valve characteristic impact on the system response. Comparisons of the simulations and the experiments conducted in this thesis should be performed. Additionally, the initiation of a collaboration with AspenTech HYSYS Dynamics should be considered to allow for the implementation of plural valve characteristic curves for various GMFs.

Work related to documenting potential variations in valve characteristics when altering the compressor speed, valve orientation and other parameters will also be of interest. Experimental investigations of slugs in relation to valve performance is also an area for further study. It is also of specific interest to compare various valve performance predictions methods and document any variations in valve performance parameters. The development of a standard for two-phase flow through control valves is also needed. The various subjects for further work are summarised below:

- Compare results using various performance models and develop a standard wet gas control valve performance calculation procedure.
- Visualisation and documentation of flow at discharge valve inlet.
- Investigate the placement of the valve inlet temperature sensor.
- Document the impact of slugs, speed variations and change in valve orientation on valve performance.
- Implement, analyse and document different valve characteristics impact on the system response in HYSYS Dynamics.
- Collaboration with HYSYS Dynamics to allow for dynamic simulations of valves' response to variations in GMF and thus characteristic.





## References

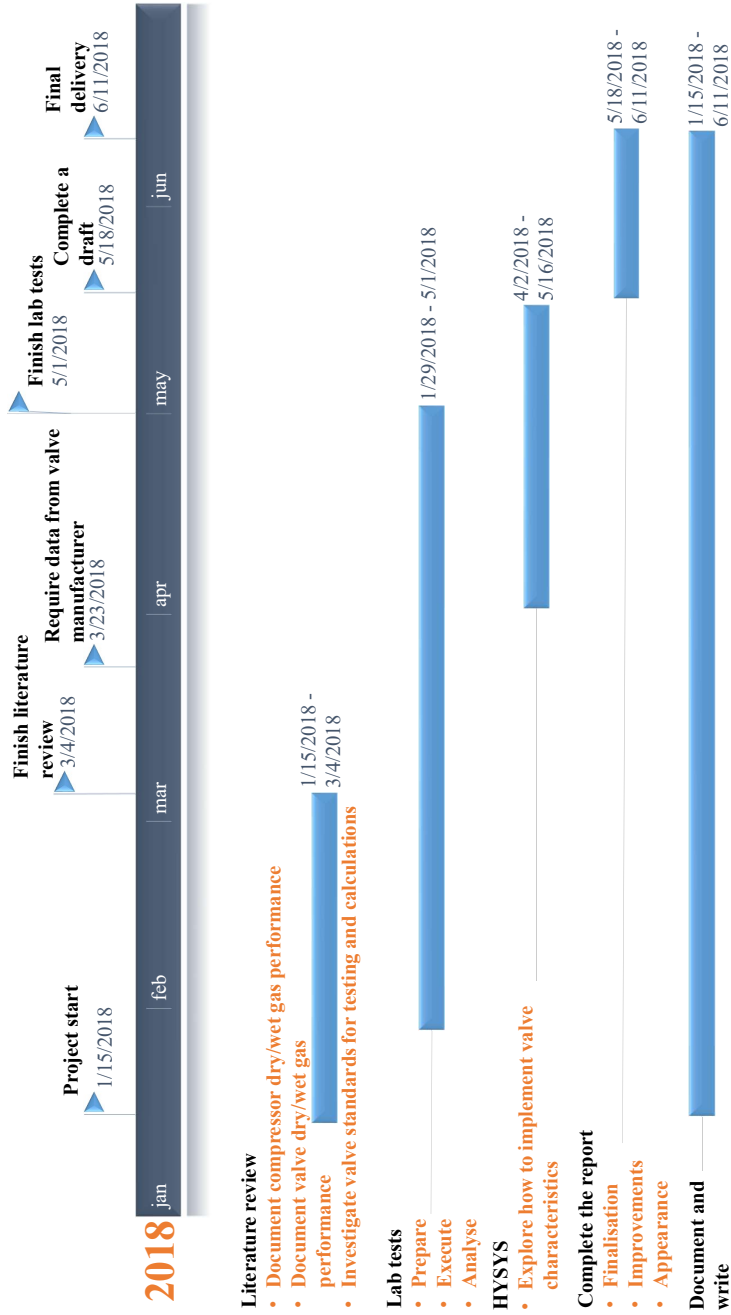
- Aspen Technology, 2016. Aspen HYSYS V9 User Manual. Version: 9. Accessed: Spring 2018.
- Bahadori, A., 2014. Sizing of valve and control valve. In: Natural Gas Processing. Elsevier Inc., Ch. 8, pp. 371–439.
- Baker, R. C., 2016. Flow measurement handbook : industrial designs, operating principles, performance, and applications, second edition. Edition. Ch. 5, pp. 116–162.
- Bakken, L. E., 2017a. Thermodynamic compression and expansion. In: TEP04 Gas Turbines and Compressors. NTNU.
- Bakken, M., 2017b. Compressor wet gas test data at 9000 rpm. Trondheim, NTNU.
- Borden, G., Friedmann, P., 1998. Control Valves. Practical guides for measurement and control. Instrument Society of America, Research Triangle Park, N.C.
- Brenne, L., Bjørge, T., Gilarranz, J. L., Koch, J. M., Miller, H. F., 2005. Performance evaluation of a centrifugal compressor operating under wet gas conditions. Proceedings of the 34th Turbomachinery Symposium, 111–120.
- Dahlhaug, O. G., 2017. Fundamental similarity considerations. In: TEP4195 Turbo Machinery. NTNU. Accessed: 13.07.17.  
URL <https://ntnu.itslearning.com>
- Darby, R., Meiller, P., Stockton, J., 2001. Select the best model for two-phase relief sizing. Chemical Engineering Progress 97, 56–64.
- Diener, R., Kiesbauer, J., Schmidt, J., March 2005. Improved control valve sizing for multiphase flow. Hydrocarbon Processing 84, 59–65.
- Diener, R., Schmidt, J., March 2005. Sizing of throttling device for gas/liquid two-phase flow part 2: Control valves, orifices, and nozzles. Process Safety Progress 24 (1), 29–37.  
URL <http://search.proquest.com/docview/28725208/>
- Dolve, I. M., 2017. Energy optimization - compressor control. Project thesis. NTNU: Department of Energy and Process Engineering.

- Equinor, 2018. Åsgard subsea gas compression. Accessed: 24.10.2017.  
URL <https://www.equinor.com/en/where-we-are/norway/asgard-subsea-gas-compression.html>
- Ferrara, V., 2016. Wet gas compressors - stability and range. Doctoral thesis. NTNU: Department of Energy and Process Engineering.
- Ferrara, V., Bakken, L. E., 2015. Wet gas compressor surge stability. Proceedings of ASME Turbo Expo: Turbine Technical Conference and Exposition 9.
- Fisher Controls, 2017. Control Valve Handbook, 4th Edition. Emerson Process Management, Marshalltown, Iowa, Ch. 1–2.
- Fisher Controls, 2018. Catalog 12. Emerson Process Managemet.  
URL [http://www.documentation.emersonprocess.com/groups/public/documents/catalog/d103182x012.pdf?\\_ga=2.224074717.735188938.1524121714-896667971.1520874298](http://www.documentation.emersonprocess.com/groups/public/documents/catalog/d103182x012.pdf?_ga=2.224074717.735188938.1524121714-896667971.1520874298)
- Forsthoffer, W. E., January 2006. Operation of a compressor in a system. In: Forsthoffer's Rotating Equipment Handbooks. Vol. 3. Elsevier Science, Ch. 4, pp. 43–51.  
URL <https://www.sciencedirect.com/science/article/pii/B9781856174725500095>
- Hundseid, Ø., Bakken, L. E., 2006a. Wet gas performance analysis. Proceedings of ASME Turbo Expo: Power for Land, Sea, and Air 5, 625–632.  
URL <http://proceedings.asmedigitalcollection.asme.org/proceeding.aspx?articleid=1590750>
- Hundseid, Ø., Bakken, L. E., 2006b. Wet gas performance analysis. Proceedings of ASME Turbo Expo: Power for Land, Sea, and Air 5, 625–632.  
URL <http://dx.doi.org/10.1115/GT2006-91035>
- Hundseid, Ø., Bakken, L. E., 2015. Integrated wet gas compressor test facility. Proceedings of ASME Turbo Expo: Turbine Technical Conference and Exposition 9.  
URL <http://proceedings.asmedigitalcollection.asme.org/proceeding.aspx?articleid=2428737>
- Hundseid, Ø., Bakken, L. E., Grüner, T. G., Brenne, L., Bjørge, T., 2008. Wet gas performance of a single stage centrifugal compressor. Proceedings of ASME Turbo Expo: Power for Land, Sea and Air 7, 661–670.

- URL <http://proceedings.asmedigitalcollection.asme.org/proceeding.aspx?articleid=1626036>
- IEC, 2011. Industrial-process control valves - part 2-1: Flow capacity - sizing equations for fluid flow under installed conditions. Standard IEC 60534-2-1:2011.  
URL <https://www.standard.no>
- IEC, 2015. Industrial process control valves - part 2-3: Flow capacity - test procedures. Standard IEC 60534-2-3:2015.  
URL <https://www.standard.no>
- ISO, 2003. Measurement of fluid flow by means of pressure differential devices inserted in circular cross-section conduits running full - part 2: Orifice plates. Standard ISO 5167-2:2003.  
URL <https://www.standard.no>
- Kaleem, K. M., 2015. Pipe flow. In: Fluid Mechanics and Machinery. Oxford University Press, p. 300.  
URL <http://app.knovel.com/hotlink/pdf/rcid:kpFMM00004/id:kt00UPLRTA/fluid-mechanics-machinery/pipe-flow?kpromoter=Summon>
- Leung, J. C., 1986. A generalized correlation for one-component homogeneous equilibrium flashing choked flow. *AIChE Journal* 32 (10), 1743–1746.  
URL <https://onlinelibrary.wiley.com/doi/abs/10.1002/aic.690321019>
- Lipták, B. G., 1995. *Instrument Engineers' Handbook : Process Control*, 3rd Edition. Butterworth-Heinemann, Oxford, p. 533.
- Musgrove, G. O., Poerner, M. A., Beck, G., Kurz, R., Bourn, G., 2014a. Perspectives and experience with wet gas compression. *Turbo Expo: Power for Land, Sea, and Air* 9.  
URL <http://dx.doi.org/10.1115/GT2016-56159>
- Musgrove, G. O., Poerner, M. A., Cirri, M., Bertoneri, M., 2014b. Overview of important considerations in wet gas compression testing and analysis. *Turbomachinery and Pump Symposia*.  
URL <https://doi.org/10.21423/R1VD1J>
- Saravanamuttoo, H. I. H., 2009. *Gas Turbine Theory*, 6th Edition. Pearson Prentice Hall, Ch. 4, pp. 157–186.

- Schmidt, J., Egan, S., 2009. Case studies of sizing pressure relief valves for two-phase flow. *Chemical Engineering and Technology* 32 (2), 263–272.
- Schultz, J. M., 1962. The polytropic analysis of centrifugal compressors. *ASME Journal of Engineering for Power* 84, 69–82.  
URL <http://gasturbinespower.asmedigitalcollection.asme.org/article.aspx?articleid=1416225>
- Sheldon, C. W., Schuder, C. B., January 1965. Sizing control valves for liquid-gas-mixtures. *Instruments Control Systems* 38.
- Thomas, P., 1999. Control valve liquid flow. In: *Simulation of Industrial Processes for Control Engineers*. Butterworth-Heinemann, Oxford, pp. 60 – 67.  
URL <https://www.sciencedirect.com/science/article/pii/B9780750641616500080>

# Appendix A: Research Plan



## Appendix B: Research Log

Table 6: Research log.

Week	Activity
8	Wet gas test
10	Dry gas test
11	Contacted Emerson for inherent data
12	Contacted Emerson and repeated request for data
12	New differential pressure sensor installed in lab
15	Contacted Emerson and repeated request for data
16	Received inherent data from Emerson
16	Dry gas retest
17	Wet gas retest

# Appendix C: Risk Assessment


NTNU	Hazardous activity identification process			
	Prepared by HSE section	Number HMSRV2601E	Date 09.01.2013	
	Approved by The Rector		Replaces 01.12.2006	

**Date: 15.02.2018**

Unit: Department of Energy and Process Engineering  
Line manager: Terese Løvås

Participants in the identification process (including their function): Ingeborg M. Dolve (student), Erik Langørge (Lab engineer)  
Short description of the main activity/main process: Master project for student: Ingeborg Møeland Dolve. Project title: Wet Gas Compression Transient Operation

Is the project work purely theoretical? (YES/NO): No  
Answer "YES" implies that supervisor is assured that no activities requiring risk assessment are involved in the work. If YES, briefly describe the activities below. The risk assessment form need not be filled out.

Signatures: Responsible supervisor: 

Student: 

ID nr.	Activity/process	Responsible person	Existing documentation	Existing safety measures	Laws, regulations etc.	Comment
1	Compressor and valve experiment dry gas	Erik Langørge	Risk Assessment Report	Procedure for Running Experiments	The Work Environment Act	There is no existing documentation on experiments involving water injection downstream the compressor. Therefor a SJA was conducted for this experimental set-up. See the following SJA named:
2	Compressor and valve experiment wet	Martin Bakken Lars E. Bakken		Safe Job Analysis (SJA)		Discharge Valve Transient Behaviour (Water injection downstream compressor)
3	Discharge valve experiment wet (water injection upstream compressor)					
4	Discharge valve experiment wet (water injection downstream compressor)					

NTNU		Risk assessment		Prepared by	Number	Date
				HSE section	HMSRV2603E	04.02.2011
HSE/KS				Approved by		Replaces
				The Rector		01.12.2006



Unit: Department of Energy and Process Engineering

Date: 15.02.2018

Line manager: Terese Løvås

Participants in the identification process (including their function): Ingeborg M. Dolve (student), Erik Langørgen (Lab engineer)  
 Short description of the main activity/main process: Master project for student: Ingeborg Møeland Dolve. Project title: Wet Gas Compression Transient Operation

Signatures: Responsible supervisor: 

Student: 

Activity from the identification process form	Potential undesirable incident/strain	Likelihood (1-5)	Consequence:		Risk Value (human)	Comments/status Suggested measures
			Human (A-E)	Environment (A-E)		
1-3	See Risk Assessment Report					
4	Water tube detaches from pulse valve. Risk of water/air spray	3	A	A	A3	Make sure water tube is protected and properly attached. Wear eye protection.
4	Accumulation of water in front of valve. Risk of reversal flow. Risk of mechanical failure when there is high levels of water in the impeller	2	C	A	C2	Visual inspection of volute to see if any backflow occurs. Should operate the compressor from the control room.
4	Ignorant control of valves may lead to parts detaching entering the compressor.	2	D	A	D2	Avoid high speeds and closed vane.
4	Throttling into surge area may lead to noise and vibrations	3	B	A	B3	Operate in stable region. Wear hearing protection
4	Rapid increase of load. Risk of mechanical failure	1	D	A	D1	Start with small slugs and gradually increase the size

Likelihood, e.g.:

1. Minimal
2. Low
3. Medium

Consequence, e.g.:

- A. Safe
- B. Relatively safe
- C. Dangerous

Risk value (each one to be estimated separately):

- Human = Likelihood x Human Consequence  
 Environmental = Likelihood x Environmental consequence  
 Financial/material = Likelihood x Consequence for Economy/material



NTNU	<b>Risk assessment</b>			Prepared by	Number	Date
				HSE section	HMSRV2603E	04.02.2011
HSE/IKS				Approved by		Replaces
		The Rector		01.12.2006		



- 4. High
- 5. Very high

- D. Critical
- E. Very critical

**Potential undesirable incident/strain**

Identify possible incidents and conditions that may lead to situations that pose a hazard to people, the environment and any materiel/equipment involved.

**Criteria for the assessment of likelihood and consequence in relation to fieldwork**

Each activity is assessed according to a worst-case scenario. Likelihood and consequence are to be assessed separately for each potential undesirable incident. Before starting on the quantification, the participants should agree what they understand by the assessment criteria:

**Likelihood**

<b>Minimal</b> 1	<b>Low</b> 2	<b>Medium</b> 3	<b>High</b> 4	<b>Very high</b> 5
Once every 50 years or less	Once every 10 years or less	Once a year or less	Once a month or less	Once a week

**Consequence**

Grading	Human	Environment	Financial/material
<b>E</b> Very critical	May produce fatality/ies	Very prolonged, non-reversible damage	Shutdown of work >1 year.
<b>D</b> Critical	Permanent injury, may produce serious serious health damage/sickness	Prolonged damage. Long recovery time.	Shutdown of work 0.5-1 year.
<b>C</b> Dangerous	Serious personal injury	Minor damage. Long recovery time	Shutdown of work < 1 month
<b>B</b> Relatively safe	Injury that requires medical treatment	Minor damage. Short recovery time	Shutdown of work < 1week
<b>A</b> Safe	Injury that requires first aid	Insignificant damage. Short recovery time	Shutdown of work < 1day


The unit makes its own decision as to whether opting to fill in or not consequences for economy/materiel, for example if the unit is going to use particularly valuable equipment. It is up to the individual unit to choose the assessment criteria for this column.

**Risk = Likelihood x Consequence**

Please calculate the risk value for "Human", "Environment" and, if chosen, "Economy/materiel", separately.

**About the column "Comments/status, suggested preventative and corrective measures":**

Measures can impact on both likelihood and consequences. Prioritise measures that can prevent the incident from occurring; in other words, likelihood-reducing measures are to be prioritised above greater emergency preparedness, i.e. consequence-reducing measures.

NTNU		Risk matrix		Number		Date	
 HSE/IKS		prepared by		HMSRV2604		8 March 2010	
		HSE Section		Page		Replaces	
		approved by		4 of 4		9 February 2010	
		Rector					

## MATRIX FOR RISK ASSESSMENTS at NTNU

		<b>CONSEQUENCE</b>									
Extremely serious	E1	E2	E3	E4	E5						
Serious	D1	D2	D3	D4	D5						
Moderate	C1	C2	C3	C4	C5						
Minor	B1	B2	B3	B4	B5						
Not significant	A1	A2	A3	A4	A5						
	Very low	Low	Medium	High	Very high						
	<b>LIKELIHOOD</b>										

Principle for acceptance criteria. Explanation of the colours used in the risk matrix.

Colour	Description
Red	Unacceptable risk. Measures must be taken to reduce the risk.
Yellow	Assessment range. Measures must be considered.
Green	Acceptable risk. Measures can be considered based on other considerations.

## SAFE JOB ANALYSIS

<b>SJA name: Discharge Valve Transient Behaviour (Water injection downstream compressor)</b>	
Date: 15.02.17	Location: Wet gas compressor test facility in cellar at the thermal energy department at NTNU.
Mark for completed checklist:	<input type="checkbox"/>

Participators:		
Ingeborg Mæland Dolve	Erik Langørgen	
SJA-responsible:	Erik Langørgen	

<p>Specification of work (What and how?):</p> <p>The main purpose is to investigate the discharge valve characteristic under transient behaviour. A change in the lab set-up has been done (See Section 6.1 for set-up details). Water is in this experiment injected downstream the compressor through the pulse valve. Variations in GMF will be investigated.</p>
<p>Risks associated with the work:</p> <ul style="list-style-type: none"> <li>• Ignorant control of valves may lead to parts detaching entering the compressor. Should avoid high compressor speeds together with closed valve.</li> <li>• Entering the surge area may lead to noise and vibrations. Should not throttle the compressor into surge area. Listen for vibrations and inspect the characteristic under operation. A rule of thumb is to only close the valve to 30 % and not further.</li> <li>• Accumulation of water in front of the discharge valve. Can happen if: 1. Valve orientation changes, 2. Water is injected at high rates while the compressor operates at low speeds or 3. The valve is closed while the water keeps being injected.</li> <li>• Risk of reversal flow and water in compressor.</li> <li>• The compressor risks mechanical failure if operated with high levels of water, especially at high speeds.</li> <li>• Water tube detaches from pulse valve. Risk of uncontrolled water/air spray.</li> </ul>
<p>Safeguards: (plan for actions, see next page):</p> <ul style="list-style-type: none"> <li>• Keep the compressor away from the surge area.</li> <li>• Only operate with valve openings between 30%-100%.</li> <li>• All experiments will be conducted together with authorized operators and there will always be two persons in the lab during tests.</li> <li>• Make sure water tube is protected and properly attached.</li> <li>• Wear protection for eyes and ears.</li> <li>• Visual inspection of pulse valve and tubes.</li> </ul>

**Conclusions/comments:**

When evaluating the consequences concerning human and material endangerment for this experiment is concluded that the risks are acceptable, and the experiment can be conducted following the safeguards.

<b>Recommended/approved</b>	<b>Date/Signature:</b>	<b>Recommended/approved</b>	<b>Date/Signature:</b>
SJA-responsible:		HSE responsible:	
Responsible for work:		Other, (position):	

HSE aspect	Yes	No	NA	Comments / actions	Resp.
<b>Documentation, experience, qualifications</b>					
Known operation or work?		x			
Knowledge of experiences / incidents from similar operations?	x			The compressor lab has been operated for years	
Necessary personnel?	x			Experiments will be done together with approved lab operators	
<b>Communication and coordinating</b>					
Potential conflicts with other operations?			x		
Handling of an eventually incident (alarm, evacuation)?			x		
Need for extra assistance / watch?	x			Will always be two persons or more in the lab.	
<b>Working area</b>					
Unusual working position		x			
Work in tanks, manhole?			x		
Work in ditch, shaft or pit?			x		
Clean and tidy?	x				
Protective equipment beyond the personal?	x			Ear and eye protection	
Weather, wind, visibility, lighting, ventilation?			x		
Usage of scaffolding/lifts/belts/ straps, anti-falling device?			x		
Work at heights?			x		
Ionizing radiation?			x		
Influence of escape routes?		x			
<b>Chemical hazards</b>					
Usage of hazardous/toxic/corrosive chemicals?			x		
Usage of flammable or explosive chemicals?			x		
Risk assessment of usage?	x			Done according to department's procedures	
Biological materials/substances?			x		

Dust/asbestos/dust from insulation?			x		
<b>Mechanical hazards</b>					
Stability/strength/tension?	x				
Crush/clamp/cut/hit?			x		
Dust/pressure/temperature?	x			Working with wet/dry gas compression	
Handling of waste disposal?			x		
Need of special tools?	x			Water is injected through pulse valve	
<b>Electrical hazards</b>					
Current/Voltage/over 1000V?			x		
Current surge, short circuit?			x		
Loss of current supply?			x		
<b>Area</b>					
Need for inspection?	x			See Procedure for Running Experiments	
Marking/system of signs/rope off?			x		
Environmental consequences?			x		
<b>Key physical security systems</b>					
Work on or demounting of safety systems?			x		
<b>Other</b>			<b>x</b>		

## Appendix D: The Schultz Polytropic Analysis of Centrifugal Compressors

In operation of compressors, real gas behaviour has to be accounted for in order to get proper performance calculations. Schultz proposed a new model for performance calculations in 1962. It should be noted that this method is developed with special regards to the centrifugal compressor. Schultz' procedure accounts for the variations in the polytropic volume exponent.

In Schultz' model the polytropic volume exponent is defined by Equation (25).

$$n_v = \frac{1 + X}{Y \left[ \frac{1}{\kappa} \left( \frac{1}{\eta_p} + X \right) - \left( \frac{1}{\eta_p} - 1 \right) \right]} \quad (25)$$

Schultz supplemented the known compressibility factor Z with two additional compressibility functions: X and Y.

$$X = \frac{T}{V} \left( \frac{\partial V}{\partial T} \right)_p - 1 \quad (26)$$

$$Y = -\frac{p}{V} \left( \frac{\partial V}{\partial p} \right)_T \quad (27)$$

To account for the variations in the polytropic volume exponent, Schultz introduced a compressor path correction factor f. This correction factor, defined in Equation (28), is the same for both polytropic and isentropic analysis.

$$f = f_s = \frac{h_{2s} - h_1}{\frac{\kappa_v}{\kappa_v - 1} [p_2 v_2 - p_1 v_1]} \quad (28)$$

Using Schultz' volume exponent the pressure-temperature relation becomes:

$$\frac{T_2}{T_1} = \frac{p_2}{p_1} \frac{n_T - 1}{n_T} \quad (29)$$

The polytropic head is then calculated based on the corrected parameters as shown in Equation (30).

$$H_p = f \frac{n_v}{n_v - 1} \frac{Z_1 R_o T_1}{MW} \left[ \frac{p_2}{p_1} \frac{n_v - 1}{n_v} - 1 \right] \quad (30)$$

When the polytropic head is determined, the polytropic efficiency can be calculated as the relationship between the polytropic head and the actual head. The polytropic efficiency is defined by Equation (31).

$$\eta_p = \frac{H_p}{H} \quad (31)$$

### Power Calculations

When the head of the process is known, it is possible to calculate the power consumption for the given compression process. Energy consumption for a compression process is given by Equation (32).

$$P = \frac{\dot{m}H}{\eta_m} = \frac{\dot{m}H_p}{\eta_m\eta_p} \quad (32)$$

$\eta_m$  is the mechanical efficiency and represents the losses in the machine that is not accounted for in neither the polytropic nor the isentropic analysis.

## Appendix E: Affinity Laws

As explained in Section 2.3.1 the compressor characteristics is often given by a set of curves for pressure and efficiency plotted against volume flow or mass flow. Only a limited number of rotational speeds, between the lowest and the highest, are included in the characteristic. So, if an operating point lies outside or between these curves, the affinity laws are used for calculating the head, efficiency and volume flow. The affinity laws provide a method for scaling the compressor from one operating point to another. The affinity laws are shown in Equation (33) and (34). (Dahlhaug, 2017)

$$\frac{Q}{Q^*} = \frac{N}{N^*} \quad (33)$$

$$\frac{H_p}{H_p^*} = \left[ \frac{N}{N^*} \right]^2 \quad (34)$$

The parameters that are unknown are marked with \*, while the parameters that are known from the given characteristic have no index. The affinity laws assume constant efficiency between the calculated and known values.



## **Appendix F: Inherent NPS 8 V150 Fisher Valve Characteristics**

The information in this appendix was retrieved through mail correspondence with Kjell Skoe (FSE Valves, Flow Control) from Emerson Automation and Jostein Bergstrom (Inside Sales Engineer, Fisher Valves) from Emerson Process Management in April 2018.

# Valve/Regulator Sizing Calculation

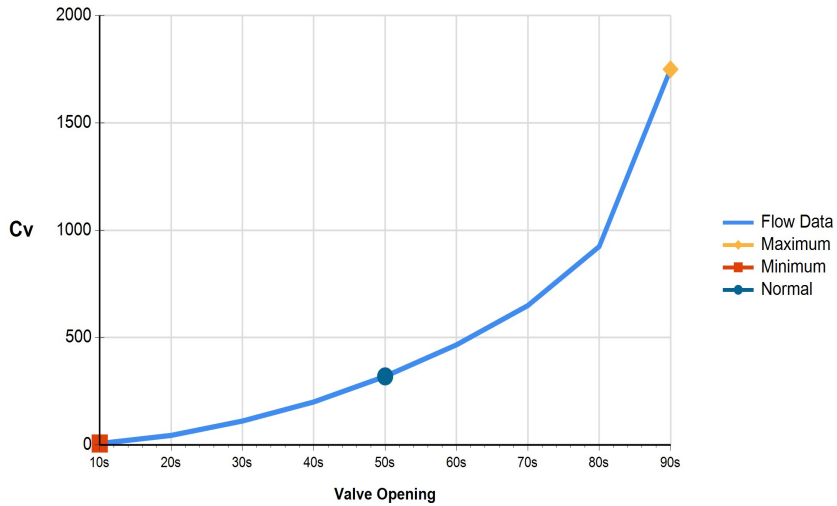
Kunde:	Emerson Process Management Norway		
Kontakt:	Kontakt: <b>Jostein Bergstrom</b>		
Customer Reference:	Sales Office Reference: <b>JTB FY18 Calc.</b>		Lead Time: <b>Day(s)</b>
Pos: <b>100</b>	Rev:	Antall: <b>1</b>	Rev: <b>NTNU</b>
Tag nr: <b>Water</b>	Date Last Modified: <b>16/04/2018</b>		
Betegnels: <b>NPS 8 V150</b>			
Service Description:			

Variable Name	Units	Minimum	Normal	Maximum
<b>SERVICE &amp; SIZING</b>				
Inlet Temperature (T1)	deg C	50.0000	50.0000	50.0000
Inlet Pressure (P1)	bar(g)	10.00000	10.00000	10.00000
Pressure Change (dP)	bar	1.00000	1.00000	1.00000
Mass Flow Rate Liquid (wl)	kg/h	5386.8700	274068.8255	1503512.3657
Pressure Recovery Factor (FI)		0.930	0.860	0.510
Valve style modifier (Fd)		0.510	0.860	0.990
Cavitation coefficient (Kc)		0.330	0.330	0.330
Atmospheric Pressure	psi	14.69	14.69	14.69
Specific Gravity (SG)		0.989	0.989	0.989
Kinematic Viscosity (Nu)	SSU	2.509	2.509	2.509
Critical Pressure (Pc)	bar(g)	219.62716	219.62716	219.62716
Vapor Pressure (Pv)	bar(g)	-0.88933	-0.88933	-0.88933
Inlet fluid density (Rho1)	kg/m3	988.48	988.48	988.48
Pipe Size Up	mm	200	200	200
Pipe Schedule Up		STD	STD	STD
Pipe Size Down	mm	200	200	200
Pipe Schedule Down		STD	STD	STD
Nominal Valve Diameter (dv)	mm	203.20	203.20	203.20
Sizing Coefficient (Cv)		6.270	319.000	1750.000
% Open		10	50	90
Application Ratio (Ar)		0.092	0.092	0.092
dP Choked	bar	9.42316	8.05801	2.83381
dP Cavitation	bar	3.59348	3.59348	3.59348
Fp		1.00	1.00	1.00
<b>NOISE CALCULATION</b>				
Hydrodynamic Trim		Standard Trim	Standard Trim	Standard Trim
Valve Lpa (LpAe1m)	dB(A)	< 50	57	67
<b>VELOCITY OUTPUTS</b>				
V1 Pipe	m/s	0.0469	2.3874	13.0969
V2 Pipe	m/s	0.0469	2.3874	13.0969
Item Notes:				

### Flow Coefficient Graph

Kunde:	Emerson Process Management Norway		
Kontakt:	Kontakt: <b>Jostein Bergstrom</b>		
Customer Reference:	Sales Office Reference: <b>JTB FY18 Calc.</b>		Lead Time: <b>Day(s)</b>
Pos: <b>100</b>	Rev:	Antall: <b>1</b>	
Tag nr: <b>Water</b>	Date Last Modified: <b>16/04/2018</b>		
Betegnelse: <b>NPS 8 V150</b>			
Service Description:			

Flow Coefficient vs. Valve Opening



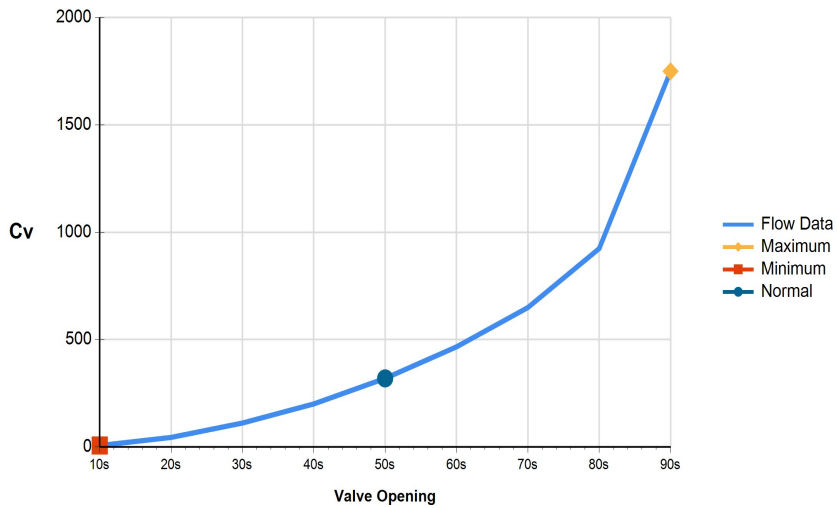
Product: V150 Valve Size=NPS 8 Flow=Forward Characteristic=Modified Equal Percent Ball Seal=Comp Ball  
 Material=CF3M SST/CRPL Valve Type=V150 Attenuator=No

## Valve/Regulator Sizing Calculation

Kunde:		Emerson Process Management Norway		
Kontakt:		Kontakt: <b>Jostein Bergstrom</b>		
Customer Reference:		Sales Office Reference: <b>JTB FY18 Calc.</b>		Lead Time: <b>Day(s)</b>
Pos: <b>200</b>	Rev:	Antall: <b>1</b>	Rev: <b>NTNU</b>	
Tag nr: <b>Air</b>		Date Last Modified: <b>16/04/2018</b>		
Betegnelse: <b>NPS 8 V150</b>				
Service Description:				
Sizing Type: Gas	Flow is Turbulent	Solving for: Q	Noise is IEC/Aerodynamic	Flow is Mass
Variable Name	Units	Minimum	Normal	Maximum
<b>SERVICE &amp; SIZING</b>				
Gas		AIR	AIR	AIR
Inlet Pressure (P1)	bar(g)	10.00000	10.00000	10.00000
Pressure Change (dP)	bar	1.00000	1.00000	1.00000
Inlet Temperature (T1)	deg C	50.0000	50.0000	50.0000
Volumetric Flow Rate Gas (Qg)	Nm3/h	436.20926	22050.22573	102541.74368
Pressure drop ratio factor (Xt)		0.703	0.615	0.156
Pressure Recovery Factor (Fl)		0.930	0.860	0.510
Valve style modifier (Fd)		0.510	0.860	0.990
Atmospheric Pressure	psi	14.69	14.69	14.69
Kinematic Viscosity (Nu)	SSU	2.50867	2.50867	2.50867
Specific heats ratio (gamma)		1.400	1.400	1.400
Molecular Weight/Specific Gravity	M	28.970	28.970	28.970
Inlet Compressibility Factor (Z1)		1.000	1.000	1.000
Pipe Size Up	mm	200	200	200
Pipe Schedule Up		STD	STD	STD
Pipe Size Down	mm	200	200	200
Pipe Schedule Down		STD	STD	STD
Nominal Valve Diameter (dv)	mm	203.20	203.20	203.20
Aerodynamic Distance (Rn)	m	1.000	1.000	1.000
Sizing Coefficient (Cv)		6.270	319.000	1750.000
% Open		10	50	90
dP Choked	bar	7.74203	6.77290	1.71800
dP/P1 Valve		0.091	0.091	0.091
Fp		1.00	1.00	1.00
<b>NOISE CALCULATION</b>				
Valve/Trim		Segmented Ball	Segmented Ball	Segmented Ball
LpAeTrim1m	dB(A)	63	81	97
LpAeOutlet1m	dB(A)	< 50	< 50	65
Valve Lpa (LpAe1m)	dB(A)	63	81	97
Valve Lpa (LpAeRn)	dB(A)	63	81	97
<b>VELOCITY OUTPUTS</b>				
Valve Outlet Area(Ao)	mm2	32429.6	32429.6	32429.6
M1 Pipe	Mach	0.001	0.057	0.267
Mo Valve	Mach	0.001	0.063	0.292
M2 Pipe	Mach	0.001	0.063	0.293
V1 Pipe	m/s	0.4089	20.6680	96.1136
Vo Valve	m/s	0.4476	22.6240	105.2101
V2 Pipe	m/s	0.4497	22.7321	105.7127
C1 Pipe	m/s	360.4419	360.4419	360.4419
Co Valve	m/s	360.4419	360.4419	360.4419
C2 Pipe	m/s	360.4419	360.4419	360.4419
Item Notes:				

Kunde:	Emerson Process Management Norway		
Kontakt:	Kontakt: <b>Jostein Bergstrom</b>		
Customer Reference:	Sales Office Reference: <b>JTB FY18 Calc.</b>		Lead Time: <b>Day(s)</b>
Pos: <b>200</b>	Rev:	Antall: <b>1</b>	
Tag nr: <b>Air</b>	Date Last Modified: <b>16/04/2018</b>		
Betegnelse: <b>NPS 8 V150</b>			
Service Description:			

Flow Coefficient vs. Valve Opening



Product: V150 Valve Size=NPS 8 Flow=Forward Characteristic=Modified Equal Percent Ball Seal=Comp Ball  
 Material=CF3M SST/CRPL Valve Type=V150 Attenuator=No

Table 7: NPS 8 V150 Fisher valve characteristics  $C_v$  1750 (Fisher Controls, 2018).

Valve opening (degrees)	Valve opening (%)	$C_v$	$K_v$	$F_d$	$F_l$	$x_t$
10	11,11	6,27	5,42	0,51	0,93	0,703
20	22,22	44	38,1	0,62	0,94	0,795
30	33,33	111	96	0,73	0,93	0,745
40	44,44	200	173	0,81	0,9	0,678
50	55,56	319	276	0,86	0,86	0,615
60	66,67	466	403	0,91	0,83	0,555
70	77,78	649	561	0,95	0,79	0,481
80	88,89	924	799	0,97	0,74	0,378
90	100	1750	1514	0,99	0,51	0,156

Table 8: NPS 8 V150 Fisher valve characteristics  $C_v$  1820 (Fisher Controls, 2018).

Valve opening (degrees)	Valve opening (%)	$C_v$	$K_v$	$F_d$	$F_l$	$x_t$
10	11,11	6,99	6,05	0,51	0,89	0,526
20	22,22	50,9	44	0,62	0,9	0,731
30	33,33	122	106	0,73	0,9	0,735
40	44,44	225	195	0,81	0,88	0,64
50	55,56	353	305	0,86	0,87	0,597
60	66,67	518	448	0,91	0,82	0,537
70	77,78	714	618	0,95	0,78	0,487
80	88,89	1030	891	0,97	0,71	0,36
90	100,00	1820	1574	0,99	0,54	0,176

## Appendix G: Lab Results

Table 9: Explanation of lab parameters used in Table 10-12.

Lab parameter	Explanation
XT-3.1P	Ambient air pressure
PT-3.3	Static inlet pressure orifice
TT-5.1	Inlet temperature orifice
PT-3.1	Differential pressure orifice
PT-3.4	Static inlet pressure compressor
Inlet_Temp	Averaged inlet temperature compressor
PT-3.5	Static inlet pressure discharge valve
Outlet_Temp	Averaged inlet temperature discharge valve
PDT-1.1	Differential pressure discharge valve
ST-1.1	Shaft speed
OV	Set point discharge valve opening
$\dot{m}_l$	Liquid mass flow

Table 10: Dry gas test results (9000 rpm).

GMF	OV	XT-3,1P	PT-3.3	TT-5.1	PT-3.4		Inlet_Temp	PT-3.5	Outlet_Temp	$\dot{m}_i$	PT-3.1		PDT-1.1	
					bar	bar					bar	bar	bar	bar
0,9996	30	1,0083	1,0075	28,0147	0,9979	27,8102	1,2348	51,0949	0,0002	0,1081	0,2315			
0,9997	40	1,0083	1,0069	28,2876	0,9890	27,8184	1,2201	49,4250	0,0002	0,2087	0,2169			
0,9998	50	1,0084	1,0058	28,5914	0,9747	28,0023	1,1873	47,6070	0,0002	0,3765	0,1846			
0,9998	60	1,0084	1,0049	28,5519	0,9610	27,8890	1,1477	45,7766	0,0002	0,5338	0,1462			
0,9998	70	1,0085	1,0042	28,5082	0,9498	27,8937	1,1135	44,3260	0,0002	0,6644	0,1116			
0,9998	80	1,0085	1,0034	28,8155	0,9386	27,9515	1,0772	43,0912	0,0002	0,7957	0,0742			
0,9998	90	1,0085	1,0027	28,7803	0,9276	27,9457	1,0418	41,4818	0,0002	0,9251	0,0357			
0,9998	100	1,0086	1,0025	27,9915	0,9242	27,5036	1,0312	40,5066	0,0002	0,9644	0,0236			



Table 11: Set-up 1 wet gas test results (9000 rpm).

GMF	OV	XT-3,1P		PT-3.3		TT-5.1		PT-3.4		Inlet_Temp		PT-3.5		Outlet_Temp		$\dot{m}_l$		PT-3.1		PDT-1.1	
		%	bar	bar	bar	°C	bar	bar	°C	°C	bar	bar	kg/s	bar	bar	bar	bar	bar	bar	bar	bar
0,9483	30	0,9944	0,9945	23,6175	0,9841	18,0697	1,2238	28,7540	0,0357	0,1038	0,2330										
0,9506	40	0,9944	0,9939	22,9149	0,9751	17,1513	1,2167	27,2794	0,0477	0,2047	0,2234										
0,9475	50	0,9912	0,9892	25,7261	0,9589	20,5033	1,1779	29,1119	0,0664	0,3572	0,1894										
0,9489	60	0,9911	0,9881	25,6008	0,9451	20,3625	1,1386	28,2113	0,0766	0,5085	0,1500										
0,9497	70	0,9911	0,9873	25,5877	0,9332	20,1711	1,1042	27,2418	0,0847	0,6477	0,1151										
0,9534	80	0,9911	0,9864	25,0699	0,9212	20,1428	1,0664	26,6609	0,0855	0,7824	0,0761										
0,9482	90	0,9911	0,9857	25,4241	0,9103	19,7870	1,0311	25,7828	0,1023	0,9037	0,0378										
0,9495	100	0,9911	0,9855	25,2174	0,9071	19,3780	1,0206	25,4232	0,1016	0,9408	0,0257										
0,8003	30	0,9910	0,9910	24,8160	0,9815	20,1595	1,2195	28,2223	0,1559	0,0953	0,2296										
0,8064	40	0,9910	0,9903	24,5010	0,9735	19,7584	1,2090	28,0605	0,2087	0,1852	0,2188										
0,7975	50	0,9911	0,9893	24,6981	0,9605	18,9480	1,1813	27,2890	0,2949	0,3340	0,1909										
0,7973	60	0,9911	0,9885	24,1310	0,9477	18,5609	1,1472	26,4897	0,3520	0,4780	0,1556										
0,8039	70	0,9911	0,9876	24,2564	0,9363	18,1151	1,1140	25,8351	0,3755	0,5959	0,1213										
0,8017	80	0,9911	0,9868	24,4315	0,9236	17,7444	1,0760	25,0011	0,4212	0,7364	0,0825										
0,8032	90	0,9911	0,9862	24,9550	0,9125	16,5477	1,0417	23,6274	0,4458	0,8477	0,0467										
0,8066	100	0,9910	0,9860	24,0145	0,9097	16,7657	1,0321	23,6477	0,4443	0,8779	0,0352										

Table 12: Set-up 2 wet gas test results (9000 rpm).

GMF	OV	XT-3,1P		PT-3.3		TT-5.1		PT-3.4		Inlet_Temp		PT-3.5		Outlet_Temp		$\dot{m}_l$		PT-3.1		PDT-1.1	
		%	bar	bar	bar	°C	bar	bar	°C	bar	bar	°C	bar	bar	°C	kg/s	bar	bar	bar	bar	
0,9487	30	0,9947	0,9945	25,4987	0,9847	25,2670	1,2194	49,0859	0,0349	0,0102	0,2291	0,0349	0,0102	49,0859	0,0349	0,0102	0,2291	0,0349	0,0102	0,2291	
0,9502	40	0,9946	0,9938	25,5051	0,9762	25,1928	1,2063	47,3966	0,0470	0,0198	0,2160	0,0470	0,0198	47,3966	0,0470	0,0198	0,2160	0,0470	0,0198	0,2160	
0,9506	50	0,9947	0,9927	25,3906	0,9626	25,1154	1,1779	45,1392	0,0620	0,0364	0,1870	0,0620	0,0364	45,1392	0,0620	0,0364	0,1870	0,0620	0,0364	0,1870	
0,9500	60	0,9946	0,9917	25,3557	0,9492	25,0140	1,1383	43,2798	0,0747	0,0510	0,1487	0,0747	0,0510	43,2798	0,0747	0,0510	0,1487	0,0747	0,0510	0,1487	
0,9497	70	0,9946	0,9909	25,2095	0,9387	24,8969	1,1077	41,7090	0,0832	0,0634	0,1174	0,0832	0,0634	41,7090	0,0832	0,0634	0,1174	0,0832	0,0634	0,1174	
0,9504	80	0,9946	0,9901	25,0662	0,9273	24,6851	1,0709	40,1661	0,0898	0,0764	0,0782	0,0898	0,0764	40,1661	0,0898	0,0764	0,0782	0,0898	0,0764	0,0782	
0,9510	90	0,9946	0,9893	24,9997	0,9153	24,6190	1,0333	38,3605	0,0961	0,0905	0,0378	0,0961	0,0905	38,3605	0,0961	0,0905	0,0378	0,0961	0,0905	0,0378	
0,9479	100	0,9946	0,9891	24,5406	0,9125	24,2498	1,0253	37,3517	0,1042	0,0935	0,0282	0,1042	0,0935	37,3517	0,1042	0,0935	0,0282	0,1042	0,0935	0,0282	
0,7934	30	0,9947	0,9946	25,6467	0,9860	25,2593	1,2191	49,5517	0,1554	0,0088	0,2278	0,1554	0,0088	49,5517	0,1554	0,0088	0,2278	0,1554	0,0088	0,2278	
0,8005	40	0,9947	0,9941	25,5061	0,9787	25,2624	1,2110	48,8477	0,2082	0,0173	0,2199	0,2082	0,0173	48,8477	0,2082	0,0173	0,2199	0,2082	0,0173	0,2199	
0,8018	50	0,9947	0,9931	25,2786	0,9660	25,1506	1,1858	46,9980	0,2787	0,0319	0,1932	0,2787	0,0319	46,9980	0,2787	0,0319	0,1932	0,2787	0,0319	0,1932	
0,7999	60	0,9947	0,9921	25,2151	0,9535	25,0038	1,1499	45,4253	0,3385	0,0465	0,1574	0,3385	0,0465	45,4253	0,3385	0,0465	0,1574	0,3385	0,0465	0,1574	
0,8025	70	0,9947	0,9913	25,5294	0,9437	25,4875	1,1208	44,3816	0,3689	0,0570	0,1275	0,3689	0,0570	44,3816	0,3689	0,0570	0,1275	0,3689	0,0570	0,1275	
0,8004	80	0,9948	0,9904	25,2449	0,9313	25,1487	1,0812	42,6819	0,4177	0,0719	0,0853	0,4177	0,0719	42,6819	0,4177	0,0719	0,0853	0,4177	0,0719	0,0853	
0,8015	90	0,9948	0,9896	25,5942	0,9206	25,3521	1,0471	41,4417	0,4465	0,0842	0,0464	0,4465	0,0842	41,4417	0,4465	0,0842	0,0464	0,4465	0,0842	0,0464	
0,7985	100	0,9949	0,9896	24,6044	0,9175	24,6893	1,0378	40,3872	0,4650	0,0879	0,0357	0,4650	0,0879	40,3872	0,4650	0,0879	0,0357	0,4650	0,0879	0,0357	

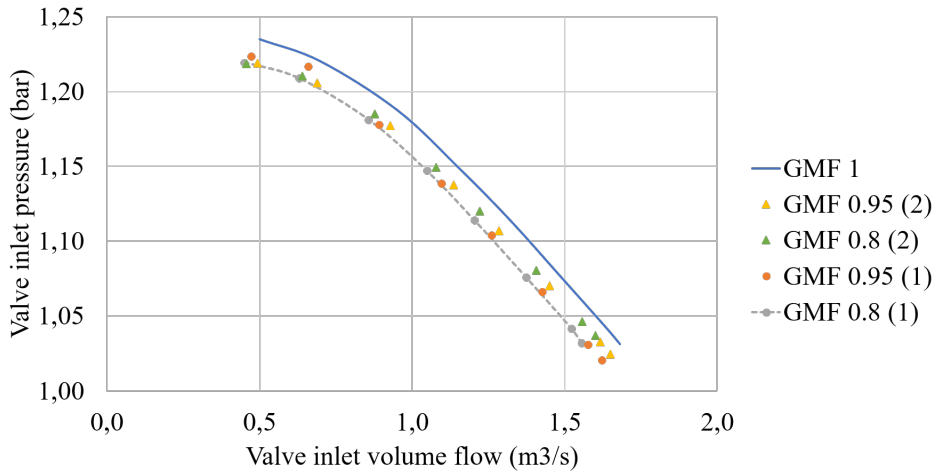


Figure 43: Valve inlet pressure curves for various GMFs in relation to volume flow (9000 rpm).

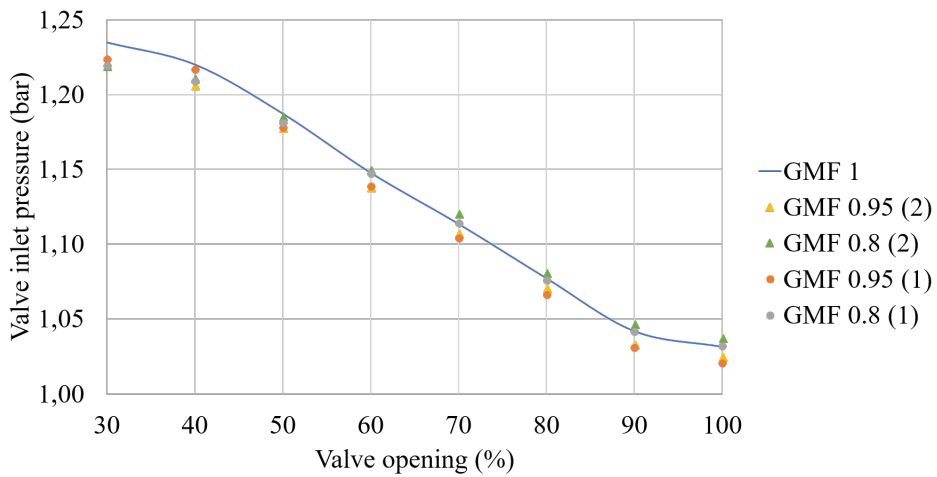


Figure 44: Valve inlet pressure curves for various GMFs in relation to valve opening (9000 rpm).

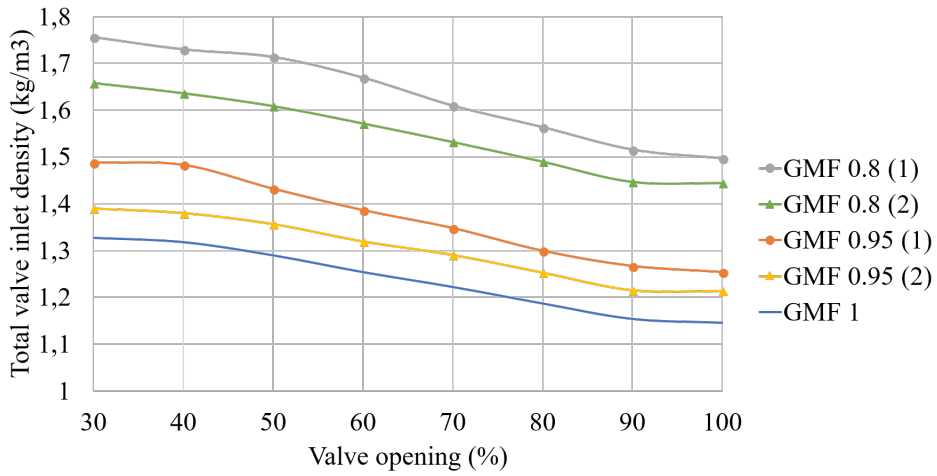


Figure 45: Total valve inlet density curves for various GMFs in relation to valve opening (9000 rpm).

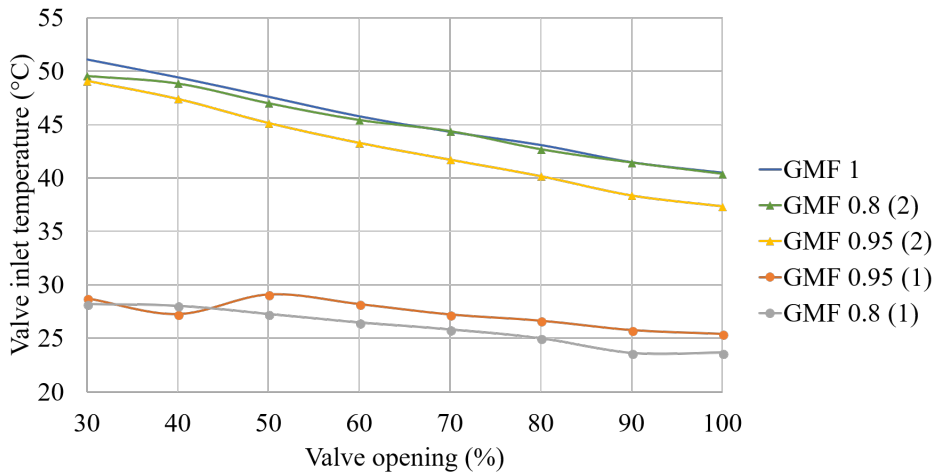


Figure 46: Valve inlet temperature curves for various GMFs in relation to valve opening (9000 rpm).

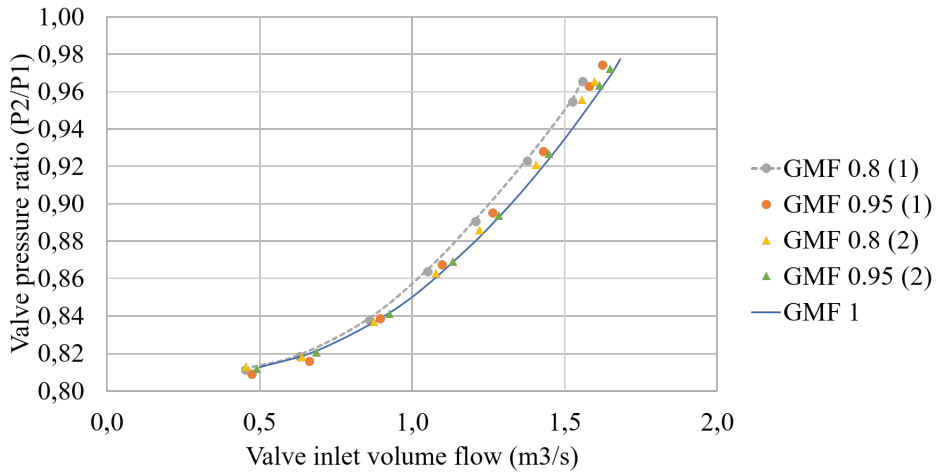


Figure 47: Valve pressure ratio ( $P_2/P_1$ ) curves for various GMFs in relation to volume flow (9000 rpm).

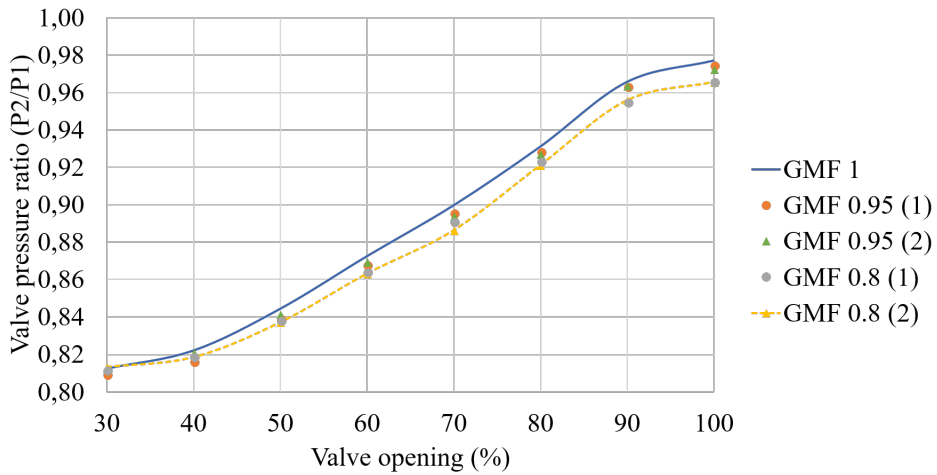


Figure 48: Valve pressure ratio ( $P_2/P_1$ ) curves for various GMFs in relation to valve opening (9000 rpm).

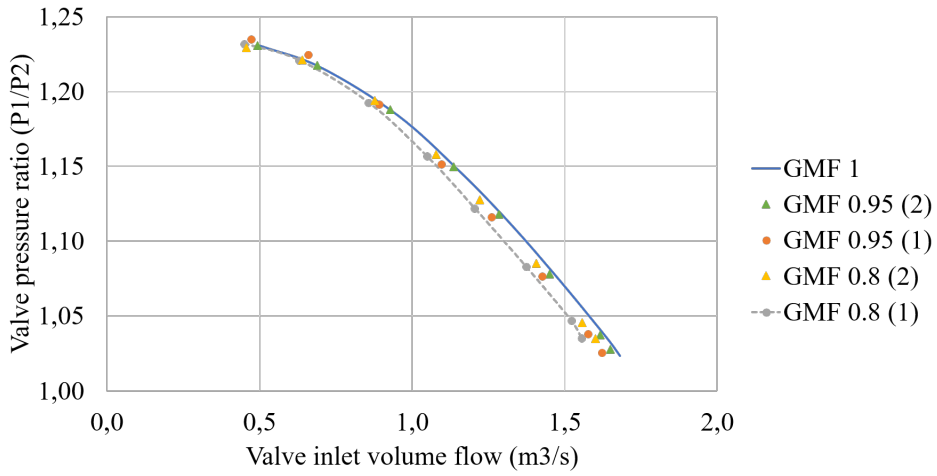


Figure 49: Valve pressure ratio ( $P_1/P_2$ ) curves for various GMFs in relation to volume flow (9000 rpm).

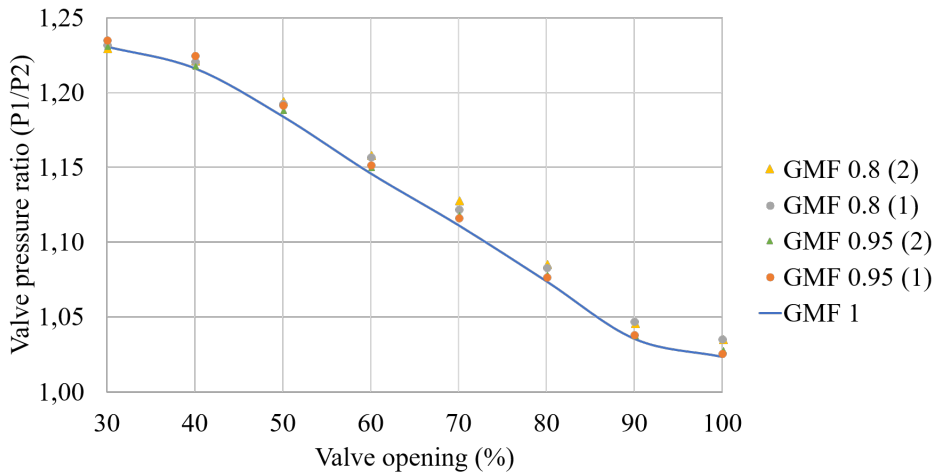


Figure 50: Valve pressure ratio ( $P_1/P_2$ ) curves for various GMFs in relation to valve opening (9000 rpm).

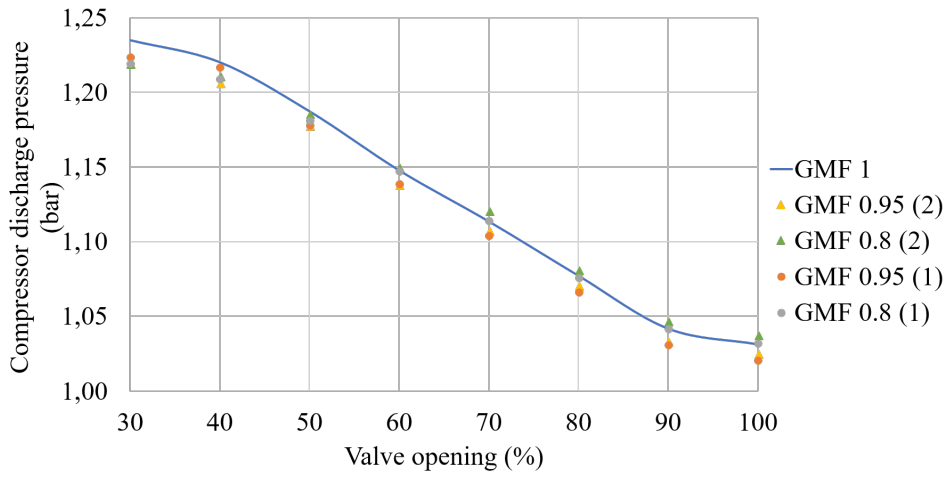


Figure 51: Compressor discharge pressure curves for various GMFs in relation to valve opening (9000 rpm).

## Appendix H: Calculated Performance Parameters

In this appendix, some of the main calculated performance parameters are presented tabulated.

Table 13: Explanation to the parameters used in Table 14-16.

Parameter	Explanation
OV	Set point discharge valve opening
$\dot{m}_g$	Gas mass flow at orifice
$Q_c$	Total compressor inlet volume flow
$Q_v$	Total valve inlet volume flow
$\rho_{tot}$	Total valve inlet density
x	Pressure ratio differential
Y	Expansion factor
$C_V$	Flow coefficient
$C_{v,rel}$	Relative flow coefficient
$P_R$	Valve pressure drop ratio



Table 14: Dry gas calculated performance parameters, based on Table 10.

GMF	OV	$\dot{m}_g$	$Q_c$	$Q_v$	$\rho_{tot}$	x	Y	$C_v$	$C_v, rel$	$P_R$
-	%	kg/s	$m^3/s$	$m^3/s$	kg/m <sup>3</sup>	-	-	-	-	-
0,9997	30	0,6638	0,5754	0,5006	1,3275	0,1874	0,9156	168,2441	9,9270	0,5000
0,9998	40	0,9205	0,8065	0,6996	1,3183	0,1778	0,9128	243,6144	14,3741	0,5000
0,9998	50	1,2267	1,0921	0,9530	1,2900	0,1555	0,9164	358,3581	21,1444	0,5000
0,9998	60	1,4505	1,3098	1,1594	1,2541	0,1274	0,9268	484,3936	28,5810	0,5000
0,9999	70	1,6145	1,4747	1,3238	1,2223	0,1002	0,9358	627,1143	37,0020	0,5000
0,9999	80	1,7557	1,6257	1,4836	1,1870	0,0688	0,9507	848,6458	50,0732	0,5000
0,9999	90	1,8848	1,7656	1,6382	1,1539	0,0343	0,9664	1328,6113	78,3929	0,5000
0,9999	100	1,9235	1,8017	1,6818	1,1458	0,0229	0,9567	1694,8105	100	0,5000

Table 15: Set-up 1 wet gas calculated performance parameters, based on Table 11.

GMF	OV	$\dot{m}_g$	$Q_c$	$Q_v$	$\rho_{tot}$	x	Y	$C_v$	$C_v, rel$	$P_R$
-	%	kg/s	$m^3/s$	$m^3/s$	kg/m <sup>3</sup>	-	-	-	-	-
0,9481	30	0,6528	0,5758	0,4710	1,4882	0,1904	0,9142	149,8808	10,0424	0,5000
0,9503	40	0,9123	0,8108	0,6594	1,4834	0,1836	0,9100	215,7979	14,4591	0,5000
0,9472	50	1,1897	1,0832	0,8918	1,4322	0,1608	0,9136	314,6822	21,0846	0,5000
0,9487	60	1,4159	1,3075	1,0948	1,3864	0,1318	0,9243	429,6565	28,7882	0,5000
0,9493	70	1,5846	1,4828	1,2601	1,3479	0,1042	0,9332	559,6943	37,5011	0,5000
0,9531	80	1,7376	1,6417	1,4257	1,2993	0,0714	0,9488	768,6714	51,5031	0,5000
0,9478	90	1,8582	1,7830	1,5760	1,2667	0,0367	0,9641	1180,4335	79,0923	0,4730
0,9491	100	1,8927	1,8225	1,6210	1,2536	0,0252	0,9523	1492,4756	100	0,4364
0,8002	30	0,6244	0,5528	0,4500	1,7561	0,1882	0,9152	121,8532	11,5001	0,5000
0,8057	40	0,8654	0,7718	0,6290	1,7299	0,1810	0,9113	176,3785	16,6460	0,5000
0,7961	50	1,1512	1,0451	0,8571	1,7137	0,1616	0,9131	253,8017	23,9530	0,5000
0,7958	60	1,3715	1,2586	1,0481	1,6695	0,1357	0,9220	340,2077	32,1077	0,4985
0,8031	70	1,5312	1,4258	1,2047	1,6096	0,1089	0,9302	443,0351	41,8122	0,4934
0,8003	80	1,6883	1,5974	1,3740	1,5637	0,0767	0,9450	601,0305	56,7233	0,4861
0,8023	90	1,8087	1,7456	1,5222	1,5156	0,0449	0,9560	876,5747	82,7283	0,4612
0,8054	100	1,8386	1,7673	1,5558	1,4969	0,0341	0,9355	1059,5827	100	0,4277

Table 16: Set-up 2 wet gas calculated performance parameters, based on Table 12.

GMF	OV	$\dot{m}_g$	$Q_c$	$Q_v$	$\rho_{tot}$	x	Y	$C_v$	$C_v, rel$	$P_R$
-	%	kg/s	$m^3/s$	$m^3/s$	kg/m <sup>3</sup>	-	-	-	-	-
0,9487	30	0,6462	0,5621	0,4901	1,3898	0,1879	0,9154	157,1691	10,8275	0,5000
0,9502	40	0,8986	0,7882	0,6852	1,3799	0,1791	0,9122	227,4562	15,6696	0,5000
0,9506	50	1,1926	1,0605	0,9248	1,3565	0,1587	0,9147	329,2302	22,6809	0,5000
0,9500	60	1,4192	1,2795	1,1322	1,3194	0,1306	0,9249	446,6134	30,7675	0,5000
0,9497	70	1,5717	1,4322	1,2821	1,2906	0,1060	0,9321	564,7436	38,9056	0,5000
0,9504	80	1,7229	1,5882	1,4467	1,2530	0,0730	0,9476	768,4392	52,9383	0,5000
0,9510	90	1,8641	1,7405	1,6127	1,2154	0,0366	0,9641	1211,7856	83,4808	0,4879
0,9479	100	1,8951	1,7728	1,6471	1,2138	0,0276	0,9478	1451,5740	100	0,4606
0,7934	30	0,5969	0,5186	0,4535	1,6585	0,1868	0,9158	122,1840	11,4116	0,5000
0,8005	40	0,8352	0,7311	0,6373	1,6366	0,1816	0,9110	177,2375	16,5534	0,5000
0,8018	50	1,1277	0,9997	0,8738	1,6091	0,1630	0,9124	259,2277	24,2110	0,5000
0,7999	60	1,3533	1,2147	1,0760	1,5718	0,1369	0,9213	349,4057	32,6333	0,5000
0,8025	70	1,4991	1,3618	1,2189	1,5321	0,1137	0,9271	438,5054	40,9549	0,5000
0,8004	80	1,6744	1,5396	1,4037	1,4899	0,0789	0,9434	605,0389	56,5085	0,4937
0,8015	90	1,8026	1,6778	1,5543	1,4466	0,0443	0,9566	897,5684	83,8297	0,4436
0,7985	100	1,8421	1,7166	1,5972	1,4441	0,0344	0,9348	1070,7042	100	0,4161